UCRL-14228 D3

UCRL-14228

University of California

Ernest O. Lawrence Radiation Laboratory

A NUMERICAL CALCULATION OF TWO-DIMENSIONAL STEADY-STATE DETONATIONS BY THE METHOD OF CHARACTERISTICS

DISTRIBUTION STATEMENT A
Approved for Public Release
Distribution Unlimited

Reproduced From Best Available Copy

Livermore, California

20000915 069

Lovelace Foundation - Document Library

14943

JAN 26 1966

DTIC QUALITY INSPECTED 4

UCRL-14228
Mathematics and Computers, UC-32
TID-4500 (43rd Ed.)

UNIVERSITY OF CALIFORNIA
Lawrence Radiation Laboratory
Livermore, California

AEC Contract No. W-7405-eng-48

A NUMERICAL CALCULATION OF TWO-DIMENSIONAL STEADY-STATE DETONATIONS BY THE METHOD OF CHARACTERISTICS

Gerald T. Richards
(Captain, U. S. Army)

May 26, 1965

Printed in USA. Price $4.00. Available from the Clearinghouse for Federal Scientific and Technical Information, National Bureau of Standards, U. S. Department of Commerce, Springfield, Virginia.

CONTENTS

CONTENTS (Continued)

ABSTRACT

This paper presents a method for finding the state of the detonation products for a plane detonation wave utilizing the two-dimensional steady-state hydrodynamics equations and the method of characteristics. It is shown that in those cases where the equation of state gives pressure along the adiabat as a function of density (only), the characteristic equations can be solved analytically in velocity space for the plane problem. A numerical method for the solution in coordinate space is then developed using the solution in velocity space in conjunction with the geometric relationship between characteristic curves in the two spaces. In this manner the difficulty encountered due to the coincidence of the detonation front and two characteristic curves in coordinate space is overcome. The derivations involved are included as appendices. The body of the paper describes the application of the technique for an ideal gas equation of state and for an equation of state developed by Mark Wilkins (UCRL-7797). A further application is described in which this solution is used to start a solution for a steady state detonation in cylindrical geometry. The results are reported for PBX 9404 in the form of graphs produced by the computing facilities on a cathode ray tube from the computer programs described.

GENERAL INTRODUCTION

In the course of work at the Lawrence Radiation Laboratory (Livermore) with the numerical calculation of the detonation of high explosives employing finite difference techniques directly on the differential equations of continuum mechanics as described in reference 1 (the HEMP code), it was decided that some kind of independent check on the ability of HEMP to calculate a steady state detonation was desirable. The objective was to establish that HEMP could sustain a steady state solution over a "long" time and to establish confidence in the numerical values of the variables calculated. It is well known that the method of characteristics enjoys the confidence of a large number of people and would, therefore, be a good method to accomplish both objectives. The work described here was undertaken with this in mind.

It will be noted that the computer programs written lack "polish" and cannot be used in present form as production codes to generate solutions to all the "practical" problems one would desire. This lack of polish should be

judged in the light of the objectives described in the paragraph above. The work was directed toward demonstrating that the method could be employed, and then working a representative problem which could be used to check against the same problem solved on HEMP. These objectives have been met. (This comparison will be made in a report by Mark Wilkins to be issued later.)

The report itself has been written with an eye toward self-containment. It seemed desirable to include everything that is necessary for a thorough understanding of the development of the numerical methods employed. For the most part this work has been confined to the appendices.

Sections I and II are devoted to the solution of a steady state detonation in plane geometry and section III describes the steady state problem in cylindrical geometry. The check of HEMP was to be made with the plane problem, and the cylindrical problem was included because it appeared that a need was developing for a production code for cylindrical steady-state detonations in connection with experimental programs under way at the Lawrence Radiation Laboratory studying material properties. Such a code employing the method of characteristics would be considerably faster than HEMP for this problem. The program described merely demonstrates that the technique of section III could be employed to build such a code.

I take this opportunity to offer my thanks to Mark Wilkins for proposing the project and encouraging me throughout, to John Hardy for his suggestions that helped transform my thoughts into deeds, to Fred Fritsch, Don Emery, and especially Gloria Scoggin for their instructions and aid in programming and debugging, and to the many people of the Technical Information Division for their talent and patience.

GENERAL DISCUSSION

It is generally accepted that the state of the detonation products of a high explosive (H. E.) can be accurately calculated using the hydrodynamics equations behind the detonation front and the Hugoniot equations across the front in conjunction with the Chapman-Jouguet hypothesis (see ref. 2). It is well known that the flow behind the front, relative to the front, is supersonic, and that if the detonation products are assumed to be nonviscous and non-conducting while the flow is assumed to be irrotational and isentropic, then the steady-state hydrodynamics equations are hyperbolic. For hyperbolic equations, the method of characteristics can be employed in those cases

where the boundary conditions are given on a curve that is not itself a characteristic curve. For the two-dimensional steady-state detonation it happens that the detonation front is both a boundary curve and a characteristic curve. In fact the front occurs where two characteristic curves become coincident. Therefore, to use the method of characteristics for this problem, it is necessary to devise a procedure to generate information behind this front where the method can be used.

Pack and Hill devised a method employing an expansion in power series from the front (see ref. 3). The method described on the following pages employs the hodograph transformation which transforms the detonation front from a line in coordinate space to a point and a characteristic curve in velocity space (see appendix 6 for details). It is then possible to use the geometric relation between characteristic curves in the two spaces to solve the problem numerically. This method requires an equation of state for the detonation products which results, through Bernoulli' s equation, in a sound speed, or relative volume, that is a function of the two velocity components. This is the same as requiring that the pressure be a function of density, only, along an adiabat. It was not possible to make a direct comparison with the Pack and Hill results because the equation of state they used was tabular but the "shapes" of the curves they give are the same as those shown in this report. The method used here seems to be easier to use and does not involve as many assumptions.

To work the plane problem using Wilkins' equation of state (see ref. 4) it was necessary to evaluate an improper integral (see part B, section II) that is shown to converge in appendix 10. As a further check on this integral it was evaluated for an ideal gas using the input constants shown in part D, section III, and the problem discussed in section I was worked using the program described in section II. The results of this are not included but when the plots obtained were compared with the plots in section I, they were identical. The ideal gas equation of state can, therefore, be included in a program written for the Wilkins equation of state, and this was done for the cylindrical program.

The data displayed in Figs. 2-15 and 17-19 were included to illustrate the kind of information available directly from the programs as written. With the exception of Fig. 19, the data were plotted by the computing facilities at Lawrence Radiation Laboratory (Livermore) from the tapes generated on the CDC 3600 high speed computer directly from the programs described.

CONCLUSIONS

The work herein described demonstrates that the method of characteristics can be employed to determine the state of the products of a plane steady-state detonation by using the hodograph transformation and the geometric relationship between the characteristic curves in the velocity space and those in the coordinate space to generate information behind the detonation front. It is also demonstrated that with some experimentation it would be possible to use the solution to the plane problem to build a production code for "rapid" solutions to cylindrical steady-state detonation problems.

I. A PLANE TWO-DIMENSIONAL DETONATION FOR AN EXPLOSIVE WITH AN IDEAL GAS EQUATION OF STATE

Introduction

In parts A through D below is presented the solution of a plane two-dimensional steady-state detonation of an explosive with an ideal gas equation of state employing the method of characteristics. Part A gives an outline of the derivation of the basic equations governing the motion; part B gives a description of the numerical method used; part C describes the example problem solved; and part D gives a description of the program card decks available.

A. Calculation of the Two-Dimensional Steady-State Detonation for an Ideal-Gas-Type Explosive

The general equations governing the motion of a steady state, non-viscous, nonconducting medium in the absence of body forces in a plane are (see appendix 1):

Conservation of Mass

$$\frac{\partial(\rho u)}{\partial x} + \frac{\partial(\rho v)}{\partial y} = 0 ,$$

Conservation of Momentum

$$- \frac{\partial p}{\partial x} = \rho u \frac{\partial u}{\partial x} + \rho v \frac{\partial u}{\partial y} ,$$

$$- \frac{\partial p}{\partial y} = \rho u \frac{\partial v}{\partial x} + \rho v \frac{\partial v}{\partial y} ,$$

Conservation of Energy

$$\rho u \frac{\partial}{\partial x}\left(\epsilon + \frac{u^2 + v^2}{2}\right) + \rho v \frac{\partial}{\partial y}\left(\epsilon + \frac{u^2 + v^2}{2}\right) = - \frac{\partial(pu)}{\partial x} - \frac{\partial(pv)}{\partial y} ,$$

Entropy Principle

$$\rho u \frac{\partial \eta}{\partial x} + \rho v \frac{\partial \eta}{\partial y} \geq 0 ,$$

where

ρ = mass density,

u = velocity in the x direction,

v = velocity in the y direction,

(x, y) = rectangular coordinates,

p = hydrostatic pressure,

ϵ = internal energy per unit mass,

η = entropy per unit mass.

If it is assumed that the material has the ideal gas equation of state,

$$\frac{p}{p_0} = \left(\frac{\rho}{\rho_0}\right)^{\gamma} \exp\left(\frac{\eta - \eta_0}{c_v}\right)$$

where

$\gamma = c_p / c_v$,

c_p = specific heat at constant pressure,

c_v = specific heat at constant volume,

and further assumed that the material is isentropic and irrotational, these equations can be replaced by the following equations (see appendix 1):

$$\begin{aligned} &(a^2 - u^2)\frac{\partial u}{\partial x} - uv\left(\frac{\partial u}{\partial y} + \frac{\partial v}{\partial x}\right) + (a^2 - v^2)\frac{\partial v}{\partial y} = 0 , \\ &\frac{\partial u}{\partial y} - \frac{\partial v}{\partial x} = 0 , \end{aligned} \tag{1}$$

where $a^2 = \left.\frac{\partial p}{\partial \rho}\right|_{\eta} = \frac{\gamma p}{\rho} \equiv$ sound speed.

It can also be shown that along path lines (flow lines)

$$u^2 + v^2 + \frac{2a^2}{\gamma - 1} = \text{constant} \tag{2}$$

so that only the variables x, y, u, v are involved in these equations. From the ideal gas equation of state it can be shown that:

$$p = p_i \left(\frac{a^2}{a_i^2}\right)^{\frac{\gamma}{\gamma-1}} ,$$

$$\rho = \frac{\gamma p}{a^2} = \frac{\rho_0}{V} , \tag{3}$$

$$\epsilon = \frac{pV}{\gamma - 1} , \text{ (see Ref. 2)}$$

$$E = \rho_0 \epsilon$$

where

ϵ = internal energy per unit mass,
p_i, ρ_i, a_i are values at some initial point,
V = relative volume,
ρ_0 = reference density.

The problem is then reduced to finding u and v and using the relations above to find the other variables of interest. In this treatment the equations (1) were solved numerically by the use of the method of characteristics. The equations can be shown to be hyperbolic (see appendix 2) and if the so-called hodograph transformation is made, i. e., if the equations are recast with u, v as the independent variables, four equations result (see appendix 3). Two equations are for characteristics in the u, v, plane (Γ) and two are for characteristics in the x, y plane (C), which last are also "compatibility relations" that hold along Γ curves. These four relations are:

$$\Gamma_1: \quad \frac{dv}{du} = -\left(\frac{uv + a\sqrt{u^2 + v^2 - a^2}}{v^2 - a^2}\right)$$

along which

$$C_1: \quad \frac{uv + a\sqrt{u^2 + v^2 - a^2}}{u^2 - a^2} \frac{dx}{d\alpha} = \frac{dy}{d\alpha}$$

$$\Gamma_2: \quad \frac{dv}{du} = -\left(\frac{uv - a\sqrt{u^2 + v^2 - a^2}}{v^2 - a^2}\right) , \tag{4}$$

along which

$$C_2: \quad \frac{uv - a\sqrt{u^2 + v^2 - a^2}}{u^2 - a^2} \frac{dx}{d\beta} = \frac{dy}{d\beta} ,$$

where α and β are parameters along Γ_1 and Γ_2 respectively, provided that $u^2 + v^2 - a^2 > 0$.

Now if one lets

ψ^+ = angle the Γ_1 curve makes with the positive u axis,

ψ^- = angle the Γ_2 curve makes with the positive u axis,

then one can show (see appendix 5) that the equations (4) may be written as

$$\begin{aligned}
&\Gamma^+: \quad v_\alpha = (\tan\psi^+)\, u_\alpha , \\
&C^+: \quad y_\alpha = \frac{-1}{\tan\psi^-}\, x_\alpha , \\
&\Gamma^-: \quad v_\beta = (\tan\psi^-)\, u_\beta , \\
&C^-: \quad y_\beta = \frac{-1}{\tan\psi^+}\, x_\beta ,
\end{aligned} \tag{5}$$

where $A_\alpha = \frac{\partial A}{\partial \alpha}$, and the Γ and C curves can be designated $\Gamma_1 = \Gamma^+$, $C_2 = C^-$, etc. because of the particular way in which they are related (see below). Note that the C^+ and Γ^- curves are perpendicular as are C^- and Γ^+.

The coordinate system used is one in which the detonation front is considered to be at rest and the initial values of the dependent variables are those determined by the Chapman-Jouguet hypothesis (see appendix 4). Only the "upper" half of the slab is considered since the other half is the reflection of the one considered.

In appendices 6 and 7 it is shown that the equations for Γ^+ and Γ^- can be solved in parametric form. They are shown to be epicycloids generated by a circle of radius $\bar{q}$ (see below) rolling on a circle of radius $a_{c\text{-}j}$, where

$a_{c\text{-}j} \equiv$ the Chapman-Jouguet sound speed,

$$\bar{q} \equiv \frac{1}{2}\left(\frac{1}{\mu} - 1\right) a_{c\text{-}j} ,$$

$$\mu^2 = \frac{\gamma - 1}{\gamma + 1} ,$$

γ = specific heat ratio.

The Γ^+ curves are generated if the circle of radius $\bar{q}$ rotates counterclockwise, and the Γ^- curves are generated if it rolls clockwise. The constant in equation (2) is determined in appendix 6 and designated $\hat{q} = a_{c\text{-}j}/\mu$, and is

shown to be the locus of points where the sound speed is zero. There are two parameters involved in the solutions. The first is the angle subtended at the center of the circle of radius a_{c-j} by the center of the rolling circle when it is in its initial position (ψ_*). The second is the angle subtended at the center of the circle of radius a_{c-j} by the center of the rolling circle as it rolls (β), measured with respect to the initial position. In terms of these parameters the Γ curves are given by

$$u = (a_{c-j} + \bar{q}) \cos(\beta + \psi_*) - \bar{q} \cos\left(\frac{a_{c-j} + \bar{q}}{\bar{q}} \beta + \psi_*\right),$$
$$v = (a_{c-j} + \bar{q}) \sin(\beta + \psi_*) - \bar{q} \sin\left(\frac{a_{c-j} + \bar{q}}{\bar{q}} \beta + \psi_*\right). \tag{6}$$

For $\psi_* \leq 0$, $\beta \geq 0$ the Γ^+ curves are generated, and for $\psi_* \geq 0$, $\beta \leq 0$ the Γ^- curves are generated.

In terms of these same variables the C curves are given by

$$y_\beta = \frac{-1}{\tan\left(\frac{\beta}{1-\mu} + \psi_*\right)} x_\beta . \tag{7}$$

For $\psi_* \geq 0$, $\beta \leq 0$ the C^+ curves are generated, and for $\psi_* \leq 0$, $\beta \geq 0$ the C^- curves are generated.

It can be shown (see appendix 6) that for this type of problem the solution in the u, v plane is contained in the region enclosed by $u^2 + v^2 = \hat{q}^2$, $v = 0$, and Γ_0^+, where Γ_0^+ is generated by (6) with $\psi_* = 0$ and $\beta \geq 0$.

Up to this point the solution has presented no particular difficulties, but equations (4) can only be written, and hence the "solutions" (6) and (7), if $u^2 + v^2 - a^2 > 0$. Using the results in appendix 4, it is seen that at the front, $u^2 + v^2 - a^2 = u_{c-j}^2 - a_{c-j}^2 = 0$. This means that the detonation front is both a C^+ and C^- characteristic (the equations are parabolic). In the theory of characteristics it is shown that the method can be applied if the boundary along which data are given is <u>not</u> a characteristic, but in this case it is. The way this difficulty was handled is discussed in appendix 6.

B. Numerical Method

The equations to be solved are (see appendix 6)

$$\Gamma^+: \frac{2U}{A_{c-j}} = \delta = R_2 \cos(\beta^+ + \psi_*^+) - R_3 \cos\left[(R_2/R_3)\beta^+ + \psi_*^+\right],$$
$$\frac{2V}{A_{c-j}} = \lambda = R_2 \sin(\beta^+ + \psi_*^+) - R_3 \sin\left[(R_2/R_3)\beta^+ + \psi_*^+\right], \tag{1}$$

along which

$$dy/dx = -1/\tan\left(\frac{\beta^-}{1-\mu} + \psi_*^-\right),$$

and

$$\Gamma^-: \frac{2U}{A_{c-j}} = \delta = R_2 \cos(\beta^- + \psi_*^-) - R_3 \cos\left[(R_2/R_3)\beta^- + \psi_*^-\right],$$
$$\frac{2V}{A_{c-j}} = \lambda = R_2 \sin(\beta^- + \psi_*^-) - R_3 \sin\left[(R_2/R_3)\beta^- + \psi_*^-\right], \tag{2}$$

along which

$$dy/dx = -1/\tan\left(\frac{\beta^+}{1-\mu} + \psi_*^+\right),$$

where

$$0 \leq \beta^+ \leq \pi(1-\mu)/2\mu, \quad 0 \geq \beta^- \geq -\pi(1-\mu)/2\mu, \text{ generally,}$$
$$\text{and} \quad 0 \geq \psi_*^+ \geq \pi(1-\mu)/2\mu, \quad 0 \leq \psi_*^- \leq \pi(1-\mu)/\mu\ . \tag{3}$$

Specifically the limits on β^+ and β^- are determined by the Γ^+ curve with $\psi_*^+ = 0$ and $\lambda = 0$ as well as by the circle $U^2 + V^2 = A_{c-j}^2/\mu^2$, as given in detail in appendix 6.

The nature of the above relations demands a numerical solution. The procedure will be to assign values of ψ_*^+ and ψ_*^- which will be used to determine β^+ and β^- and hence U and V, then to determine X and Y by making numerical integration of the compatibility conditions.

To that end several general relations will be derived below: Suppose that one is given ψ_*^+ and ψ_*^- and is required to find β^- and β^+ at the intersection of Γ^+ and Γ^-. Equations (1) and (2) are used to give

$$R_2 \cos(\beta^+ + \psi_*^+) - R_3 \cos\left(\frac{R_2}{R_3}\beta^+ + \psi_*^+\right) = R_2 \cos(\beta^- + \psi_*^-)$$
$$- R_3 \cos\left(\frac{R_2}{R_3}\beta^- + \psi_*^-\right) \tag{4a}$$

and

$$R_2 \sin(\beta^+ + \psi_*^+) - R_3 \sin\left[(R_2/R_3)\beta^+ + \psi_*^+\right] = R_2 \sin(\beta^- + \psi_*^-) - R_3 \sin\left[(R_2/R_3)\beta^- + \psi_*^-\right] . \quad (4b)$$

Eq. (4) may be rewritten as

$$R_2\left[\cos(\beta^+ + \psi_*^+) - \cos(\beta^- + \psi_*^-)\right] = R_3\left\{\cos\left[(R_2/R_3)\beta^+ + \psi_*^+\right] - \cos\left[(R_2/R_3)\beta^- + \psi_*^-\right]\right\} \quad (5a)$$

and

$$R_2\left[\sin(\beta^+ + \psi_*^+) - \sin(\beta^- + \psi_*^-)\right] = R_3\left\{\sin\left[(R_2/R_3)\beta^+ + \psi_*^+\right] - \sin\left[(R_2/R_3)\beta^- + \psi_*^-\right]\right\} . \quad (5b)$$

The following relations are easily derived from trigonometry:

$$\cos\psi - \cos\theta = 2 \sin \tfrac{1}{2}(\theta + \psi) \sin \tfrac{1}{2}(\theta - \psi) ,$$
$$\sin\theta - \sin\psi = 2 \cos \tfrac{1}{2}(\theta + \psi) \sin \tfrac{1}{2}(\theta - \psi) . \quad (6)$$

Using (6) in (5):

$$2R_2 \sin \tfrac{1}{2}(\beta^+ + \beta^- + \psi_*^+ + \psi_*^-) \sin \tfrac{1}{2}(\beta^+ - \beta^- + \psi_*^+ - \psi_*^-) = 2R_3 \sin \tfrac{1}{2}\left[(R_2/R_3)(\beta^+ + \beta^-) + \psi_*^+ + \psi_*^-\right] \sin \tfrac{1}{2}\left[(R_2/R_3)(\beta^+ - \beta^-) + \psi_*^+ - \psi_*^-\right] \quad (7)$$

and

$$2R_2 \cos \tfrac{1}{2}(\beta^+ + \beta^- + \psi_*^+ + \psi_*^-) \sin \tfrac{1}{2}(\beta^+ - \beta^- + \psi_*^+ - \psi_*^-) = 2R_3 \cos \tfrac{1}{2}\left[(R_2/R_3)(\beta^+ + \beta^-) + \psi_*^+ + \psi_*^-\right] \sin \tfrac{1}{2}\left[(R_2/R_3)(\beta^+ - \beta^-) + \psi_*^+ - \psi_*^-\right] . \quad (8)$$

Dividing equation (7) by (8):

$$\tan \tfrac{1}{2}(\beta^+ + \beta^- + \psi_*^+ + \psi_*^-) = \tan \tfrac{1}{2}\left[(R_2/R_3)(\beta^+ + \beta^-) + \psi_*^+ + \psi_*^-\right] . \quad (9)$$

From equation (9):

$$\beta^+ + \beta^- + \psi_*^+ + \psi_*^- = (R_2/R_3)(\beta^+ + \beta^-) + \psi_*^+ + \psi_*^-$$

or

$$(1 - R_2/R_3)(\beta^+ + \beta^-) = 0 . \tag{10}$$

Recalling the definitions of R_2 and R_3 from equation (53), appendix 6:

$$1 - R_2/R_3 = 1 - \frac{1+\mu}{1-\mu} = \frac{-2\mu}{1-\mu} \neq 0 ;$$

hence, (10) yields

$$\beta^+ = -\beta^- . \tag{11}$$

Hence, the general statement: <u>At the intersection of any pair of Γ^+ and Γ^- characteristics one need only determine one of β^+ and β^- since $\beta^+ = -\beta^-$ at such intersection points.</u>

Now putting (11) in (7) and (8) yields:

$$2R_2 \sin\frac{1}{2}\left(\psi_*^+ + \psi_*^-\right) \sin\frac{1}{2}\left(2\beta^+ + \psi_*^+ - \psi_*^-\right) = 2R_3 \sin\frac{1}{2}\left(\psi_*^+ + \psi_*^-\right) \times \sin\frac{1}{2}\left(\frac{2R_2}{R_3}\beta^+ + \psi_*^+ - \psi_*^-\right) ,$$

$$2R_2 \cos\frac{1}{2}\left(\psi_*^+ + \psi_*^-\right) \sin\frac{1}{2}\left(2\beta^+ + \psi_*^+ - \psi_*^-\right) = 2R_3 \cos\frac{1}{2}\left(\psi_*^+ + \psi_*^-\right) \times \sin\frac{1}{2}\left(\frac{2R_2}{R_3}\beta^+ + \psi_*^+ - \psi_*^-\right) ,$$

from which

$$\sin\left[\beta^+ + \frac{1}{2}\left(\psi_*^+ - \psi_*^-\right)\right] - \frac{R_3}{R_2}\sin\left[\frac{R_2}{R_3}\beta^+ + \frac{1}{2}\left(\psi_*^+ - \psi_*^-\right)\right] = 0 . \tag{12}$$

Equation (12) is then solved for β^+. As indicated in appendix 6, along the boundary $\lambda = 0$, $\psi_*^+ = -\psi_*^-$. Using this relation in (12), the value of β^+ along $\lambda = 0$ is given by the solution of

$$\sin(\beta^+ + \psi_*^+) - \frac{R_3}{R_2}\sin\left(\frac{R_2}{R_2}\beta^+ + \psi_*^+\right) = 0 , \tag{13}$$

which is seen to agree with setting $v = 0$ in (1).

The other boundary where β^+ is in question is the Γ_0^+ curve along which $\psi_*^+ = 0$. The value of β^+ along Γ_0^+ is then found from the solution of

$$\sin\left(\beta^{+} - \frac{1}{2}\psi_{*}^{-}\right) - \frac{R_3}{R_2}\sin\left[\frac{R_2}{R_3}\beta^{+} - \frac{1}{2}\psi_{*}^{-}\right] = 0 . \tag{14}$$

From equation (17), appendix 6, the sound speed A may be determined from

$$A^2 = \left(\frac{A_{c-j}^2}{\mu^2} - U^2 - V^2\right)\left(\frac{\gamma - 1}{2}\right) . \tag{15}$$

Therefore, given a pair of Γ curves, by specifying ψ_{*}^{+} and ψ_{*}^{-} one determines β^{+} from (13) or (14). With β^{+}, one can use (1) or (2) to determine U and V and (15) to determine A so that the problem is completely solved in the U, V plane since knowing A one can find the pressure from equation (19), appendix 1, and the density from equation (18), appendix 1, etc. The problem now is to determine X and Y at each β^{+} in the U, V plane. The known values of X, Y are (see Fig. 1):

$Y = 0$ along $\lambda = 0$,

$X = 0$, $Y = b$ along Γ_0^{+},

$X = Y = \infty$ along $U^2 + V^2 = A_{c-j}^2/\mu^2$,

$X = 0$, $0 \leq Y \leq b$ at $V = 0$, $U = A_{c-j}$,

$0 \leq X < \infty$, $b \leq Y < \infty$ at the intersection of Γ_0^{+} and $U^2 + V^2 = A_{c-j}^2/\mu^2$.

The approach is to assign a value of $\Delta\psi_{*}$, let $\psi_{*(1)}^{+} = 0$; $\psi_{*(2)}^{+} = -\Delta\psi_{*}, \ldots$, out to

$$\psi_{*(n)}^{+} \geq \frac{-\pi(1 - \mu)}{2\mu} ;$$

determine values of ψ_{*}^{-} that give the Γ^{-} curves that intersect these Γ^{+} curves along $\lambda = 0$ so that the region is covered with a mesh of Γ curves; determine β^{+} at each intersection point; and then use an average value of the slopes in (1) and (2) to obtain the X, Y point at each intersection.

At this point it is necessary to convert the equations for use in the numerical solution. To do this the characteristic curves are numbered with the Γ^{+} curves designated by $k = 1, 2, \ldots$, and the Γ^{-} curves designated by $j = 1, 2, \ldots$ (see Fig. 1a). To do this, let

$$\psi_{*}^{+} = W_k^{+} \text{ and } \psi_{*}^{-} = W_j^{-} . \tag{16}$$

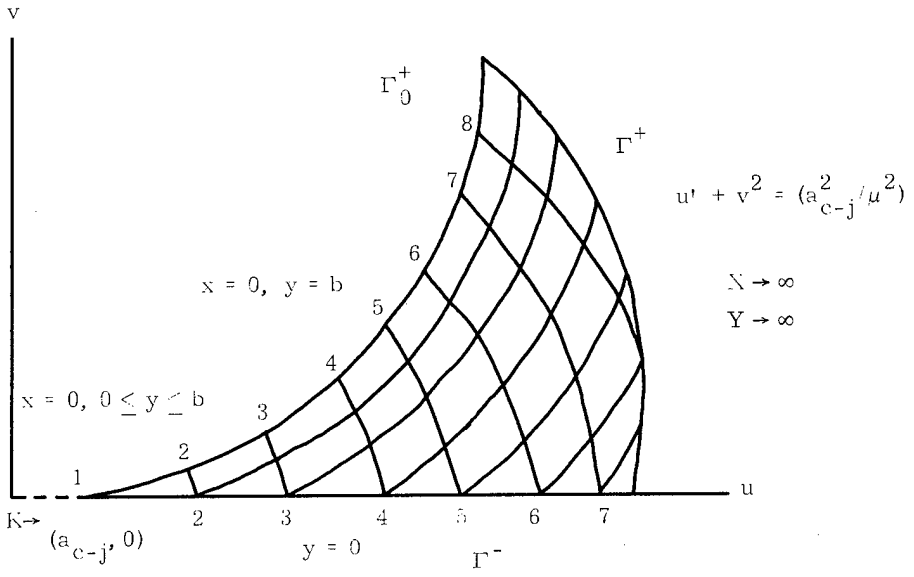

(a)

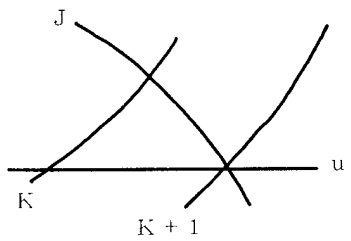

$X_{J,K}$ and $Y_{J,K}$ known
$Y_{J,K+1} = Y_{min}$ known
Find: $X_{J,K+1}$

(b)

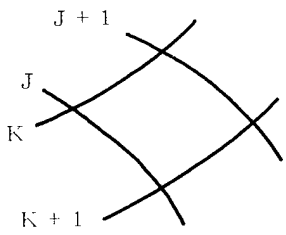

$X_{J,K}$; $Y_{J,K}$; $X_{J+1,K}$; $Y_{J+1,K}$;
$X_{J,K+1}$; $Y_{J,K+1}$ known
Find:
$X_{J+1,K+1}$ and $Y_{J+1,K+1}$

(c)

Fig. 1. The problem.

Since $\beta^- = -\beta^+$ at the intersection points, one need only compute β^+ and so let

$$\beta^+ = B_{j,k} \text{ then } U = U_{j,k},\ V = V_{j,k},\ \text{and } A = A_{j,k}\,. \tag{17}$$

For convenience let

$$\begin{aligned} R_1 &= \frac{1}{\mu}\,, \\ R_4 &= \frac{1}{1-\mu} = R_1/R_3\,, \\ R_5 &= R_2/R_3, \\ R_6 &= R_3/R_2\,. \end{aligned} \tag{18}$$

Then rewriting (12), (13), (14), (15), (1), and (2):

$$\sin\left[B_{j,k} + \tfrac{1}{2}(W_k^+ - W_j^-)\right] - R_6 \sin\left[R_5 B_{j,k} + \tfrac{1}{2}(W_k^+ - W_j^-)\right] = 0 \text{ for a general } B_{j,k}\,,$$

$$\sin\left[B_{j,k} + W_k^+\right] - R_6 \sin\left[R_5 B_{j,k} + W_k^+\right] = 0 \text{ for a } B_{j,k} \text{ along } V_{j,k} = 0, \tag{19}$$

$$\sin\left[B_{j,k} - \tfrac{1}{2} W_j^-\right] - R_6 \sin\left[R_5 B_{j,k} - \tfrac{1}{2} W_j^-\right] = 0 \text{ for a } B_{j,k} \text{ along } W_1^+ = 0,$$

$$\begin{aligned} U_{j,k} &= A_{c-j}\left[R_2 \cos\left(B_{j,k} + W_k^+\right) - R_3 \cos\left(R_5 B_{j,k} + W_k^+\right)\right]\,, \\ V_{j,k} &= A_{c-j}\left[R_2 \sin\left(B_{j,k} + W_k^+\right) - R_3 \sin\left(R_5 B_{j,k} + W_k^+\right)\right]\,, \\ A_{j,k} &= \sqrt{\left[\frac{A_{c-j}^2}{\mu^2} - \left(U_{j,k}\right)^2 - \left(V_{j,k}\right)^2\right]\left(\frac{\gamma - 1}{2}\right)}\,. \end{aligned} \tag{20}$$

Then one assigns values to W_k^+ and W_j^- for each k, j, and calculates $B_{j,k}$ from (19) using the Newton-Raphson Method (see appendix 8). Equations (20) are then used to determine $U_{j,k}$, $V_{j,k}$, and $A_{j,k}$ at each $B_{j,k}$.

In order to determine $x = X_{j,k}$ and $y = Y_{j,k}$, define

$$F_{j+\frac{1}{2},k} = \tan\left[-\frac{R_4}{2}(B_{j,k} + B_{j+1,k}) + \frac{1}{2}(W_j^- + W_{j+1}^-)\right] \tag{21}$$

and

$$F_{j,k+\frac{1}{2}} = \tan\left[\frac{R_4}{2}(B_{j,k} + B_{j,k+1}) + \frac{1}{2}(W_k^+ + W_{k+1}^+)\right] \tag{22}$$

and calculate $F_{j+\frac{1}{2}, k}$ and $F_{j, k+\frac{1}{2}}$ from the given W_k^+, W_j^- and the calculated $B_{j, k}$. The two compatibility conditions from (1) and (2) may now be written as

$$-(Y_{j+1, k} - Y_{j, k}) F_{j+\frac{1}{2}, k} = X_{j+1, k} - X_{j, k} \text{ (along } \Gamma^+), \tag{23}$$

$$-(Y_{j, k+1} - Y_{j, k}) F_{j, k+\frac{1}{2}} = X_{j, k+1} - X_{j, k} \text{ (along } \Gamma^-). \tag{24}$$

To carry out the computation using the known values of x, y the procedure is to first obtain the x value at k = 2 using (24), then obtain x, y values along Γ_1^+ for each "j" using both (23) and (24). The process is then repeated for each "k." Referring to the diagrams in Fig. 1, Fig. 1b represents the situation along the U axis and Fig. 1c represents the situation in the U, V plane generally. The computations in these two cases are the ones used and will be carried out here as an illustration:

To determine the x value along V = 0 for a given "k" value, assume $X_{j, k}$, $Y_{j, k}$, $Y_{j, k+1}$ = YMIN are known; then from (24),

$$X_{j, k+1} = X_{j, k} - (Y_{j, k+1} - Y_{j, k}) F_{j, k+\frac{1}{2}}. \tag{25}$$

To determine subsequent values of $X_{j, k+1}$ and $Y_{j, k+1}$, X and Y are known at j, k; j+1, k; and j, k+1 and from (23) and (24):

$$Y_{j+1, k+1} = \frac{X_{j+1, k} - X_{j, k+1} + F_{j+1, k+\frac{1}{2}} Y_{j+1, k} - F_{j+\frac{1}{2}, k+1} Y_{j, k+1}}{F_{j+1, k+\frac{1}{2}} - F_{j+\frac{1}{2}, k+1}} \tag{26}$$

and

$$X_{j+1, k+1} = X_{j+1, k} - (Y_{j+1, k+1} - Y_{j+1, k}) F_{j+1, k+\frac{1}{2}}. \tag{27}$$

C. Example Problem

As an application of this method, a problem was solved for a typical explosive utilizing a CDC 3600 high speed computer. The data used was for PBX 9404 (see ref. 4):

Chapman-Jouguet pressure = P_{c-j} = 0.39 megabar,
Detonation speed = D = 0.88 cm/μsec,
Density of unburnt explosive = ρ_0 = 1.84 g/cm^3.

Using the relations in appendix 4 the effective γ was calculated to be:

Specific heat ratio = $\gamma \cong 2.6535795$.

The initial half-thickness of the H. E. was taken as 0.5.

The idea was to assign a value of zero to W_1^+ and W_1^-, and a fixed value ΔW to be added to W_j^- to get W_{j+1}^- and subtracted from W_k^+ to get W_{k+1}^+. The grid thus generated in the u, v plane was to be used to solve the problem. While this gave a rather finely spaced grid in the u, v plane with $\Delta W = 1°$ (or 0.01745 radian), the resulting grid in the x, y plane had a relatively large space between the detonation front and the first C^+ curve. When smaller values of ΔW were tried, the gap was seen to close very slowly and it became obvious that variable grid spaces would be required. Without any attempt to optimize the system of spacing, 30 C^+ curves were inserted between the original C^+ lines and the front ranging in spacing from $\Delta W_1 = 5 \times 10^{-7} \times \Delta W$ to $\Delta W_{30} = 4 \times 10^{-2} \times \Delta W$. From there on the spaces were equal with $\Delta W_i = 2 \times 10^{-1} \times \Delta W$. The solution was obtained with $\Delta W = 1°$ so the majority of the spacing was with 0.2° intervals. Figures 2 and 3 show some representative Γ^+ and C^+ curves respectively.

In considering the accuracy of the method used, the C^+ curve nearest the front is the most important. The initial point on this curve along y = 0 is determined by extending a straight line from the point x = 0, y = 0.5. Referring to Fig. 3 it seems obvious that a curve drawn from the point (0., 0.5) to the x axis without crossing the first C^+ curve cannot differ much from a straight line. By taking smaller value for ΔW_i, the first point on this C^+ curve can be placed as near to the front as desired and hence the x, y values can be made as accurate as desired.

As a check, ΔW was set to 0.5° giving $\Delta W_1 = (2.5 \times 10^{-7})°$, etc., and the resulting values of x and y were the same to four significant figures near y = 0 and to less than 1% everywhere.

Figure 4 shows the pressure in megabars as a function of the distance from the front expressed in units of the original thickness for various values of y. Table 1, appendix 11, lists output from which this figure was plotted.

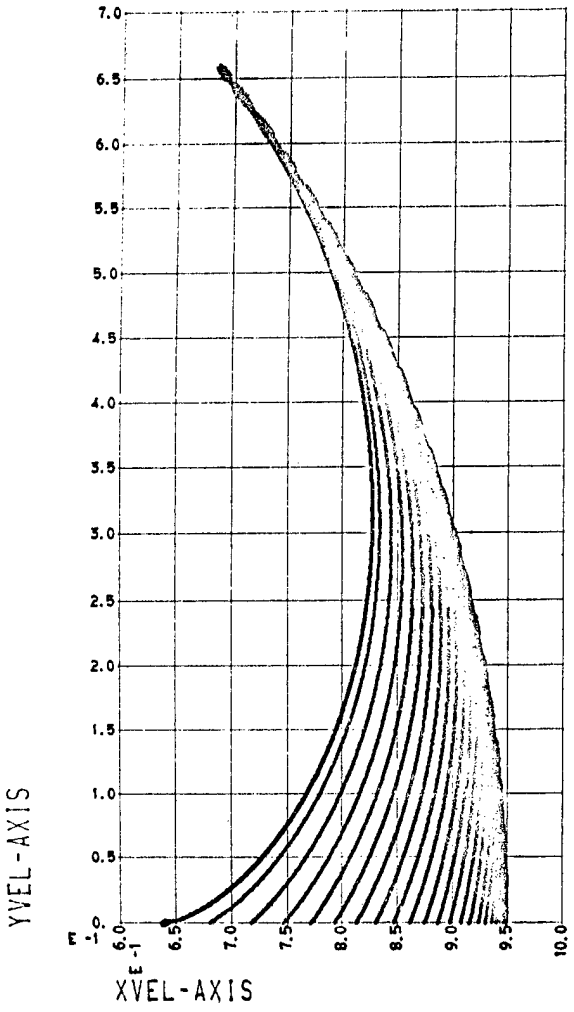

Fig. 2. Γ^+ characteristics for ideal gas equation of state in plane geometry.

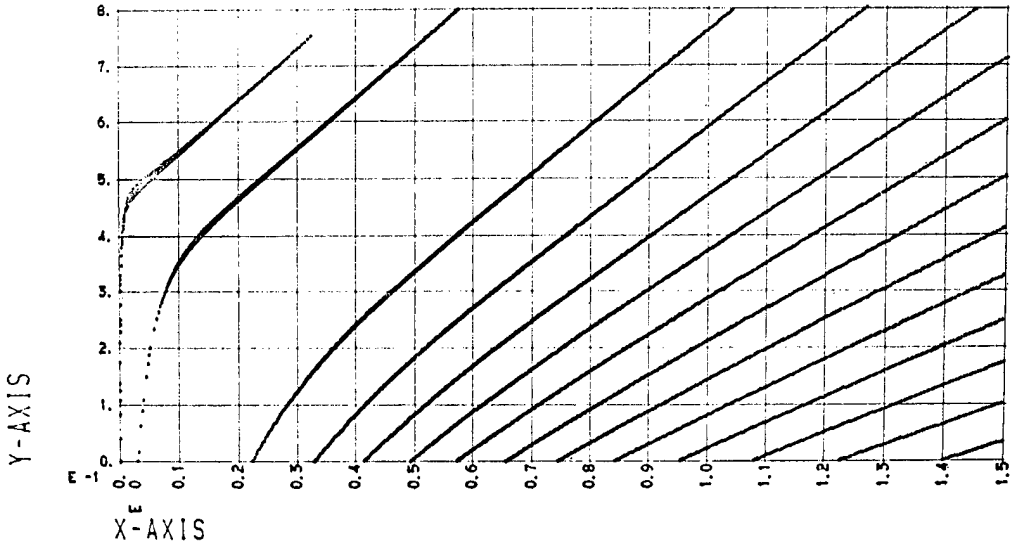

Fig. 3. C^+ characteristics for ideal gas equation of state in plane geometry.

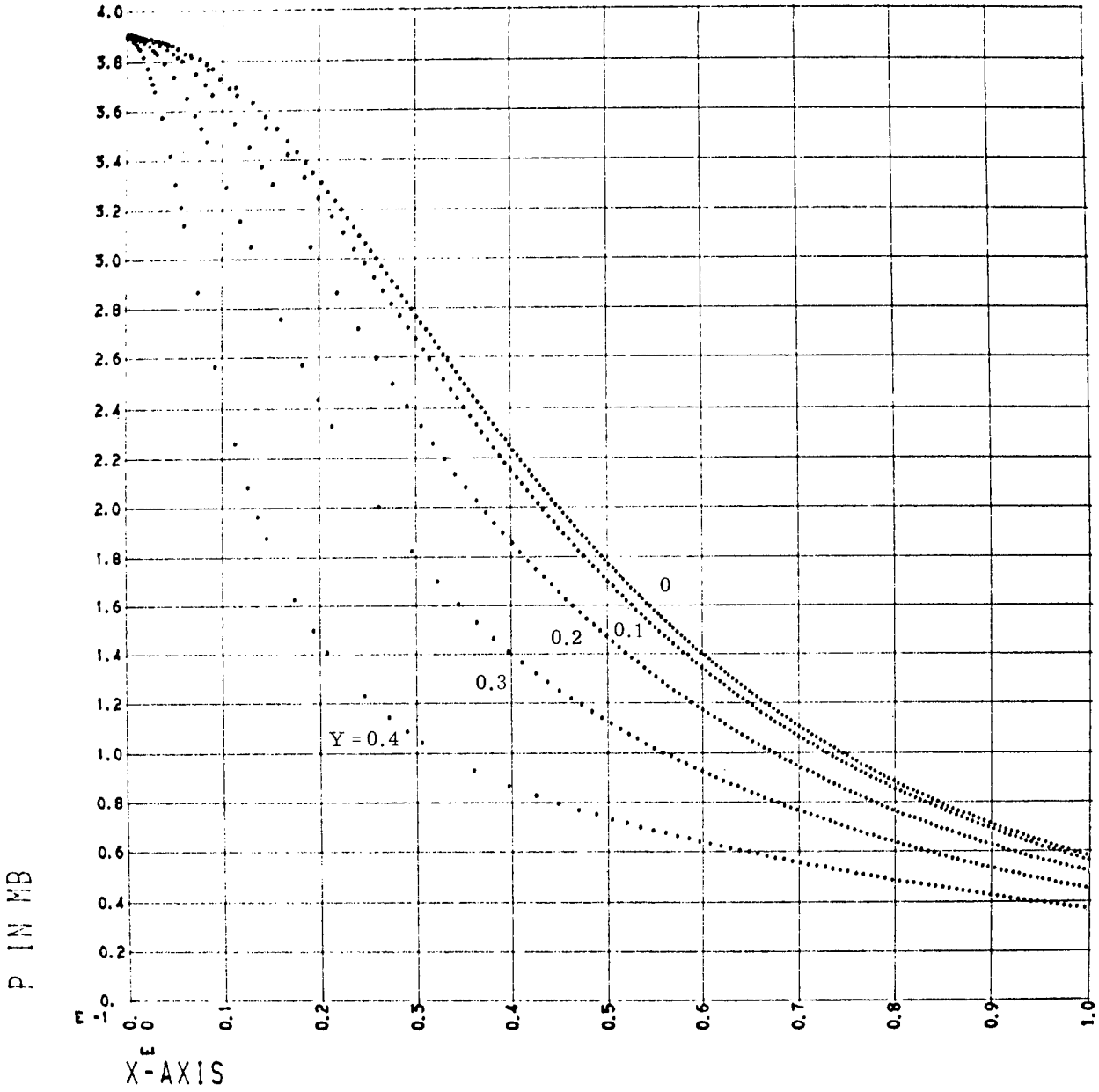

Fig. 4. Pressure profiles at various distances from the centerline of the H. E. as a function of the distance from the front in units of the initial slab thickness, for an ideal gas equation of state in plane geometry.

Figures 5, 6, and 7 show pressure in megabars, velocity in the x direction relative to the front, and velocity in the y direction as a function of the distance from the x axis for various distances from the front.

Figure 8 shows constant relative volume contours in the x-y plane.

D. The Program Card Decks

The code name given this program is 2D-STEDET. One basic program was written in FORTRAN for the CDC 3600 high speed computer. There are two versions available and they differ only in output and COMMON statements. Both binary and FORTRAN decks are available along with copies of the compilations. If the decks are desired, they may be obtained by contacting Mark Wilkins.

No attempt was made to optimize the program to achieve rapid calculations or uniform distribution of grid points in the x, y plane. This, of course, could be done. Anyone desiring to use the program will find the following comments of interest.

2D-STEDET

The program allows for a $\gamma \geq 2.6535795$ and gives as output along each j and k curve:

P = pressure,
VOL = relative volume,
E = internal energy in units of original volume,
U = velocity in the x direction relative to the front,
V = velocity in the y direction,
B = parameter on Γ^+ and Γ^-,
WPOS = generating parameter for Γ^+,
WNEG = generating parameter for Γ^-,
X = distance from the front,
Y = distance from the centerline of H. E.,
ULB = maximum value of B on each k line.

In addition there are linear interpolation routines which were put in to get information needed to show the variations along constant X, Y, and VOL lines. The first routine prints out P and X for Y = .1, .2, .3, .4. The second prints out U, V, P, D-U = UPRI, and Y for X = .25, .50, .75, 1.0. The third prints out X and Y for VOL = .8, .9, 1.0, 1.1, 1.2, 1.3, 1.4, 1.5, 1.6, 1.7, 1.8.

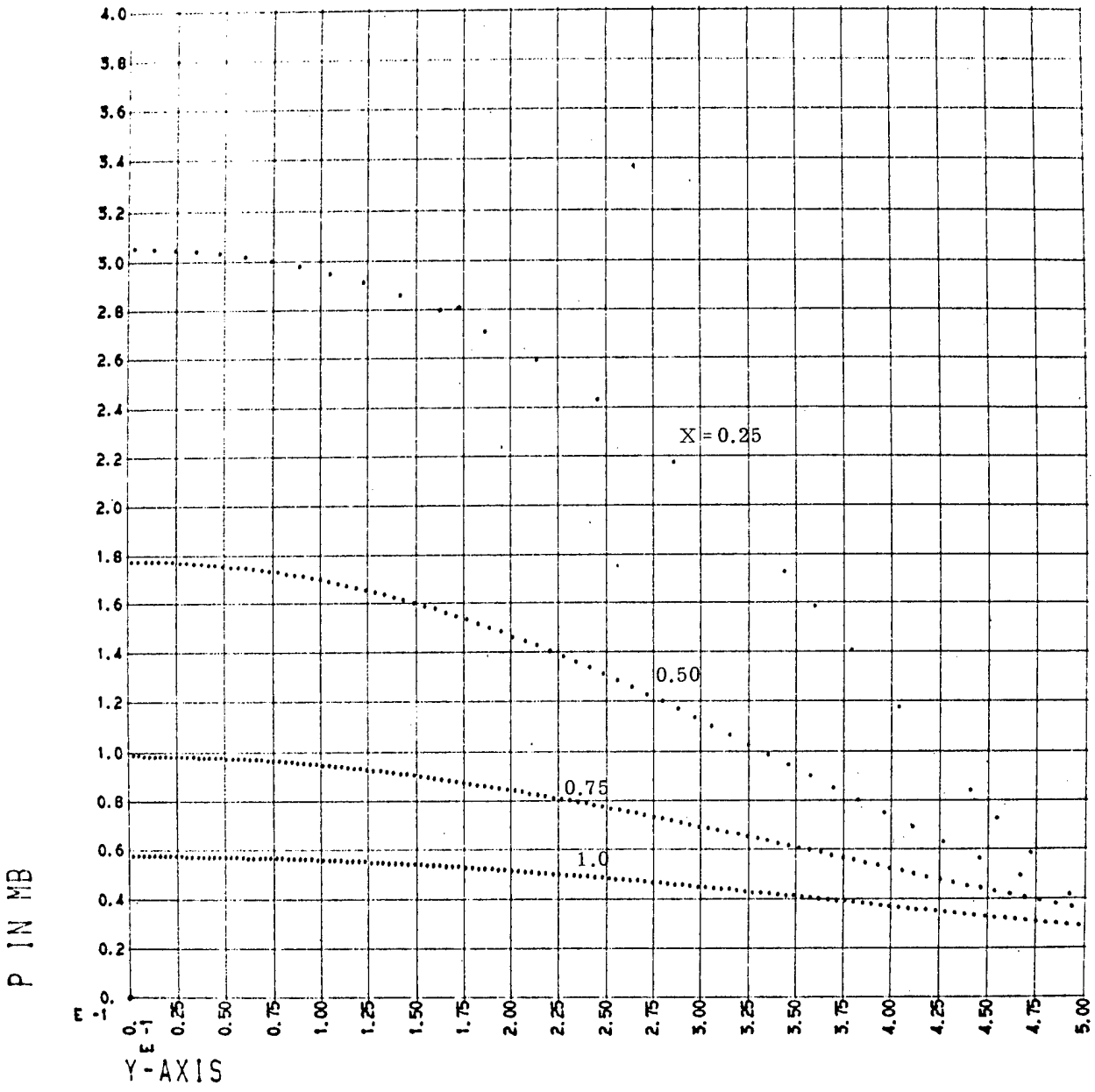

Fig. 5. Pressure as a function of distance from the centerline of the H. E. for various distances from the front in units of the initial slab thickness, for an ideal gas equation of state in plane geometry.

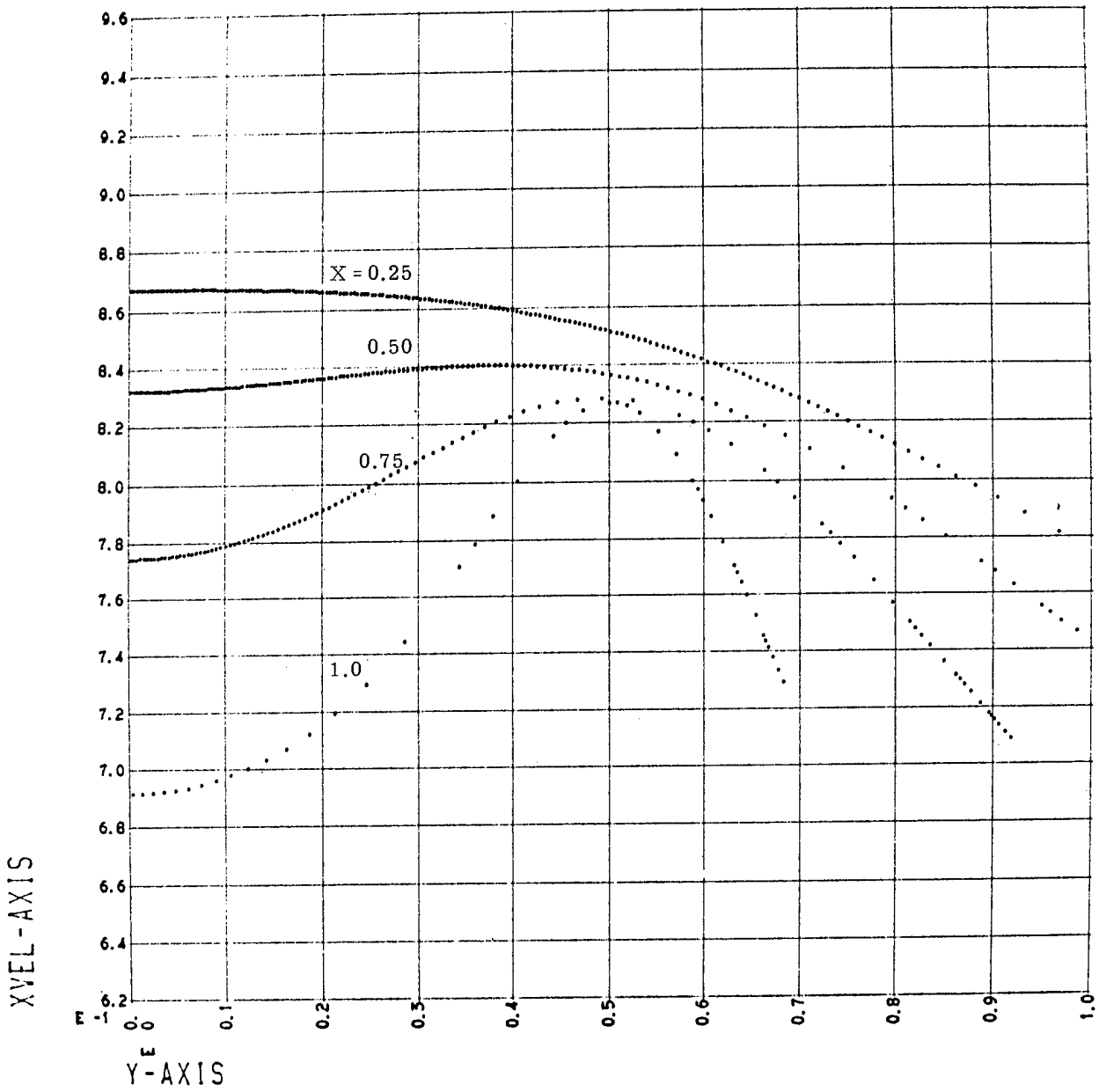

Fig. 6. Velocity normal to the front as a function of distance from the centerline of the H. E. for various distances from the front in units of the initial slab thickness, for an ideal gas equation of state in plane geometry.

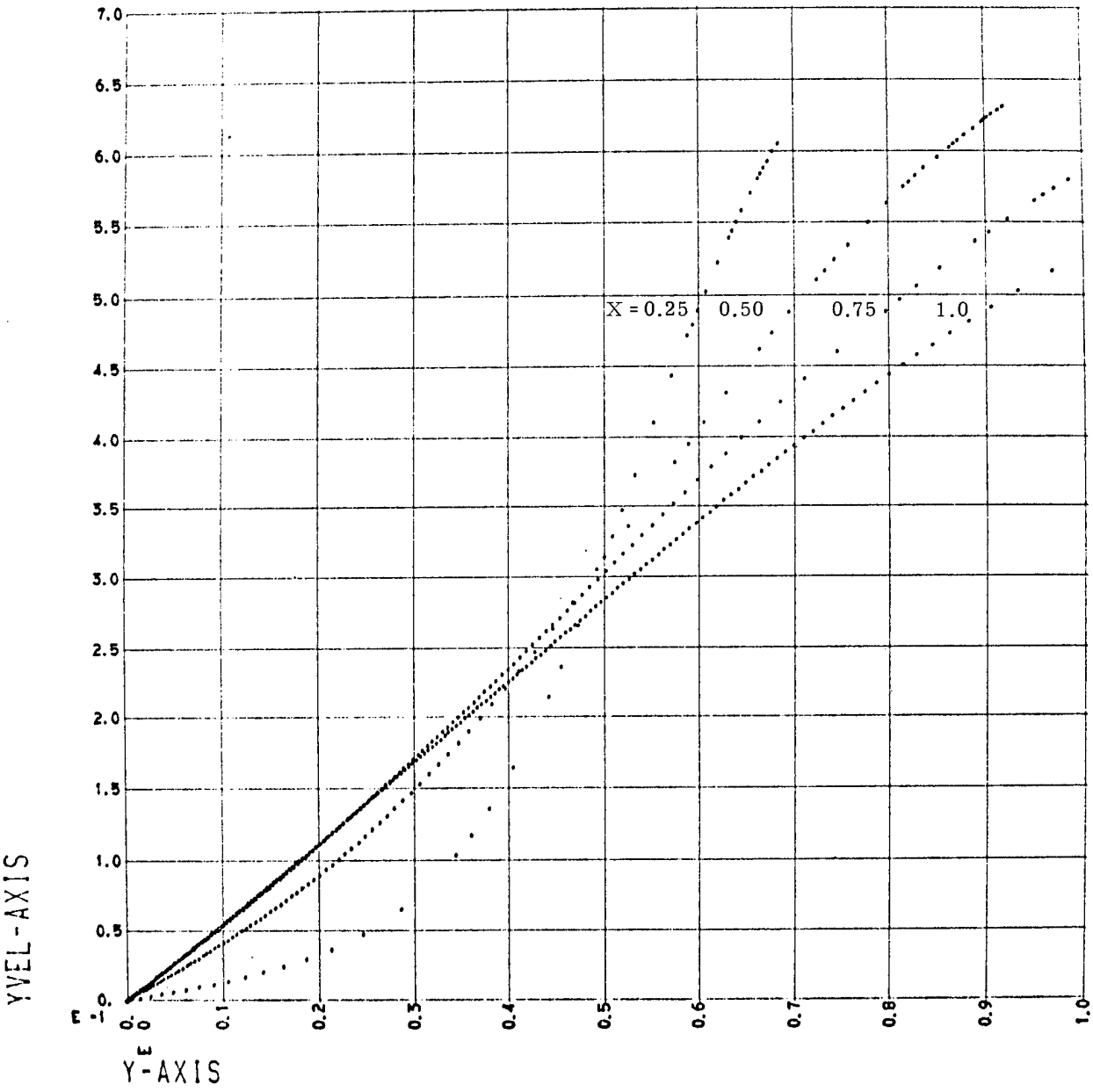

Fig. 7. Velocity parallel to the front as a function of distance from the centerline of the H. E. for various distances from the front in units of the initial slab thickness, for an ideal gas equation of state in plane geometry.

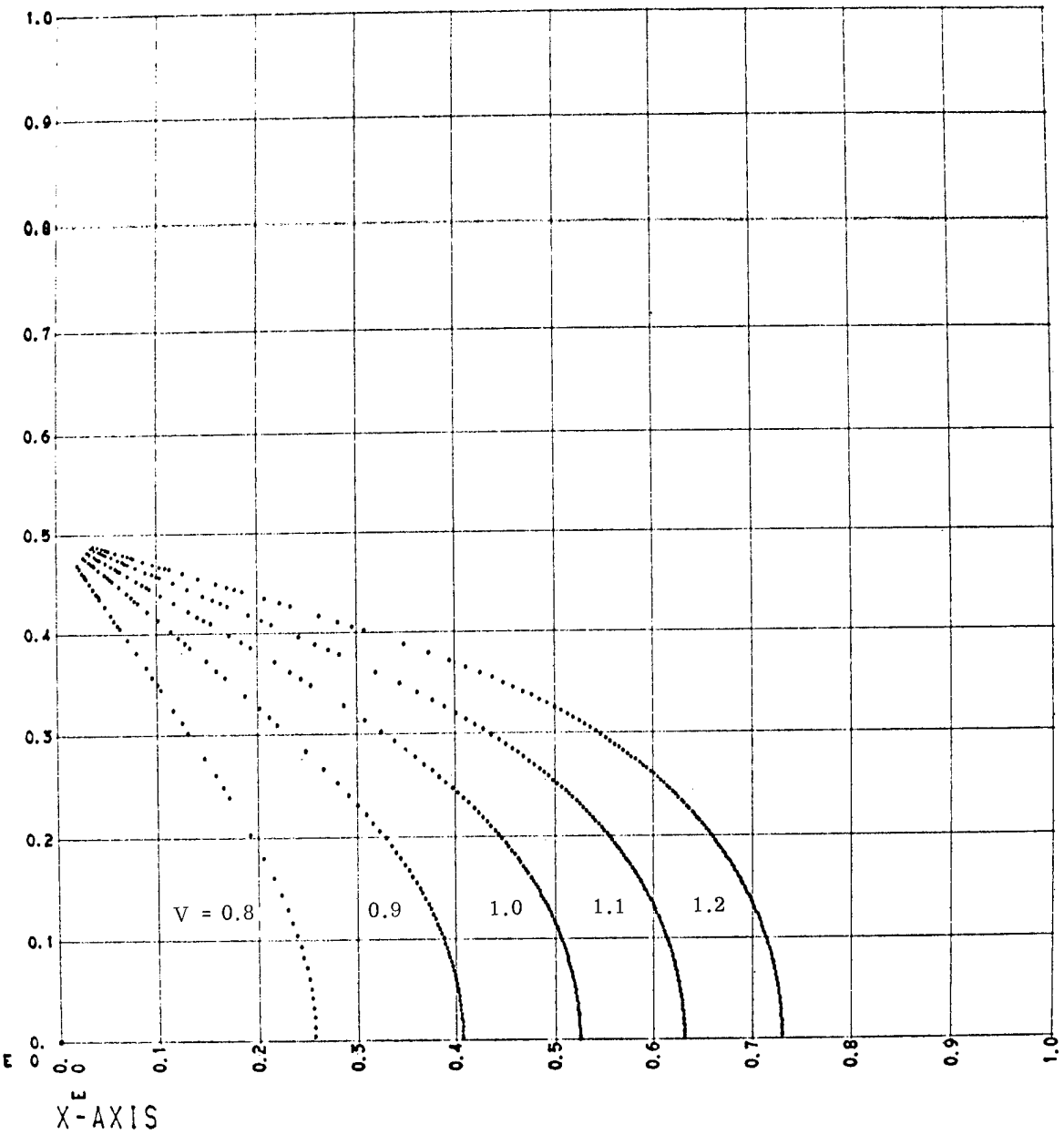

Fig. 8. Constant relative volume contour curves for the ideal gas equation of state in plane geometry.

With ΔW = DELWS = 0.01745 this takes about 20 minutes to run to completion.

2D-STEDET W/OOP

The program was set up to run with $\gamma \geq 2.6535795$ and $\Delta W = 0.008725$. If $\Delta W = 0.01745$, a smaller γ would be possible (see below). This program differs from 2D-STEDET in that the first set of output (P, VOL, etc.) is printed out only at WPOS = 0.01745 and WPOS = 0.1745 for each j, and in addition to the interpolation, prints out P, D-U, and X for Y = 0.

With $\Delta W = 0.008725$ this takes about 6 minutes to run to completion.

General Comments

In either program if sense switch 1 (SS1) is depressed, the problem will come off after completion of calculations along a k-line. The on-line printer will give the k-line number just calculated and the maximum number of k-lines, and will indicate "PROBLEM FINISHED" after the output data has been written on the output tape. Everything calculated to that point is printed out but the problem must be resubmitted if the complete calculation is desired.

The size of the region in the U, V plane is dependent on γ but the grid spacing is constant or at least dependent on an unrelated input quantity DELWS. As a result, a change in γ results in a change in the number of grid lines. The number of j-lines is determined as follows:

$$j_{max} \leq \frac{\pi\left(\frac{1}{\mu} - 1\right)}{0.2*\text{DELWS}} + 29, \quad \mu^2 = \frac{\gamma - 1}{\gamma + 1} .$$

In 2D-STEDET j_{max} should not exceed 600 and in 2D-STEDET W/OOP j_{max} should not exceed 1200.

If the program were to be used often, it would be advisable to establish a fixed number of grid lines with a grid spacing dependent only on γ. As it is, if a problem is to be run where j_{max} is too large, the COMMON statements in the FORTRAN deck will have to be changed. Care must be taken in this case since 2D-STEDET W/OOP currently uses about 45,000 words of memory in the CDC 3600.

To run a problem with one of the binary decks one needs only to put a *ID card in front of the deck followed by a *XEQ card, the binary deck, a *DATA card, and three input cards. The input cards must be in the F10.7 format and in the following order:

Card 1:

DELWS, YSTRT = half, thickness of H. E., XSTRT = 0., WSTRT = 0., YM = 0., ULA = 0.001

Card 2:

GAMMA = γ, SPEED = D = detonation velocity, ROE = ρ_0 = reference density of the H. E.

Card 3:

CY1 = 0.1, XC1 = 0.25, CVOL1 = 0.8

The three input quantities on Card 3 are used to activate the interpolation routines. CY1 gives P and X for a fixed Y; XC1 gives U, V, P, D-U = UPRI, and Y for a fixed X, CVOL1 gives X and Y for a fixed VOL. If any of these is not desired, then the corresponding activation number (CY1, etc.) should be put on Card 3 as a "0." since the program is set to bypass for that value.

2D-STEDET W/OOP PLUS PLOT

This program is the same as 2D-STEDET W/OOP except that a plot routine has been added which will plot the output obtained from the interpolation routine plus every twentieth Γ^+ and C^+ curve. The Γ^+ curves start with k = 1 while the C^+ curves start with k = 2. The plot routine can be bypassed completely or the Γ^+ and C^+ curves may be left out in addition to the bypass already available for the interpolation routines.

To use this program with a binary check an additional card is required in the I10 format:

Card 4:

IPLOT = IA, IPLOT1 = IB

If IA = 0 and IB = 0, no plot results.

If IA = 1 and IB = 0, C^+ and Γ^+ are not plotted.

If IA = 1 and IB = 1, C^+ and Γ^+ are plotted and the interpolation curves are calculated and plotted according to the data on Card 3.

An example of these plots is shown in Figs. 2-8.

II. A PLANE TWO-DIMENSIONAL DETONATION FOR AN EXPLOSIVE WITH A "WILKINS"[2] EQUATION OF STATE

Introduction

In parts A through D below is presented the solution of a plane two-dimensional steady-state detonation of an explosive with a "Wilkins-type" equation of state employing the method of characteristics. Part A gives an outline of the derivation of the basic equations; part B gives a description of the numerical method used; part C describes the example problem solved; and part D gives a description of the program card decks available.

A. Calculation of the Two-Dimensional Steady-State Detonation for an Explosive Having a "Wilkins" Equation of State

The equation of state used here is that given in ref. 4. The basic equations of motion are the same as those in section I, part A, Eq. (1). The difference comes in Eq. (2), section I, part A, which is replaced by (see appendix 9):

$$u^2 + v^2 + 2\int_{s_0}^{s_1} \frac{a^2}{\rho}\, d\rho = \text{const.} \tag{1}$$

By definition $a^2 = \left.\frac{\partial p}{\partial \rho}\right|_{\eta}$, and from the Wilkins equation of state:

$$a^2 = \frac{1}{\rho_0}\left[\frac{AQ}{V^{Q-1}} + BR\, V^2 e^{-RV} + \frac{(1+\omega)C_s}{V^{\omega}}\right] . \tag{2}$$

When (2) is substituted in (1):

$$u^2 + v^2 + \frac{2}{\rho_0}\left[\frac{AQ}{(Q-1)V^{Q-1}} + B\left(V + \frac{1}{R}\right)e^{-RV} + \frac{(1+\omega)C_s}{\omega V^{\omega}}\right] = \text{const.} \tag{3}$$

The constant in (3) can be evaluated at the detonation front where $v = 0$, $u = a_{c\text{-}j}$, $V = V_{c\text{-}j}$. This implies that through (3) the relative volume (V) is a function of u and v and, since $a^2 = a^2(V)$, that a is a function of u and v. Hence, the hodograph transformation can be made for this set of equations just as in section I, part A, and in fact all the results through appendix 5 are unaffected. Hence, we have:

$$\Gamma^+: \quad v_\alpha = \tan\psi^+ \, u_\alpha \,,$$

$$C^+: \quad y_\alpha = -\frac{1}{\tan\psi^-} x_\alpha \,, \tag{4}$$

$$\Gamma^-: \quad v_\beta = \tan\psi^- \, u_\beta \,,$$

$$C^-: \quad y_\beta = \frac{-1}{\tan\psi^+} x_\beta \,.$$

The problem from here is different. The solution for Γ^+ and Γ^- cannot be found in closed form as in section I, but a numerical integration must be performed to obtain the values of ψ^+ and ψ^-, the slopes of the tangents of Γ^+ and Γ^- respectively (see appendix 10). Having determined these parameters, the equations for C^+ and C^- can be used to determine x and y. Otherwise, the solution is very similar to the ideal gas equation of state problem.

B. Numerical Method

Referring again to Fig. 1c, the equations (4) of part A, section I, can be put in difference form as:

$$Y_{j+1,\,k+1} - Y_{j,\,k+1} = \frac{-1}{TF2}\,(X_{j+1,\,k+1} - X_{j,\,k+1}),$$

$$Y_{j+1,\,k+1} - Y_{j+1,\,k} = \frac{-1}{TF1}\,(X_{j+1,\,k+1} - X_{j+1,\,k}), \tag{1}$$

which, when solved for $X_{j+1,\,k+1}$, $Y_{j+1,\,k+1}$, yield:

$$Y_{j+1,\,k+1} = \frac{X_{j,\,k+1} - X_{j+1,\,k} + TF2\,Y_{j,\,k+1} - TF1\,Y_{j+1,\,k}}{TF2 - TF1}, \tag{2}$$

$$X_{j+1,\,k+1} = X_{j+1,\,k} + TF1\,(Y_{j+1,\,k} - Y_{j+1,\,k+1}),$$

where

$$TF1 = \tan\frac{1}{2}\left(\psi^+_{j+1,\,k+1} + \psi^+_{j+1,\,k}\right), \tag{3}$$

$$TF2 = \tan\frac{1}{2}\left(\psi^-_{j+1,\,k+1} + \psi^-_{j,\,k+1}\right).$$

The equations involving u and v are solved in appendix 10 and yield the following:

$$\psi^+ = -\int_{V_*}^{V} F(v)dV + \psi^+_*,$$

$$\psi^- = \int_{V_*}^{V} F(v)dV + \psi^-_*, \tag{4}$$

where

$$F(v) = \frac{\frac{1}{2}\frac{da^2}{dV} - \frac{a^2}{V}}{ga} \tag{5}$$

and g, a, a^2 are all known functions of V.

In order to begin the solution it is necessary to integrate (4) which is an improper integral. Using the knowledge gained in section I, it is seen that the Γ^+ curve corresponding to the uppermost point on the detonation front (Γ^+_0) has $\psi^+_* = 0$ and $V_* = V_{c\text{-}j}$. At $V = V_{c\text{-}j}$, $g = 0$ and hence care must be taken with (4). The evaluation procedure consisted of three steps: (1) the integral was shown to exist for $V_* = V_{c\text{-}j}$ in appendix 10, (2) an estimate of ψ^+ for a value of V slightly greater than $V_{c\text{-}j}$ (0.7263 for PBX 9404 and 0.731575 for LX-04-01) was obtained by fixing the upper limit and varying the lower limit toward $V_{c\text{-}j}$ as far as possible and then extrapolating to $V_{c\text{-}j}$, (3) and finally, the value of this first ψ^+ was arbitrarily varied to give a positive value of the y-velocity (v) which is required physically. The latter was possible because the other quantities calculated were not very sensitive to small changes in the small first value of ψ^+. The integration was performed using the subroutine ROMBRG.[5]

With this first value of ψ^+ calculated, arbitrary values of V were assigned up to V = 10 and ψ^+ was calculated for each V from (4). Equation (15), appendix 10 , was then used to calculate ψ^- for each V. This gives everything on Γ^+_0 since x and y are constant along this curve as shown in section I.

The value of V_* for the next Γ^+ curve is found using equation (18), appendix 10, and calculating ψ^+_* and ψ^-_* from equations (16) and (17), appendix 10. Equation (19), appendix 10, is used to calculate V for succeeding points on this Γ^+ curve, and then equation (15) is used to calculate ψ^-. Equations (13), appendix 10, was used to calculate u and v and equations (14) and (16) in UCRL-7797 (reproduced below) were used to calculate p and E. With

values of ψ^+, ψ^-, a, g on two k lines, X and Y can be calculated from (2) above. The process is then repeated for the next k line.

$$p(V) = \frac{A}{V^Q} + BC^{-RV} + \frac{C_s}{V^{1+\omega}} ,$$

$$E(V) = \frac{p(V)V}{\omega} - \frac{C}{\omega V^{Q-1}} - \frac{B\left(V - \frac{\omega}{R}\right)}{\omega} e^{-RV} ,$$

where C, A, B, R, C_s, w are constants defined in part D below.

C. Example Problem

As an application the same problem was solved as that discussed in section I. The results are shown in Figs. 9-15.

Figure 9 shows some Γ^+ curves.

Figure 10 shows some C^+ curves.

Figure 11 shows pressure in megabars as a function of the distance from the front expressed in units of the original thickness for various values of y. Table 2, appendix 11, lists output from which this figure was plotted.

Figures 12, 13, 14 show pressure in megabars, velocity in the x direction relative to the front, and velocity in the y direction as a function of the distance from the x axis for various distances from the front.

Figure 15 shows constant relative volume contours in the x, y plane.

D. The Program Card Decks

The code name given to this program is 2D-STEDET – W/WEOS. One program was written in FORTRAN for the CDC 3600 high speed computer. Both binary and FORTRAN decks are available along with copies of the compilations. If the decks are desired, they may be obtained by contacting Mark Wilkins. As in the ideal gas equation of state case, no attempt was made to "tidy up" the program.

The output available consists of:

SCJ = Chapman-Jouguet sound speed,
D = constant in equation (3), appendix 10,
V = relative volume,
XVEL = velocity in the x direction relative to the front,
YVEL = velocity in the y direction,

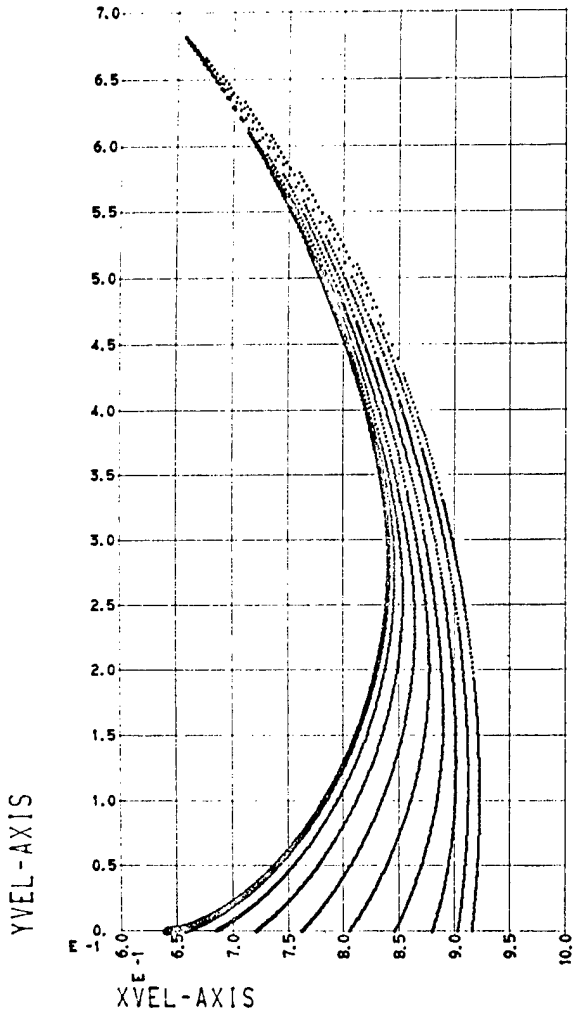

Fig. 9. Γ^+ characteristics for the Wilkins equation of state in plane geometry.

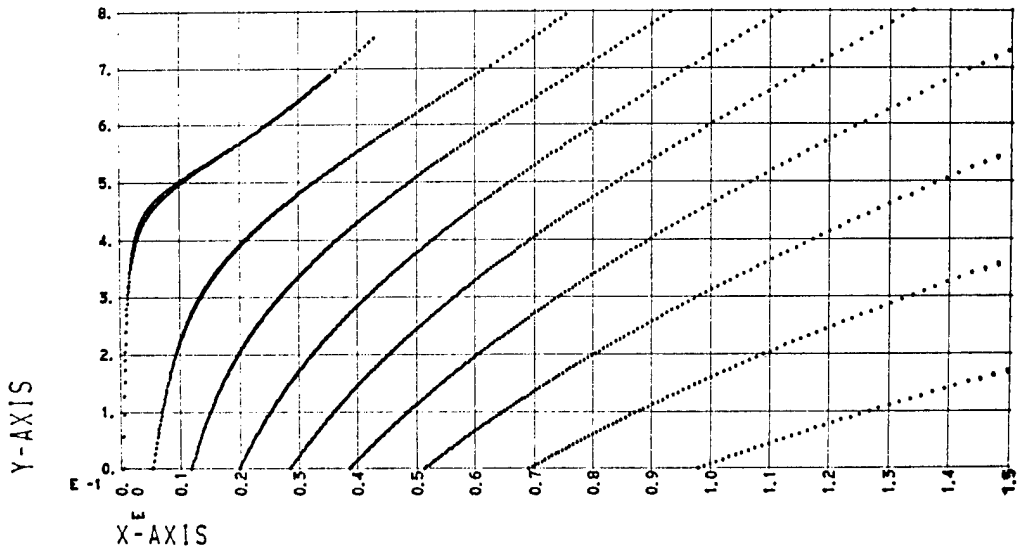

Fig. 10. C^+ characteristics for the Wilkins equation of state in plane geometry.

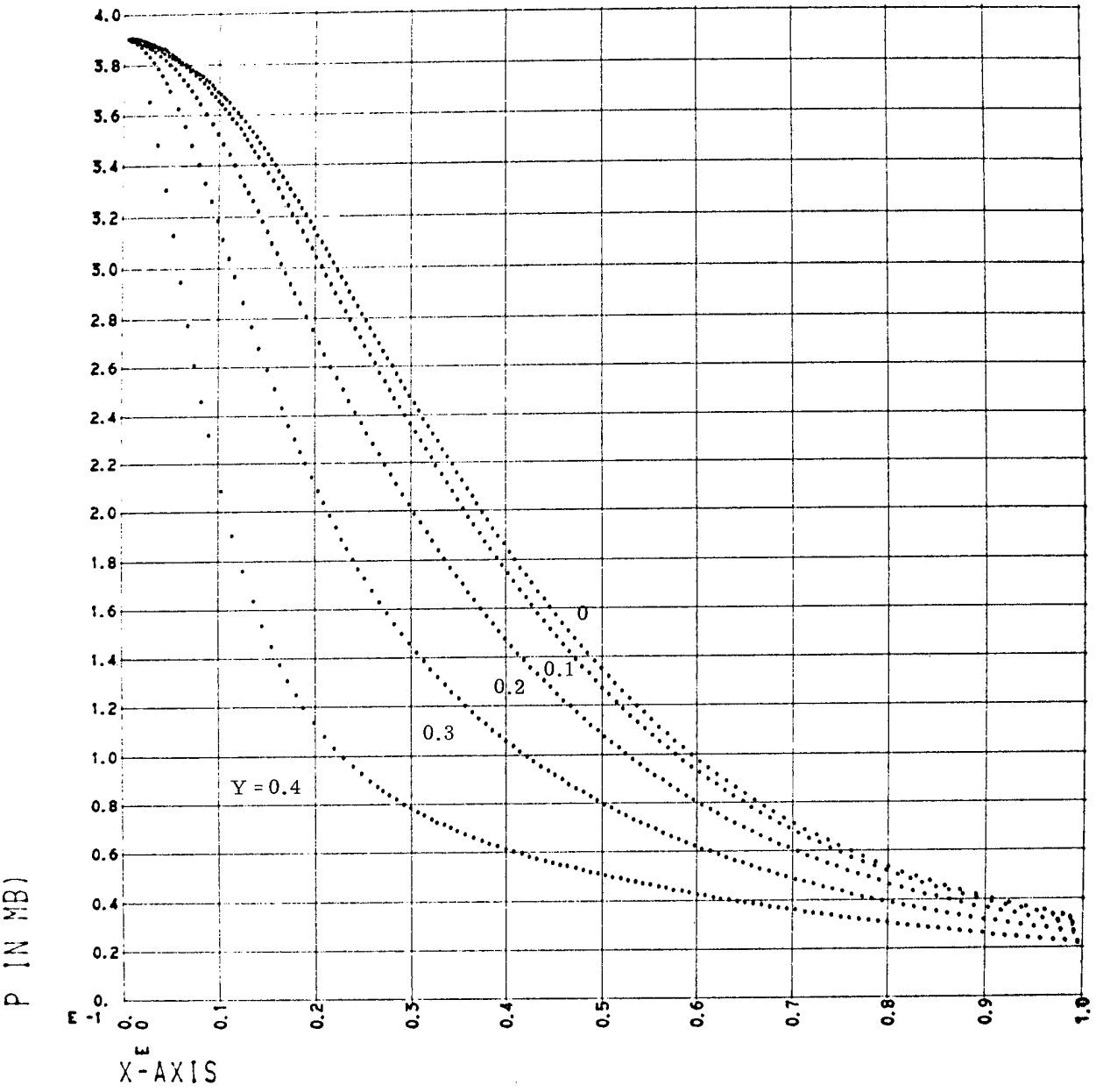

Fig. 11. Pressure profiles at various distances from the centerline of the H. E. as a function of distance from the front in units of the initial slab thickness, for the Wilkins equation of state in plane geometry.

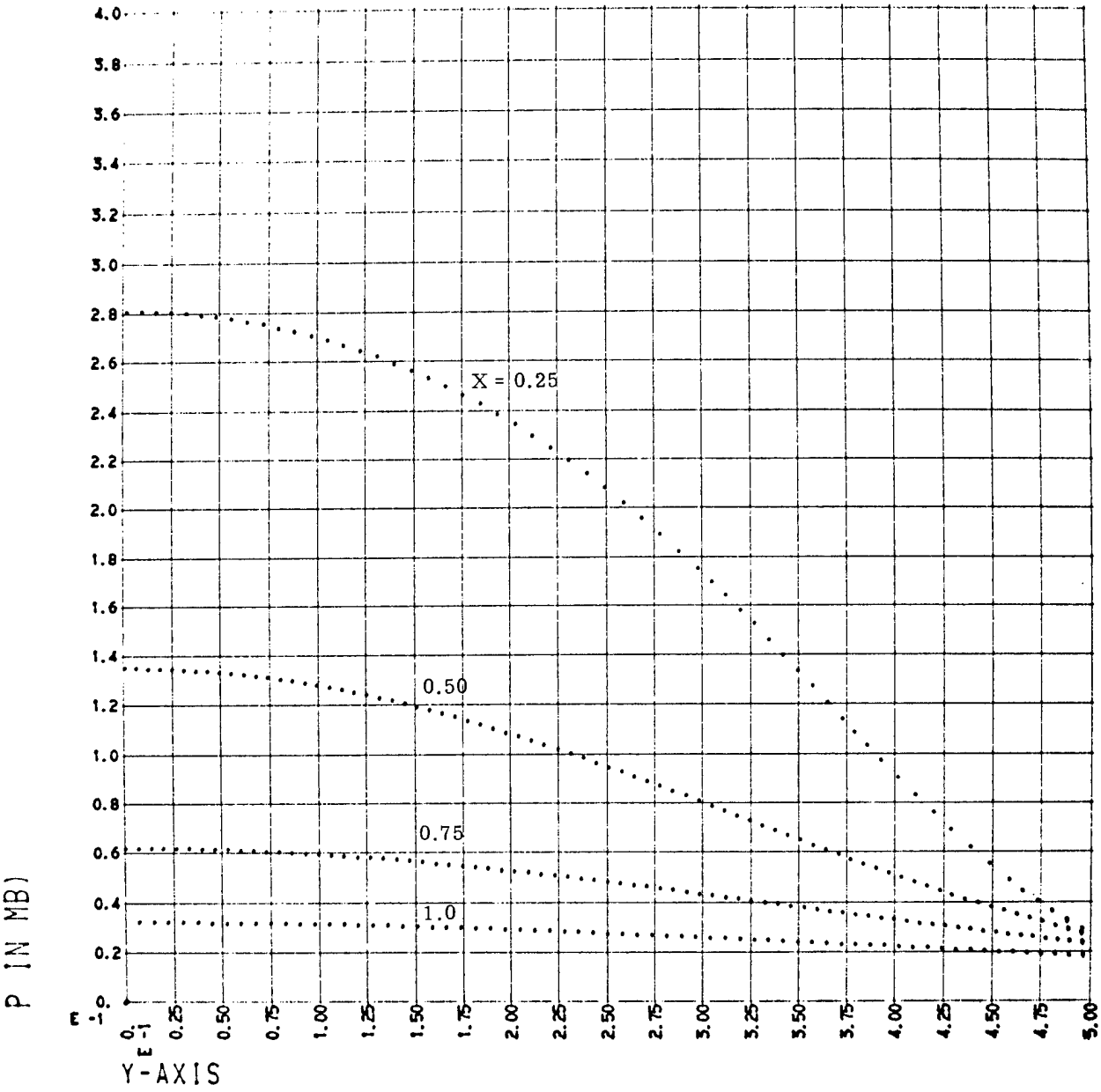

Fig. 12. Pressure as a function of distance from the centerline of the H. E. for various distances from the front in units of the initial slab thickness, for the Wilkins equation of state in plane geometry.

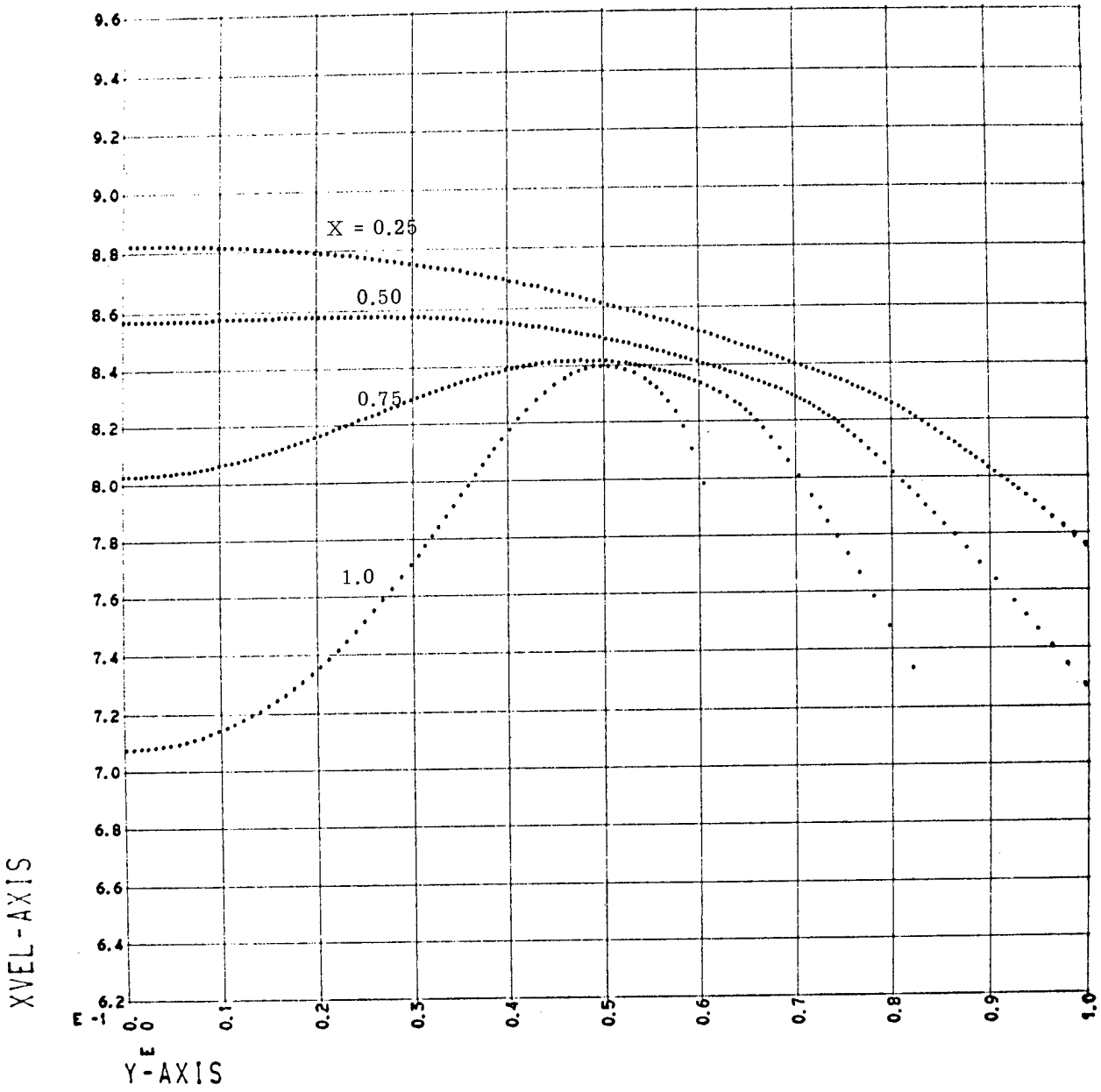

Fig. 13. Velocity normal to the front as a function of distance from the centerline of the H. E. for various distances from the front in units of the initial slab thickness, for the Wilkins equation of state in plane geometry.

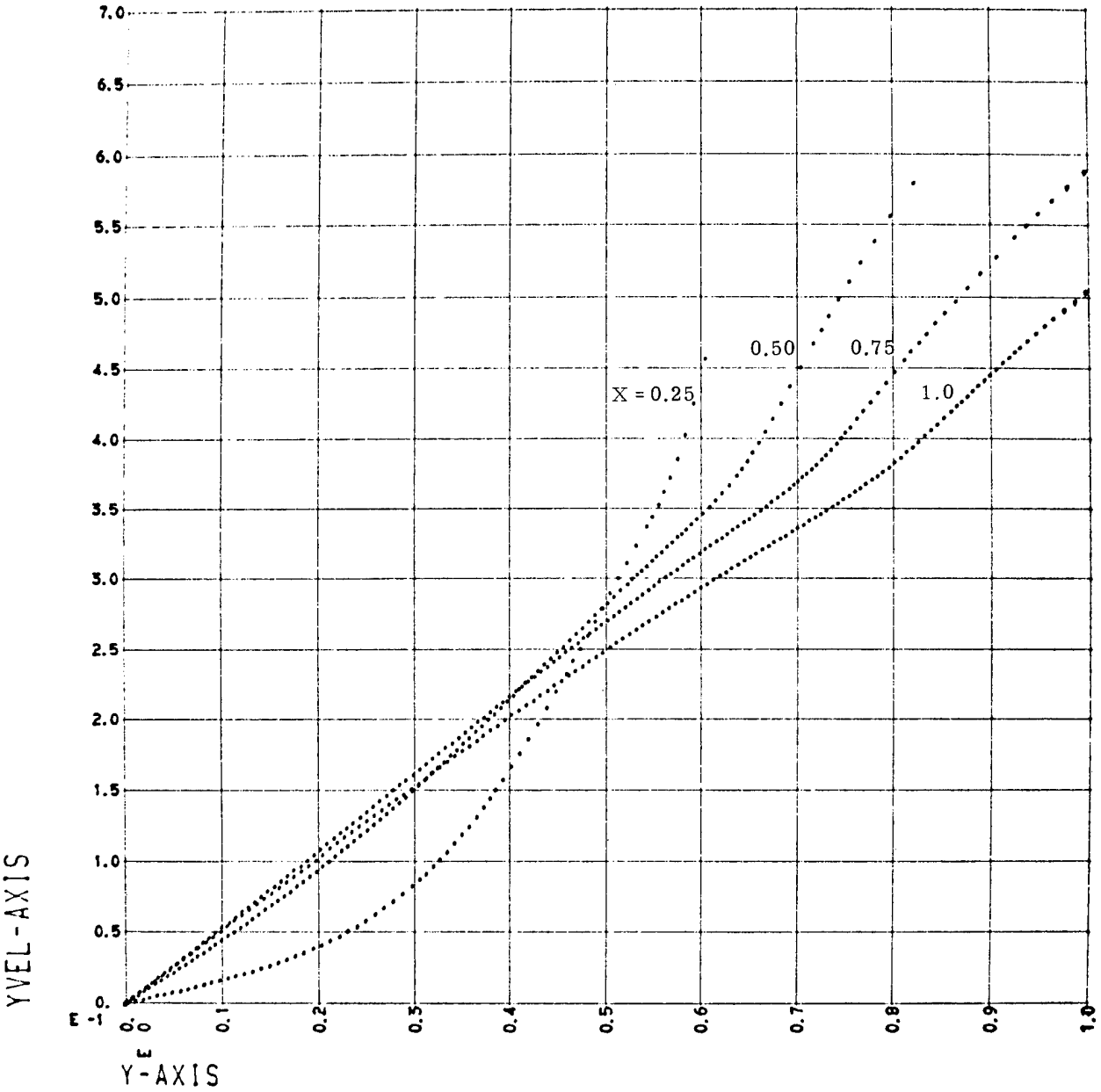

Fig. 14. Velocity parallel to the front as a function of distance from the centerline of the H. E. for various distances from the front in units of the initial slab thickness, for the Wilkins equation of state in plane geometry.

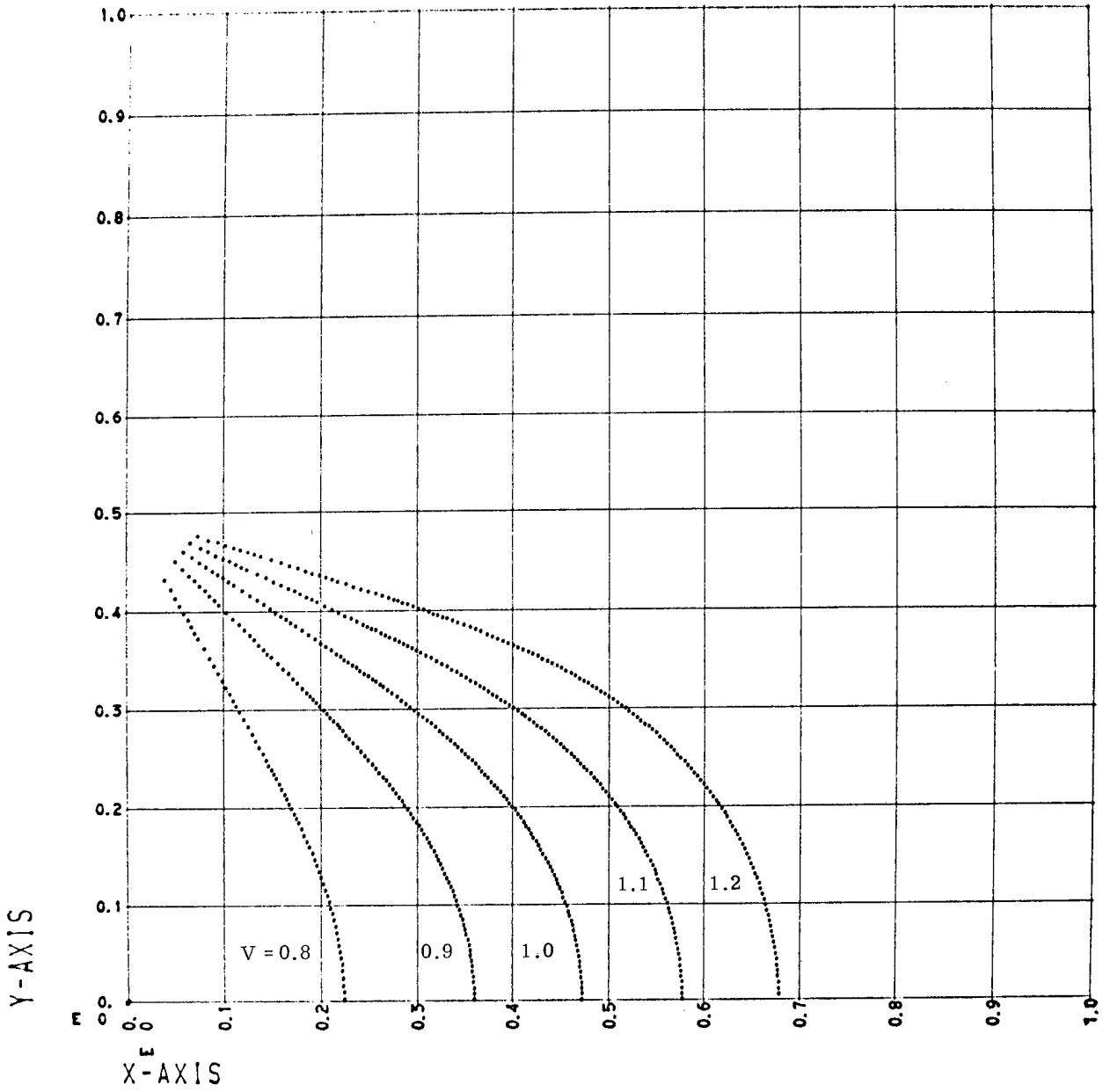

Fig. 15. Constant relative volume contour curves for the Wilkins equation of state in plane geometry.

P = pressure,

E = internal energy in units of the original volume,

PSIP = angle ψ^+ made by Γ^+ with v = 0,

PSIN = angle ψ^- made by Γ^- with v = 0,

X = distance from front,

Y = distance from centerline of H. E.,

UPRI = velocity in the x direction,

U = XVEL.

In addition there is a linear interpolation routine exactly like that described for 2D-STEDET W/OOP PLUS PLOT.

To run a problem with one of the binary decks one needs only to put a *ID card and a *XEQ in front of the deck, the binary deck, a *DATA card, and five input cards. These cards are:

Card 1: 5F 10.7 format

C, Q, R, B, W

The five quantities are the constants a, Q, R, B, ω that appear as equation (15) in UCRL-7797.

Card 2: 5F 10.7 format

ROE, CS, VCJ, SPEED, YSTRT

These five quantities are:

ρ_0 = ROE = reference density of the H. E.,

CS = C_s = the constant referred to at the top of page 12 in UCRL-7797,

VCJ = Chapman-Jouguet reference volume,

SPEED = detonation velocity,

YSTRT = half-thickness of the H. E.

Card 3: 3F 10.7 format

CY1 = 0.1, XC1 = 0.25, CV1 = 0.8

Card 4: 3I 10 format

ISTRT = IC, IPRT1 = ID, IPRT2 = IE

where:

IC = 0 for PBX 9404,

IC = 1 for LX-04-01,

ID = 1 yields printout of XVEL, YVEL, P, E, V for each j, k,

ID = 0 yields no printout of XVEL, YVEL, P, E, V,

IE = 1 yields printout of X, Y, V for each j, k,

IE = 0 yields no printout of X, Y, V.

Card 5: 2I 10 format

IPLOT, IPLOT1 (See explanation for 2D-STEDET W/OOP PLUS PLOT)

This program will run a problem for either PBX 9404 or LX-04-01. The data required for each is:

PBX 9404	LX-04-01
C = -0.004563	C = -0.0008335
Q = 4.0	Q = 4.0
R = 4.0	R = 4.0
B = 6.572	B = 5.943
W = 0.35	W = 0.4
ROE = 1.84	ROE = 1.865
CS = 0.032	CS = 0.029
VCJ = 0.7262958	VCJ = 0.7315694
SPEED = 0.88	SPEED = 0.848
ISTRT = 0	ISTRT = 1

III. A CYLINDRICAL TWO-DIMENSIONAL DETONATION FOR AN EXPLOSIVE WITH A "WILKINS" EQUATION OF STATE

Introduction

In parts A through D below is presented the solution of a cylindrical two-dimensional steady-state detonation of an explosive with a "Wilkins" equation of state employing the solution to the plane problem discussed in section II to start the solution, and then employing the method of characteristics for the cylindrical problem from there on. Part A gives an outline of the derivation of the basic equations governing the motion; part B gives a description of the numerical method used; part C describes the example problem solved; and part D describes the program card decks available.

A. Calculation of a Steady-State Detonation in Cylindrical Coordinates for an Explosive with a "Wilkins" Equation of State

In considering the cylindrical case it is only necessary to note that there is no change in the basic derivation given in section II except that the conservation of mass equation is altered to:

$$v \frac{\partial \rho}{\partial y} + u \frac{\partial \rho}{\partial x} + \rho \frac{\partial v}{\partial y} + \rho \frac{\partial u}{\partial x} = - \rho \frac{v}{y} \tag{1}$$

where $x \equiv$ coordinate along the axis of the cylinder,

$y \equiv$ coordinate normal to the axis of the cylinder,

and it is assumed that there is no rotation about the axis. The other conservation equations and Bernoulli's equation remain the same.

Following the same procedure used in section II, the set of equations to be solved is:

$$\begin{aligned} &(a^2 - u^2) \frac{\partial u}{\partial x} - uv \frac{\partial v}{\partial x} - uv \frac{\partial u}{\partial y} + (a^2 - v^2) \frac{\partial v}{\partial y} = - \frac{a^2 v}{y}, \\ &0 \frac{\partial u}{\partial x} + \frac{\partial v}{\partial x} - \frac{\partial u}{\partial y} + 0 \frac{\partial v}{\partial y} = 0 . \end{aligned} \tag{2}$$

Due to the presence of the term $- \frac{a^2 v}{y}$ on the right of (2), the hodograph transformation used in section I will no longer yield a set of uncoupled equations in characteristic velocity space. The derivation of the characteristic equations in the x, y plane, however, follows the same procedure but this time the vector

$$\underset{\sim}{C} = \left[-\frac{a^2 v}{y} \quad 0\right]. \tag{3}$$

With this value of $\underset{\sim}{C}$, a straightforward application of the technique followed in appendix 2 yields:

$$C_1: \left.\frac{dy}{dx}\right|_{\alpha} = \frac{uv - a\sqrt{u^2 + v^2 - a^2}}{u^2 - a^2} \tag{4}$$

along which

$$\left.\frac{du}{dx}\right|_{\alpha} + \left(\frac{uv + a\sqrt{u^2 + v^2 - a^2}}{u^2 - a^2}\right)\left.\frac{dv}{dx}\right|_{\alpha} = \left.\frac{a^2 v}{y(u^2 - a^2)}\right|_{\alpha},$$

and

$$C_2: \left.\frac{dy}{dx}\right|_{\beta} = \frac{uv + a\sqrt{u^2 + v^2 - a^2}}{u^2 - a^2} \tag{5}$$

along which

$$\left.\frac{du}{dx}\right|_{\beta} + \left(\frac{uv - a\sqrt{u^2 + v^2 - a^2}}{u^2 - a^2}\right)\left.\frac{dv}{dx}\right|_{\beta} = \left.\frac{a^2 v}{y(u^2 - a^2)}\right|_{\beta}.$$

In addition, the following relations from section II obtain:

$$a^2 = \frac{1}{\rho_0}\left[\frac{AQ}{V^{Q-1}} + BRV^2 e^{-RV} + \frac{(1+\omega)C_s}{V^{\omega}}\right], \tag{6}$$

$$q^2 = u^2 + v^2 = D - \frac{2}{\rho_0}\left[\frac{AQ}{(Q-1)V^{Q-1}} + B\left(V + \frac{1}{R}\right)e^{-RV} + \frac{(1+\omega)C_s}{\omega V^{\omega}}\right], \tag{7}$$

and

$$D = a^2_{c\text{-}j} + \frac{2}{\rho_0}\left[\frac{AQ}{(Q-1)V^{Q-1}_{c\text{-}j}} + B\left(V_{c\text{-}j} + \frac{1}{R}\right)e^{-RV_{c\text{-}j}} + \frac{(1+\omega)C_s}{\omega V^{\omega}_{c\text{-}j}}\right]. \tag{8}$$

In order to start the solution, it is assumed that "near" the front (small x) the solution is approximately the same as that for the plane case, and hence, approximate values of u, v, V and therefore p, a, E at specified values of y on an x line "near" the front can be obtained from the solution with 2D-STEDET W/WEOS as described in section II. This assumption appears reasonable for a sufficiently small x, but no attempt has been made

to check the assumption or even to vary the value of the "small x," due to lack of time. The program was written with the latter in mind, and it could easily be done.

In order to solve equations (4) and (5), use is made of the fact that along the x axis, $y = 0$ and $v = 0$. Since the term v/y occurs in (2), one cannot simply set y and v to zero in (4) and (5). Taking the limit of the first of (2) as y and v tend to zero yields:

$$(a^2 - u^2)\frac{\partial u}{\partial x} - 0\frac{\partial u}{\partial y} - 0\frac{\partial v}{\partial x} + a^2\frac{\partial v}{\partial y} = -a^2\frac{\partial v}{\partial y}, \tag{9}$$

since v/y is, in fact, $(v - 0)/(y - 0)$, and as y tends to zero is, by definition, $\frac{\partial v}{\partial y}$. With (9) and the second of (2) in place of (2), the characteristic equations along $y = 0$ are:

$$C_1: \left.\frac{dy}{dx}\right|_\alpha = \frac{-\sqrt{2}\,a}{u^2 - a^2} \tag{10}$$

along which

$$\left.\frac{du}{dx}\right|_\alpha + \frac{\sqrt{2}\,a}{u^2 - a^2}\left.\frac{dv}{dx}\right|_\alpha = 0 \text{ (along } y = 0),$$

and

$$C_2: \left.\frac{dy}{dx}\right|_\beta = \frac{\sqrt{2}\,a}{u^2 - a^2} \tag{11}$$

along which

$$\left.\frac{du}{dx}\right|_\beta - \frac{\sqrt{2}\,a}{u^2 - a^2}\left.\frac{dv}{dx}\right|_\beta = 0 \text{ (along } y = 0).$$

Equations (4) through (8), (10), and (11) along with the equations for p and E from part B, section II, constitute the set of equations required for the solution of the cylindrical steady-state detonation problem.

B. Numerical Method

The numerical procedure is rather straightforward. The idea is to replace the characteristic equations of part A, section III, with difference equations, to use values for all the variables along a selected x = constant line determined from the program described in section II for generating values on an adjacent curve in the "cylindrical region," and to repeat the generating process until the problem is finished. To that end define:

$$\tau^- = \frac{uv - a\sqrt{u^2 + v^2 - a^2}}{u^2 - a^2} \quad \text{in general,}$$

$$\tau^- = \frac{-\sqrt{2}\,a}{u^2 - a^2} \quad \text{on } y = 0, \tag{1}$$

$$\tau^+ = \frac{uv + a\sqrt{u^2 + v^2 - a^2}}{u^2 - a^2} \quad \text{in general,}$$

$$\tau^+ = \frac{\sqrt{2}\,a}{u^2 - a^2} \quad \text{on } y = 0, \tag{2}$$

$$\theta = \frac{a^2 v}{u^2 - a^2} \quad \text{in general,}$$

$$\theta = 0 \quad \text{on } y = 0, \tag{3}$$

$\Delta G = G_i - G_j$ for i, j = 1, 2, or 3 and G = any of the variables x, y, etc. Then the characteristic equations (4), (5), (10), and (11) in part A, section III, become:

$$C^-\text{: } \Delta y = \tau^- \Delta x \text{ along which } \Delta u + \tau^+ \Delta v = \frac{\theta \Delta x}{y},$$

$$C^+\text{: } \Delta y = \tau^+ \Delta x \text{ along which } \Delta u + \tau^- \Delta v = \frac{\theta \Delta x}{y}. \tag{4}$$

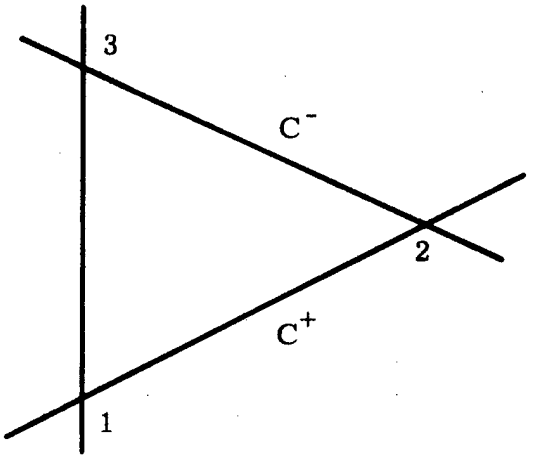

Fig. 16. The general situation.

If Fig. 16 represents the general situation in which all values of the variables concerned are known at points 1 and 3, then the equations (4) can be written as follows:

$$\text{on } C^-: \quad y_2 - y_3 = \frac{1}{2}\,\Sigma_2^-\,(x_2 - x_3)\,, \tag{5}$$

$$u_2 - u_3 + \frac{1}{2}\,\Sigma_2^+\,(v_2 - v_3) = \frac{1}{2}\,\delta_2\,(x_2 - x_3)\,. \tag{6}$$

$$\text{On } C^+: \quad y_2 - y_1 = \frac{1}{2}\,\Sigma_1^+\,(x_2 - x_1)\,, \tag{7}$$

$$u_2 - u_1 + \frac{1}{2}\,\Sigma_1^-\,(v_2 - v_1) = \frac{1}{2}\,\delta_1\,(x_2 - x_1)\,. \tag{8}$$

In these equations,

$$\Sigma_1^p = \tau_2^p + \tau_1^p \text{ with } p = + \text{ or } -, \tag{9}$$

$$\Sigma_2^p = \tau_2^p + \tau_3^p \text{ with } p = + \text{ or } -, \tag{10}$$

$$\delta_1 = \frac{\theta_2}{y_2} + \frac{\theta_1}{y_1}\,, \tag{11}$$

$$\delta_2 = \frac{\theta_2}{y_2} + \frac{\theta_3}{y_3}\,. \tag{12}$$

Equations (5)-(8) constitute a set of equations to be solved for the values at 2, ignoring for the moment the problem of evaluating τ^-, τ^+ and θ at 2. Solving (5) and (7) yields:

$$x_2 = \frac{2(y_3 - y_1) + \Sigma_1^{\pm}\,x_1 - \Sigma_2^-\,x_3}{\Delta_1}\,, \tag{13}$$

and

$$y_2 = y_1 + \frac{1}{2}\,\Sigma_1^{\pm}\,(x_2 - x_1), \tag{14}$$

where

$$\Delta_1 = \Sigma_1^+ - \Sigma_2^-\,, \tag{15}$$

and the value of x_2 from (13) is used in (14). Solving (6) and (8) yields

$$v_2 = \frac{2(u_3 - u_1) - \Sigma_1^- v_1 + \Sigma_2^+ v_3 + \delta_2(x_2 - x_3) - \delta_1(x_2 - x_1)}{\Delta_2} \tag{16}$$

and

$$u_2 = u_1 - \frac{1}{2}\Sigma_2^-(v_2 - v_1) + \frac{1}{2}\delta_1(x_2 - x_1) \tag{17}$$

where

$$\Delta_2 = \Sigma_2^+ - \Sigma_1^- \tag{18}$$

and the values of x_2 and y_2 from (13) and (14) are used in (16) and (17) and the value of v_2 from (16) is used in (17).

In order to start the solution, the values of τ^-, τ^+, and θ at 2 are set to zero. The value of the quantities in (9) through (12) are multiplied by 2 and a first estimate for x_2, y_2, v_2, and u_2 is determined from (13), (14), (16), and (17). To get a second estimate it is necessary to determine a value for a at 2. To determine a_2, it is necessary to determine V at 2. To that end equation (7), part A, section III, is used as follows.

Assume the values of u_2 and v_2 as calculated in the first estimate are correct, then one must solve

$$\phi(V) = u_2^2 + v_2^2 - D + \frac{2}{\rho_0}\left[\frac{AQ}{(Q-1)V^{Q-1}} + B\left(V + \frac{1}{R}\right)e^{-RV} + \frac{(1+\omega)C_s}{\omega V^{\omega}}\right] = 0. \tag{19}$$

This will be solved using the Newton-Raphson method described in appendix 8. If V^i is the ith estimate of the V which solves $\phi(V) = 0$, then

$$V^i = V^{i-1}\left[1 + \frac{\phi(V^{i-1})}{2a^2(V^{i-1})}\right]. \tag{20}$$

Equation (20) is applied until $|V^i - V^{i-1}| \leq e$, where e is an arbitrary small number set equal to 10^{-8} in this case. Equation (6), part A, section III, is used to calculate $a^2(V^{i-1})$.

One is then in a position to calculate values of τ^-, τ^+, and θ at 2. Having done so, the entire process is repeated to get new estimates of x, y, u, v, and V at 2. It was decided (for no particular reason) that when two successive values of u_2 differed by 10^{-8} or less, then the values of all variables at 2 were sufficiently accurate.

If the point 2 is on y = 0, then from (5) and (6):

$$x_2 = x_3 - \frac{2y_3}{\Sigma_2^-} \tag{21}$$

and

$$u_2 = u_3 + \frac{1}{2}\ \Sigma_2^+ v_3 + \frac{1}{2}\ \delta_2(x_2 - x_3) \tag{22}$$

where the values of τ^-, τ^+, θ for 2 are determined using the expressions in (1), (2), and (3) on y = 0. If point 1 is on y = 0, then there is no change from (13) through (18) except in the calculation of τ^-, τ^+, and θ at 1 as indicated for y = 0.

In the process just described it is obvious that if one has all the variables determined on some line $x = x_s$ for N values of y, then the first set of calculations will give all the variables at N - 1 new points. This will, after N sets of calculations, reduce the number of new points to 1. However, if the first point on x_s is used in conjunction with the line y = 0 through (21) and (22), then a new point is added on the first set of calculations, and on every other set of calculations thereafter. The result is that new points are reduced to 1 after 2N - 1 sets of calculations instead of after N - 1 with the last point being on y = 0. (In the program written the problem terminates after 2N - 2.) Hence, the area covered by the solution is determined by the number of points brought forward from the initiating plane solution to the line $x = x_s$ and to some extent upon the distribution of these points. In the program as written no effort was made to select an "ideal" distribution of points on $x = x_s$, and in fact, an arbitrary number of points was selected which will vary with the equation of state in an unknown manner. The distribution of these points is equally arbitrary. The object of the program was to demonstrate that the method works. A clever programmer could devise a routine to give a constant number of points on $x = x_s$ with an "ideal" distribution. Further, the value of x_s was set equal to 0.05 for no particular reason. This number (x_s) should be determined from experimentation with the program in conjunction with physical experiments and/or other computer programs such as HEMP (see ref. 4).

C. Example Problem

As an application of this method the same problem was solved as that discussed in section I. The results are shown in Figs. 17-19.

Figure 17 shows the C^- curves in the part of the problem where the cylindrical equations were solved. The blank space to the left of the line $x = 0.05$ represents the part of the space where the plane solution was assumed to hold. The points calculated there were not plotted because it was felt they would only confuse the figure. It will be noted that the distance between the characteristic curves near the top of the area becomes quite large toward the end of the solution area. This distance is probably too great for the straight line approximations made. However, the addition of several more points would eliminate this objection. Note also that there is a relatively large gap between the highest point on the figure and the line $y = 0.5$ which later represents the original boundary of the H. E. This gap could be reduced by the addition of more curves in the solution to the left of $x = 0.05$. The curves are shown merely as an illustration of the type of information produced by the code.

Figure 18 shows the pressure profile in megabars as a function of the distance from the front expressed in units of the initial thickness of the H. E. for various values of y as plotted by the plot routine directly on the CRT (cathode ray tube) by the computer.

Figure 19 shows the same information as Fig. 18, with the points for the plane solution ($x < 0.05$) removed, hand-plotted on a different scale for clarity. Table 3, appendix 11, lists output from which this figure was plotted.

D. The Program Card Decks

The code name given to this program is CYL-STEDET. One program was written in FORTRAN for the CDC 3600 high speed computer. Both binary and FORTRAN decks are available along with copies of the compilations. If decks are desired, they may be obtained by contacting Mark Wilkins.

The output quantities are the same as those listed in part D, section II, with the addition of

S = sound speed.

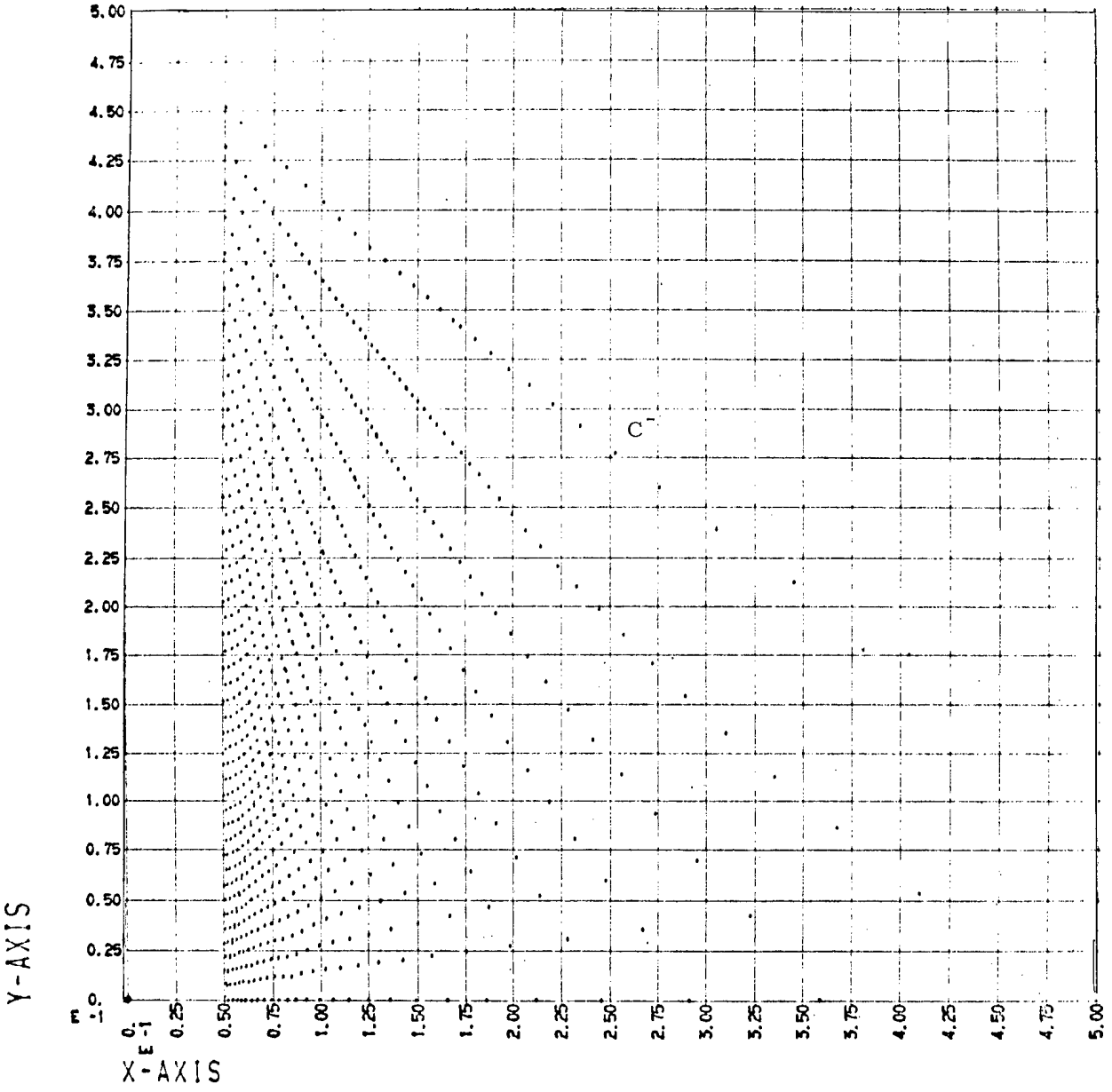

Fig. 17. C^- characteristics for cylindrical geometry with the Wilkins equation of state.

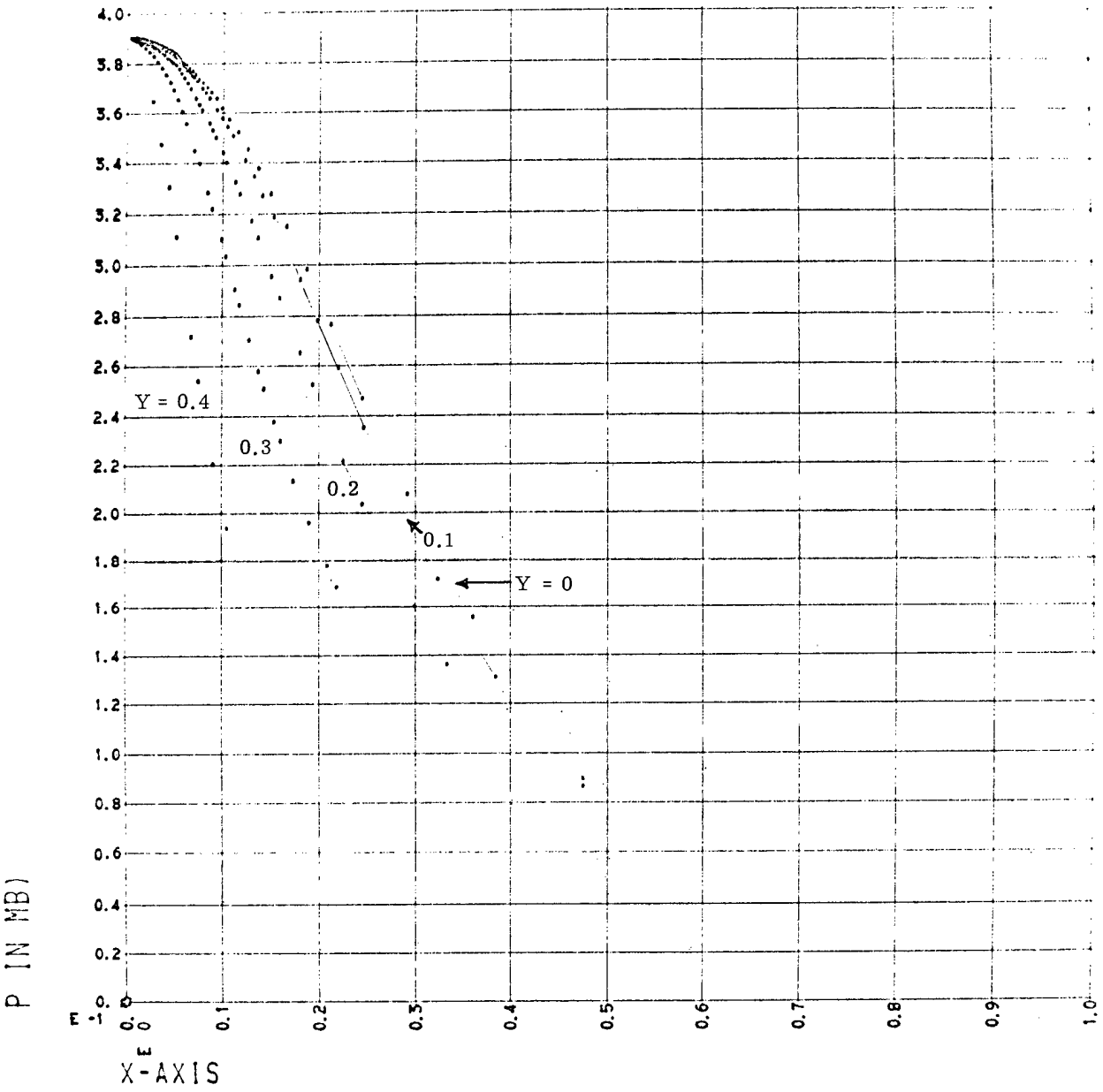

Fig. 18. Pressure profiles at various distances from the centerline of the H. E. as a function of distance from the front in units of the initial thickness, for the Wilkins equation of state in cylindrical geometry.

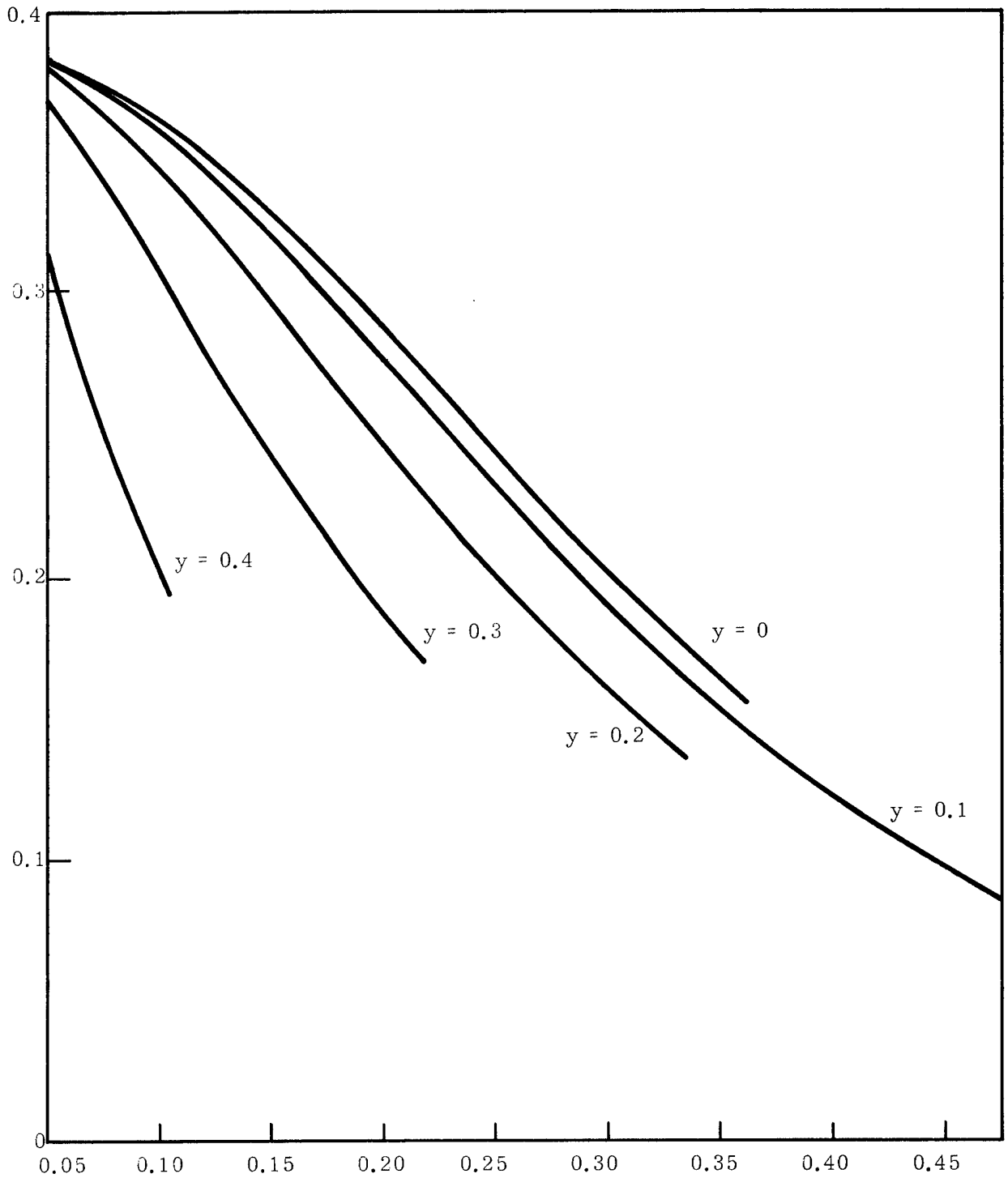

Fig. 19. Pressure profiles at various distances from the centerline of the H. E. as a function of distance from the front in units of the initial thickness, for the Wilkins equation of state in cylindrical geometry.

The linear interpolation routines are the same as in the two plane cases (see note below).

To run a problem with the binary deck, follow the instructions given in part D, section II, with the following change:

CARD 5: 3I10 format

IPLOT, IPLOT1, IPLOT2

IPLOT and IPLOT1 are unchanged from the plane cases.

IPLOT2 = 0 yields no plot of the characteristics in the plane part of the solution.

IPLOT 2 = 1 yields a plot of the characteristics in the plane part of the solution.

It is also possible to solve a problem for an ideal gas equation of state for PBX 9404. The following input data is required to do this:

C = 0.
Q = 4.0
R = 4.0
B = 0.
W = 1.65358
ROE = 1.84
CS = 0.1668537
VCJ = 0.7262958
SPEED = 0.88
ISTRT = 2

When this input was tried, the problem ran to completion, but due to the fixed selection of curves in the plane part of the solution, the maximum value of x obtained was 0.258. That was not enough for a useful solution. The important thing is that this problem ran.

NOTE: Output curves corresponding to Figs. 12-15 are not displayed for this program because the area covered by the solution obtained was too small to include more than a few points on x = 0.25, 0.50, 0.75, and 1.0 and almost no points on the constant volume contours.

APPENDIX 1

DERIVATION OF THE TWO-DIMENSIONAL, STEADY, IRROTATIONAL, ISENTROPIC HYDRODYNAMICS EQUATIONS

The general equations governing continuous media are (ref. 6, Ch. 2, 3, 4):

Conservation of Mass

$$\frac{\partial \rho}{\partial t} + (\rho u^i)_{;i} = 0,$$

Conservation of Momentum

$$t^{ij}_{\ ;i} + \rho \left(f^j - \frac{Du^j}{Dt} \right) = 0,$$

$$t^{ij} = t^{ji},$$

Conservation of Energy

$$\rho \frac{D}{Dt} \left(\epsilon + \frac{u^2}{2} \right) = \rho f^i u_i + \left(t^{ij} u_j \right)_{;i},$$

Entropy Principle

$$\rho \frac{D\eta}{Dt} \geq 0,$$

where

$\rho \equiv$ mass density,

$\underset{\sim}{u} \equiv$ velocity vector,

$t^{ij} \equiv$ stress tensor,

$\underset{\sim}{f} \equiv$ body force vector per unit mass,

$\epsilon \equiv$ internal energy per unit mass,

$\eta \equiv$ entropy per unit mass,

$A^i_{\ ;j} \equiv$ covariant partial derivative of A^i,

$\frac{D}{Dt} \equiv$ material derivative.

If one considers a nonviscous, nonconducting medium in which $\underset{\sim}{u} = [u, v, 0]$, $p = p(x, y)$, $\rho = \rho(x, y)$, $\underset{\sim}{u} = \underset{\sim}{u}(x, y)$, $\epsilon = \epsilon(x, y)$, $\eta = \eta(x, y)$, $f^i \equiv 0$, and $t^{ij} = -p\delta^{ij}$, then these equations become:

Conservation of Mass

$$\frac{\partial(\rho u)}{\partial x} + \frac{\partial(\rho v)}{\partial y} = 0, \tag{1}$$

Conservation of Momentum

$$-\frac{\partial p}{\partial x} = \rho u \frac{\partial u}{\partial x} + \rho v \frac{\partial u}{\partial y}, \tag{2}$$

$$-\frac{\partial p}{\partial y} = \rho u \frac{\partial v}{\partial x} + \rho v \frac{\partial v}{\partial y}, \tag{3}$$

Conservation of Energy

$$\rho u \frac{\partial}{\partial x}\left(\epsilon + \frac{U^2}{2}\right) + \rho v \frac{\partial}{\partial y}\left(\epsilon + \frac{U^2}{2}\right) = -\frac{\partial}{\partial x}(pu) - \frac{\partial}{\partial y}(pv), \tag{4}$$

Entropy Principle

$$\rho u \frac{\partial \eta}{\partial x} + \rho v \frac{\partial \eta}{\partial y} \geq 0, \tag{5}$$

where

$p \equiv$ hydrostatic pressure,

$x, y \equiv$ rectangular coordinates,

$U^2 \equiv u^2 + v^2$.

The equation of state for an ideal gas is

$$\frac{p}{p_0} = \left(\frac{\rho}{\rho_0}\right)^{\gamma} \exp\left(\frac{\eta - \eta_0}{c_v}\right) \quad \text{(see Ref. 2, p. 6 ff)} \tag{6}$$

where

$\gamma \equiv \frac{c_p}{c_v} \equiv$ gas constant, or specific heat ratio,

$c_p \equiv$ specific heat at constant pressure,

$c_v \equiv$ specific heat at constant volume,

The sound speed is given by

$$a^2 = \left.\frac{\partial p}{\partial \rho}\right|_{\eta},$$

so that using (6):

$$a^2 = \left.\frac{\partial p}{\partial \rho}\right|_{\eta} = \frac{\gamma p}{\rho}. \tag{7}$$

Consider the right-hand side of (4):

$$-\left[\frac{\partial}{\partial x}(pu) + \frac{\partial}{\partial y}(pv)\right] = -\left[u\frac{\partial p}{\partial x} + v\frac{\partial p}{\partial y} + p\left(\frac{\partial u}{\partial x} + \frac{\partial v}{\partial y}\right)\right].$$

From (1)

$$\frac{\partial u}{\partial x} + \frac{\partial v}{\partial y} = -\left(\frac{u}{\rho}\frac{\partial \rho}{\partial x} + \frac{v}{\rho}\frac{\partial \rho}{\partial y}\right),$$

and with this relation one can write:

$$-\left[\frac{\partial}{\partial x}(pu) + \frac{\partial}{\partial y}(pv)\right] = -\left[u\frac{\partial p}{\partial x} + v\frac{\partial p}{\partial y} - \frac{pu}{\rho}\frac{\partial \rho}{\partial x} - \frac{pv}{\rho}\frac{\partial \rho}{\partial y}\right]$$

$$= -\rho\left(u\frac{\partial}{\partial x}\frac{p}{\rho} + v\frac{\partial}{\partial y}\frac{p}{\rho}\right).$$

Hence, (4) may be written as

$$\left(u\frac{\partial}{\partial x} + v\frac{\partial}{\partial y}\right)\left(\epsilon + \frac{U^2}{2} + \frac{p}{\rho}\right) = 0.$$

Now $u\frac{\partial}{\partial x} + v\frac{\partial}{\partial y} = \frac{d}{dS}$

where S is the arc length along the particle path. Therefore, (4) becomes

$$\epsilon + \frac{U^2}{2} + \frac{p}{\rho} = \text{constant along the particle path.} \qquad (8)$$

The first law of thermodynamics may be written as

$$T d\eta = d\epsilon + p d\frac{1}{\rho} \qquad (9)$$

with T = absolute thermodynamic temperature. In terms of derivatives along the particle path (5) is

$$\rho\frac{d\eta}{dS} \geq 0,$$

and if one considers a system in which $d\eta = 0$ along the particle path, then (9) becomes

$$d\epsilon = -p d\frac{1}{\rho} \text{ along path lines.} \qquad (10)$$

From (8):

$$d\epsilon + u\,du + v\,dv + \frac{1}{\rho}dp + p d\frac{1}{\rho} = 0 \text{ along path lines.} \qquad (11)$$

Using (10) and (11) yields

$$u\,du + v\,dv = -\frac{1}{\rho}dp \text{ along path lines.} \qquad (12)$$

Since (12) is valid along path lines, one can also write

$$u \frac{du}{dS} + v \frac{dv}{dS} = - \frac{1}{\rho} \frac{dp}{dS} . \tag{13}$$

Remembering that $\frac{d}{dS} = u \frac{\partial}{\partial x} + v \frac{\partial}{\partial y}$, (13) becomes

$$u^2 \frac{\partial u}{\partial x} + uv \frac{\partial u}{\partial y} + uv \frac{\partial v}{\partial x} + v^2 \frac{\partial v}{\partial y} = - \frac{1}{\rho} \frac{dp}{dS} , \tag{14}$$

and since along path lines $d\eta = 0$, (7) may be written as

$$a^2 = \left.\frac{\partial p}{\partial \rho}\right|_{\eta} = \frac{dp}{d\rho} \text{ along path lines}$$

or, what is the same thing, as

$$\frac{dp}{dS} = a^2 \frac{d\rho}{dS} . \tag{15}$$

By using (15), (14) becomes

$$u^2 \frac{\partial u}{\partial x} + uv\left(\frac{\partial u}{\partial y} + \frac{\partial v}{\partial x}\right) + v^2 \frac{\partial v}{\partial y} = - \frac{a^2}{\rho} \frac{d\rho}{dS} . \tag{16}$$

Now (1) may be written as follows:

$$u \frac{\partial \rho}{\partial x} + \rho \frac{\partial u}{\partial x} + v \frac{\partial \rho}{\partial y} + \rho \frac{\partial v}{\partial y} = \frac{d\rho}{dS} + \rho\left(\frac{\partial u}{\partial x} + \frac{\partial v}{\partial y}\right) = 0$$

which, solved for $\frac{d\rho}{dS}$, yields

$$\frac{d\rho}{dS} = - \rho \left(\frac{\partial u}{\partial x} + \frac{\partial v}{\partial y}\right).$$

Putting this last expression in (16):

$$a^2 \left(\frac{\partial u}{\partial x} + \frac{\partial v}{\partial y}\right) = u^2 \frac{\partial u}{\partial x} + uv \left(\frac{\partial u}{\partial y} + \frac{\partial v}{\partial x}\right) + v^2 \frac{\partial v}{\partial y}$$

or

$$(a^2 - u^2) \frac{\partial u}{\partial x} - uv\left(\frac{\partial u}{\partial y} + \frac{\partial v}{\partial x}\right) + (a^2 - v^2) \frac{\partial v}{\partial y} = 0 . \tag{17}$$

If one considers (6) along path lines ($d\mu = 0$), then

$$\frac{p}{p_0} = \left(\frac{\rho}{\rho_0}\right)^{\gamma} \text{ or } \rho = \rho_0 \left(\frac{p}{p_0}\right)^{1/\gamma} , \tag{18}$$

where ρ_0, p_0 are the values at some initial point, and using (18) in (7):

$$a^2 = \frac{\gamma p}{\rho_0}\left(\frac{p}{p_0}\right)^{-1/\gamma} = \frac{\gamma p_0}{\rho_0}\left(\frac{p}{p_0}\right)^{\frac{\gamma-1}{\gamma}} = a_0^2\left(\frac{p}{p_0}\right)^{\frac{\gamma-1}{\gamma}},$$

whence

$$p = p_0\left(\frac{a^2}{a_0^2}\right)^{\frac{\gamma}{\gamma-1}}, \text{ where } a_0^2 = \frac{\gamma p_0}{\rho_0}. \tag{19}$$

Operating on (19):

$$dp = p_0 \frac{\gamma}{\gamma-1}\left(\frac{a^2}{a_0^2}\right)^{\frac{\gamma}{\gamma-1}}\left(\frac{a^2}{a_0^2}\right)^{-1}\frac{da^2}{a_0^2} = \frac{\gamma}{\gamma-1}\, p\, \frac{da^2}{a^2}$$

or

$$\frac{dp}{p} = \frac{\gamma}{\gamma-1}\frac{da^2}{a^2}. \tag{20}$$

From (7):

$$-\frac{1}{\rho}\,dp = -\frac{a^2}{\gamma p}\,dp,$$

and using (20):

$$-\frac{1}{\rho}\,dp = -\frac{1}{\gamma-1}\,da^2.$$

Putting this last in (12):

$$\frac{1}{2}\,d(u^2+v^2) = -\frac{da^2}{\gamma-1}$$

which, when integrated along path lines, yields

$$u^2 + v^2 = -\frac{2a^2}{\gamma-1} + \text{constant, along path lines.} \tag{21}$$

For use elsewhere, note that if $\gamma = 3$:

$$u^2 + v^2 + a^2 = \text{constant, along path lines.} \tag{22}$$

Note, also, that (21) implies that $a^2 = a^2(u^2+v^2)$, so that (17) is an equation in (u, v) as functions of (x, y). In order to use the method of characteristics here we need another differential equation in (u, v) as functions of (x, y).

To that end, consider the conservation equations for a general hydrodynamic material with $t^{ij} = -p\delta^{ij}$ and $f^i = 0$. First convert these equations

from tensor to vector notation by noting that:

$$t^{ij}{}_{;i} = -\left(p\delta^{ij}\right)_{,i} = -p_{,j} = -\nabla p$$

and

$$\left(t^{ij}u_j\right)_{;i} = -\left(p\delta^{ij}u_j\right)_{;i} = -\left(pu_i\right)_{;j} = -\nabla \cdot (p\underset{\sim}{u}) .$$

With these, the conservation equations become:

$$\dot{\rho} + \rho\nabla \cdot \underset{\sim}{u} = 0, \tag{23}$$

$$\rho\dot{\underset{\sim}{u}} + \nabla p = 0, \tag{24}$$

$$\rho\dot{\epsilon} + \rho\,\dot{\frac{U^2}{2}} = -\nabla \cdot (p\underset{\sim}{u}), \tag{25}$$

$$\rho\dot{\eta} \geq 0, \tag{26}$$

where $\dot{(\ )} = \frac{D}{Dt} = \frac{\partial}{\partial t} + \underset{\sim}{u} \cdot \nabla$ for unsteady motion,

and $\dot{(\ )} = \frac{D}{Dt} = \frac{d}{dS} = \underset{\sim}{u} \cdot \nabla$ for steady motion.

For steady motion, (23) may be written as

$$\underset{\sim}{u} \cdot \nabla\rho + \rho\nabla \cdot \underset{\sim}{u} = 0$$

or

$$\nabla \cdot \underset{\sim}{u} = -\frac{1}{\rho}\underset{\sim}{u} \cdot \nabla\rho . \tag{27}$$

Considering the right-hand side of (25),

$$\nabla \cdot (p\underset{\sim}{u}) = p\nabla \cdot \underset{\sim}{u} + (\nabla p) \cdot \underset{\sim}{u} ,$$

and using (27),

$$\nabla \cdot (p\underset{\sim}{u}) = -\frac{p}{\rho}\underset{\sim}{u} \cdot \nabla\rho + \underset{\sim}{u} \cdot \nabla p = \rho\underset{\sim}{u} \cdot \left(\frac{1}{\rho}\nabla p - \frac{p}{\rho^2}\nabla\rho\right)$$

or

$$\nabla \cdot (p\underset{\sim}{u}) = \rho\underset{\sim}{u} \cdot \left(\nabla\frac{p}{\rho}\right) . \tag{28}$$

Using (28) in steady (25):

$$\rho\underset{\sim}{u} \cdot \nabla\left(\epsilon + \frac{u^2}{2} + \frac{p}{\rho}\right) = 0 . \tag{29}$$

Now (9) may be written as:

$$T\frac{d\eta}{dS} = \frac{d\epsilon}{dS} + p\frac{d}{dS}\left(\frac{1}{\rho}\right) \quad \text{or} \quad \underset{\sim}{u}\cdot T\nabla\eta = \underset{\sim}{u}\cdot\nabla\epsilon + \underset{\sim}{u}\cdot p\nabla\frac{1}{\rho}\ . \tag{30}$$

From (24) for steady motion,

$$\dot{\underset{\sim}{u}} = (\underset{\sim}{u}\cdot\nabla)\underset{\sim}{u} = -\frac{1}{\rho}\nabla p, \tag{31}$$

and, in general,

$$\nabla\left(\epsilon + \frac{p}{\rho}\right) = \nabla\epsilon + \frac{1}{\rho}\nabla p + p\nabla\frac{1}{\rho}\ ,$$

so that,

$$\underset{\sim}{u}\cdot\nabla\left(\epsilon + \frac{u^2}{2} + \frac{p}{\rho}\right) = \underset{\sim}{u}\cdot\nabla\left(\frac{u^2}{2}\right) + \underset{\sim}{u}\cdot\nabla\left(\epsilon + \frac{p}{\rho}\right) = \underset{\sim}{u}\cdot\nabla\left(\frac{u^2}{2}\right)$$

$$+ \underset{\sim}{u}\cdot\left(\nabla\epsilon + p\nabla\frac{1}{\rho} + \frac{1}{\rho}\nabla p\right)\ .$$

Using (30) in this:

$$\underset{\sim}{u}\cdot\nabla\left(\epsilon + \frac{u^2}{2} + \frac{p}{\rho}\right) = \underset{\sim}{u}\cdot\nabla\frac{u^2}{2} + \underset{\sim}{u}\cdot\left(\nabla\epsilon + p\nabla\frac{1}{\rho}\right) - \underset{\sim}{u}\cdot(u\cdot\nabla)\underset{\sim}{u}\ . \tag{32}$$

In general,

$$(\underset{\sim}{u}\cdot\nabla)\frac{u^2}{2} = 2\,\underset{\sim}{u}\cdot(\underset{\sim}{u}\cdot\nabla)\frac{\underset{\sim}{u}}{2} = \underset{\sim}{u}\cdot(\underset{\sim}{u}\cdot\nabla)\underset{\sim}{u}\ ,$$

so that (32) becomes

$$\underset{\sim}{u}\cdot\nabla\left(\epsilon + \frac{u^2}{2} + \frac{p}{\rho}\right) = \underset{\sim}{u}\cdot\left(\nabla\epsilon + p\nabla\frac{1}{\rho}\right)\ . \tag{33}$$

Using (30) in (33) and recalling (29):

$$\underset{\sim}{u}\cdot T\nabla\eta = \underset{\sim}{u}\cdot\nabla\left(\epsilon + \frac{u^2}{2} + \frac{p}{\rho}\right) = \frac{d}{dS}\left(\epsilon + \frac{u^2}{2} + \frac{p}{\rho}\right) = 0, \text{ along path lines.} \tag{34}$$

Since $\underset{\sim}{u}\cdot T\nabla\eta = T\,\underset{\sim}{u}\cdot\nabla\eta = T\frac{d}{dS}\eta$, (34) implies:

$$\epsilon + \frac{u^2}{2} + \frac{p}{\rho} = \text{constant and } \eta = \text{constant along path lines.} \tag{35}$$

This is the same result obtained in (8); it was repeated because the vector equations were needed for what follows.

Now the expression $(\underset{\sim}{u} \cdot \nabla)\underset{\sim}{u}$ while in vector notation is a tensor the way it stands. In order to write it as a vector expression, we revert to tensor notation for a moment to find that

$$(\underset{\sim}{u} \cdot \nabla)\underset{\sim}{u} = u^i \frac{\partial(u_j \underset{\sim}{e}^j)}{\partial x^i} = u^i u_{j;i} \underset{\sim}{e}^j \tag{36}$$

where

$u^i \equiv$ contravariant components of $\underset{\sim}{u}$,

$u_j \equiv$ covariant components of $\underset{\sim}{u}$,

$\underset{\sim}{e}^j \equiv$ reciprocal base vector.

Operating on the right-hand side of (36):

$$u^i u_{j;i} \underset{\sim}{e}^j = u^i u_{i;j} \underset{\sim}{e}^j - u^i u_{i;j} \underset{\sim}{e}^j + u^i u_{j;i} \underset{\sim}{e}^j = \frac{1}{2} \nabla u^2$$

$$- \left[u^i u_{i;j} \underset{\sim}{e}^j - u^j u_{i;j} \underset{\sim}{e}^i \right]$$

$$= \frac{1}{2} \nabla u^2 - \delta^{k\ell}_{ji} \, u^i u_{\ell;k} \underset{\sim}{e}^j \quad \text{(see footnote*)}$$

$$= \frac{1}{2} \nabla u^2 - \epsilon_{jim} u^i \epsilon^{k\ell m} u_{\ell;k} \underset{\sim}{e}^j .$$

Now $\epsilon^{k\ell m} u_{\ell;k} \underset{\sim}{e}^j = \text{curl } \underset{\sim}{u} = \underset{\sim}{\omega} \equiv$ vorticity vector, and $\epsilon_{jim} u^i \omega^m \underset{\sim}{e}^j = \underset{\sim}{u} \wedge \underset{\sim}{\omega}$ where $\wedge \equiv$ cross product or vector product, hence

---

* $\delta^{k\ell}_{ji}$ is the generalized Kronecker symbol which has value 1 for $j = k$, $i = \ell$, and -1 for $j = \ell$, $i = k$.

ϵ_{jik} and ϵ^{jik} (not to be confused with ϵ for energy) are related to the permutation symbols $e_{k\ell m}$, $e^{k\ell m}$ as follows

$e^{k\ell m}, e_{k\ell m}$ { = 1 when $k\ell m$ is an even permutation of 123; = -1 when $k\ell m$ is an odd permutation of 123; = 0 otherwise }

and $\epsilon_{jik} = e_{jik} \sqrt{g}$

$\epsilon^{jik} = \dfrac{e^{jik}}{\sqrt{g}}$

where $g \equiv$ determinant of the metric tensor.

$$u^i u_{j;i} \underset{\sim}{e}^j = \frac{1}{2}\nabla u^2 - \underset{\sim}{u} \wedge \underset{\sim}{\omega} = \frac{1}{2}\nabla u^2 - \underset{\sim}{u} \wedge \text{curl } \underset{\sim}{u} .$$

Therefore, (36) becomes

$$(\underset{\sim}{u} \cdot \nabla)\underset{\sim}{u} = \frac{1}{2}\nabla u^2 - \underset{\sim}{u} \wedge \text{curl } \underset{\sim}{u}. \tag{37}$$

From (30)

$$T\nabla\eta = \nabla\epsilon + p\nabla\frac{1}{\rho} . \tag{38}$$

From (31) and (38)

$$\frac{1}{2}\nabla u^2 - \underset{\sim}{u} \wedge \text{curl } u = -\frac{1}{\rho}\nabla p,$$

hence

$$\nabla\left(\epsilon + \frac{p}{\rho}\right) = \nabla\epsilon + p\nabla\frac{1}{\rho} + \frac{1}{\rho}\nabla p$$

and

$$\frac{1}{2}\nabla u^2 - \underset{\sim}{u} \wedge \text{curl } \underset{\sim}{u} + \nabla\left(\epsilon + \frac{p}{\rho}\right) = \nabla\epsilon + p\nabla\frac{1}{\rho} = T\nabla\eta$$

or

$$T\nabla\eta = \nabla\left(\epsilon + \frac{u^2}{2} + \frac{p}{\rho}\right) - \underset{\sim}{u} \wedge \text{curl } \underset{\sim}{u} . \tag{39}$$

From (39) it is easily seen that if $\nabla\eta = 0$ everywhere and curl $\underset{\sim}{u} = 0$, then

$$\nabla\left(\epsilon + \frac{u^2}{2} + \frac{p}{\rho}\right) = 0 \text{ everywhere}$$

or

$$\epsilon + \frac{u^2}{2} + \frac{p}{\rho} = \text{constant, throughout the material.}$$

Therefore, for an isentropic, irrotational, steady process $\epsilon + u^2/2 + p/\rho$ = constant everywhere and the relations (8) through (22) are seen to hold everywhere instead of just along path lines with the additional requirement on the (u, v)'s that

$$-\text{curl } \underset{\sim}{u} = \frac{\partial u}{\partial y} - \frac{\partial v}{\partial x} = 0 . \tag{40}$$

Equations (17) and (40) are seen to be the desired pair of equations.

APPENDIX 2
DERIVATION OF THE CHARACTERISTIC EQUATIONS*

The set of two differential equations to be solved in this instance are:

$$(a^2 - u^2)\frac{\partial u}{\partial x} - uv\frac{\partial v}{\partial x} - uv\frac{\partial u}{\partial y} + (a^2 - v^2)\frac{\partial v}{\partial y} = 0,$$

$$0\frac{\partial u}{\partial x} + \frac{\partial v}{\partial x} - \frac{\partial u}{\partial y} + 0\frac{\partial v}{\partial y} = 0 . \qquad (1)$$

In general, a set of first-order partial differential equations in two independent variables may be written as

$$L[\underset{\sim}{U}] = \underset{\sim}{C} \qquad (2)$$

where

$$L[\underset{\sim}{U}] = A\underset{\sim}{U}_x + B\underset{\sim}{U}_y ,$$

$A, B \equiv$ matrices,

$\underset{\sim}{C} \equiv$ vector,

$\underset{\sim}{U} \equiv$ vector representing the dependent variables,

$\underset{\sim}{U}_i \equiv \frac{\partial \underset{\sim}{U}}{\partial i}$.

It is readily seen that to write (1) in the form of (2), one defines

$$\underset{\sim}{U} = [u, v] ,$$

$$A = \begin{bmatrix} a^2 - u^2 & -uv \\ 0 & 1 \end{bmatrix},$$

$$B = \begin{bmatrix} -uv & a^2 - v^2 \\ -1 & 0 \end{bmatrix} ,$$

$$\underset{\sim}{C} = [0 \;\; 0] .$$

In this case (2) is of the form

$$A\underset{\sim}{U}_x + B\underset{\sim}{U}_y = 0, \qquad (3)$$

which may be written as

$$\underset{\sim}{U}_x + A^{-1}B\underset{\sim}{U}_y = 0 \qquad (4)$$

---

*The treatment here follows closely that in Ch. 5 of ref. 7.

provided $|A| \neq 0$, where

$|A|$ = determinant of A,

A^{-1} = inverse of A.

Suppose it is given that U has some known value on a curve $C[\phi(x, y) = 0]$ along which the inner (or tangential) derivative (see ref. 7, pp. 132-133) of U is also known. In that case, the outward normal to C is given by

$$\nabla\phi = \frac{\partial\phi}{\partial x}\underset{\sim}{i} + \frac{\partial\phi}{\partial y}\underset{\sim}{j} \tag{5}$$

and the unit normal vector is given by

$$\underset{\sim}{n} = \frac{\frac{\partial\phi}{\partial x}\underset{\sim}{i} + \frac{\partial\phi}{\partial y}\underset{\sim}{j}}{\sqrt{\left(\frac{\partial\phi}{\partial x}\right)^2 + \left(\frac{\partial\phi}{\partial y}\right)^2}} \quad \text{if } \left(\frac{\partial\phi}{\partial x}\right)^2 + \left(\frac{\partial\phi}{\partial y}\right)^2 \neq 0\,. \tag{6}$$

The derivative of a function F along a curve with S the arc length is given by

$$\left(\frac{\partial F}{\partial x}\underset{\sim}{i} + \frac{\partial F}{\partial y}\underset{\sim}{j}\right) \cdot S \tag{7}$$

where $\underset{\sim}{S}$ is the unit tangent vector. If $\underset{\sim}{S} = [S_1, S_2]$ and $\underset{\sim}{n} = [n_1, n_2]$, it is well known that

$$S_1 = -n_2 \text{ and } n_1 = S_2;$$

therefore if we let $\frac{\partial\phi}{\partial i} = \phi_i$, etc. then

$$\underset{\sim}{S} = \frac{1}{\sqrt{\phi_x^2 + \phi_y^2}}\left[-\phi_y, \phi_x\right]$$

so that (7) becomes

$$-\frac{F_x\phi_y + F_y\phi_x}{\sqrt{\phi_x^2 + \phi_y^2}}\,. \tag{8}$$

Since we are assuming the inner derivative of U is known on C, (8) can be used to express the inner derivative of U assuming $\phi_x^2 + \phi_0^2 \neq 0$:

$$-\underset{\sim}{U}_x\phi_y + \underset{\sim}{U}_y\phi_x = \text{known quantities}, \tag{9}$$

and since $\phi(x, y)$ is known, ϕ_x and ϕ_y are known, so define

$$\tau = -\frac{\phi_x}{\phi_y} \tag{10}$$

and using (10) in (9) and solving for $\underset{\sim}{U}_x$,

$$\underset{\sim}{U}_x = -\tau \underset{\sim}{U}_y + \text{(known quantities)}, \text{ and substituting (11) in (5),} \tag{11}$$

$$-\tau \underset{\sim}{U}_y + A^{-1}B\underset{\sim}{U}_y + \text{(known quantities)} = 0. \tag{12}$$

In order to determine $\underset{\sim}{U}_y$ from this expression, the determinant Q of the coefficients of $\underset{\sim}{U}_y$ must satisfy

$$Q = \left|A^{-1}B - \tau I\right| \neq 0, \text{ where I} \equiv \text{identity matrix.}$$

If, on the other hand, $Q = 0$, the curve C is called characteristic and the characteristic condition is

$$Q = \left|A^{-1}B - \tau I\right| = 0. \tag{13}$$

The system is classified as hyperbolic if (13) has two distinct real roots. In that case a solution by the use of characteristics is possible. Using (3):

$$|A| = a^2 - u^2,$$

$$A^{-1} = \begin{bmatrix} \frac{1}{a^2-u^2} & \frac{uv}{a^2-u^2} \\ 0 & 1 \end{bmatrix} \quad \text{if } a^2 \neq u^2, \tag{14}$$

$$A^{-1}B = \begin{bmatrix} \frac{-2uv}{a^2-u^2} & \frac{a^2-v^2}{a^2-u^2} \\ -1 & 0 \end{bmatrix}.$$

Putting (14) in (13):

$$Q = \left| \begin{bmatrix} \frac{-2uv}{a^2-u^2} & \frac{a^2-v^2}{a^2-u^2} \\ -1 & 0 \end{bmatrix} - \tau \begin{bmatrix} 1 & 0 \\ 0 & 1 \end{bmatrix} \right| = 0. \tag{15}$$

The characteristic condition (15) is solved as follows:

$$Q = \begin{vmatrix} \frac{-2uv}{a^2-u^2} - \tau & \frac{a^2-v^2}{a^2-u^2} \\ -1 & -\tau \end{vmatrix} = \tau^2 + \frac{2uv}{a^2 - u^2}\tau + \frac{a^2 - v^2}{a^2 - u^2} = 0 ,$$

$$\tau_{1,2} = \frac{uv \mp a\sqrt{u^2 + v^2 - a^2}}{u^2 - a^2} . \tag{16}$$

From (16) it is clear that there are two distinct real roots if

$$u^2 + v^2 - a^2 > 0 . \tag{17}$$

If $\left|A^{-1}B - \tau I\right| = 0$, then there exists a vector $\underset{\sim}{\ell}$ such that

$$\underset{\sim}{\ell} A^{-1}B - \underset{\sim}{\ell}\tau I = 0 \quad \text{or} \quad \underset{\sim}{\ell} A^{-1}B = \underset{\sim}{\ell}\tau I . \tag{18}$$

Letting $\underset{\sim}{\ell}^{\alpha}$ correspond to τ_{α} ($\alpha = 1, 2$), (18) may be written as

$$\ell_i^{\alpha}(A^{-1}B)_{ij} = \ell_i^{\alpha}\tau_{\alpha}\delta_{ij} = \ell_j^{\alpha}\tau_{\alpha} \tag{19}$$

from which one must find ℓ^{α}. Expanding (19) and solving:

$$\ell_1^{\alpha}\left[(A^{-1}B)_{11} - \tau_{\alpha}\right] + \ell_2^{\alpha}(A^{-1}B)_{21} = 0,$$

$$\ell_1^{\alpha}(A^{-1}B)_{12} + \ell_2^{\alpha}\left[(A^{-1}B)_{22} - \tau_{\alpha}\right] = 0,$$

whence

$$\ell_1^{\alpha} = \frac{-(A^{-1}B)_{21}}{\left[(A^{-1}B)_{11} - \tau_{\alpha}\right]}\ell_2^{\alpha}, \text{ or } \ell_1^{\alpha} = \frac{(A^{-1}B)_{22} - \tau_{\alpha}}{(A^{-1}B)_{12}}\ell_2^{\alpha} . \tag{20}$$

Using (14) and (16) in the second of (20):

$$\ell_1^{1,2} = -\frac{\tau_{1,2}\ell_2^{1,2}}{\frac{a^2 - v^2}{a^2 - u^2}} = \frac{uv \mp a\sqrt{u^2 + v^2 - a^2}}{a^2 - v^2}\ell_2^{1,2} . \tag{21}$$

Now, operate on (5) with $\underset{\sim}{\ell}^{\alpha}$ and make use of (18):

$$\ell_i^{\alpha}U_x^i + \ell_i^{\alpha}(A^{-1}B)_{ij}U_y^j = \ell_i^{\alpha}U_x^i + \ell_i^{\alpha}\tau_{\alpha}\delta_{ij}U_y^j$$

$$= \ell_i^{\alpha}U_x^i + \ell_i^{\alpha}\tau_{\alpha}U_y^i = 0 .$$

This last may be written as

$$\ell_i^{\alpha} D_{\alpha} U^i = 0, \text{ where } D_{\alpha} = \frac{\partial}{\partial x} + \tau_{\alpha} \frac{\partial}{\partial y}, \tag{22}$$

the derivative along the $\underset{\sim}{\ell}^{\alpha}$ direction.

Using (21) in (22):

$$\frac{uv - a\sqrt{u^2 + v^2 - a^2}}{a^2 - v^2} D_1 U^1 + D_1 U^2 = 0 \quad \text{along 1,} \tag{23}$$

and

$$\frac{uv + a\sqrt{u^2 + v^2 - a^2}}{a^2 - v^2} D_2 U^1 + D_2 U^2 = 0 \text{ along 2.}$$

In order to determine the curve C, think of $\phi(x, y) = 0$ solved for $y = y(x)$, and since

$$\begin{aligned} d\phi &= \frac{\partial \phi}{\partial x} dx + \frac{\partial \phi}{\partial y} dy = 0, \\ \frac{dy}{dx} &= -\frac{\phi_x}{\phi_y} = \tau \quad [\text{see (10)}] \ . \end{aligned} \tag{24}$$

Using (16), (24), and (23) one can then write the differential equations for the characteristic curves and the compatibility equations which must be satisfied along them as:

$$C_2: \ \frac{dy}{dx} = +\tau_2 = \frac{uv + a\sqrt{u^2 + v^2 - a^2}}{u^2 - a^2}$$

along which

$$-\frac{uv + a\sqrt{u^2 + v^2 - a^2}}{v^2 - a^2} \frac{du}{dx_2} = \frac{dv}{dx_2}, \tag{25}$$

and

$$C_1: \ \frac{dy}{dx} = +\tau_1 = \frac{uv - a\sqrt{u^2 + v^2 - a^2}}{u^2 - a^2}$$

along which

$$-\frac{uv - a\sqrt{u^2 + v^2 - a^2}}{v^2 - a^2} \frac{du}{dx_1} = \frac{dv}{dx_1} \ .$$

APPENDIX 3
DERIVATION OF THE CHARACTERISTIC EQUATIONS IN THE HODOGRAPH PLANE*

The set of partial differential equations

$$\begin{aligned} (a^2 - u^2)\frac{\partial u}{\partial x} - uv\frac{\partial v}{\partial x} - uv\frac{\partial u}{\partial y} + (a^2 - v^2)\frac{\partial v}{\partial y} &= 0, \\ 0\,\frac{\partial u}{\partial x} + \frac{\partial v}{\partial x} - \frac{\partial u}{\partial y} + 0\,\frac{\partial v}{\partial y} &= 0, \end{aligned} \tag{1}$$

is a set of equations to be solved for $u = u(x, y)$ and $v = v(x, y)$. Since there are two dependent and two independent variables it is possible to transform (1) into a set which is to be solved for $x = x(u, v)$ and $y = y(u, v)$. To that end, we write:

$$\begin{aligned} du &= \frac{\partial u}{\partial x}dx + \frac{\partial u}{\partial y}dy, \\ dv &= \frac{\partial v}{\partial x}dx + \frac{\partial v}{\partial y}dy, \end{aligned} \tag{2}$$

and consider (2) as a set of equations to be solved for dx and dy. Hence

$$\begin{aligned} dx &= \frac{\begin{vmatrix} du & \frac{\partial u}{\partial y} \\ dv & \frac{\partial v}{\partial y} \end{vmatrix}}{J} = \frac{1}{J}\frac{\partial v}{\partial y}du - \frac{1}{J}\frac{\partial u}{\partial y}dv, \\ dy &= \frac{\begin{vmatrix} \frac{\partial u}{\partial x} & du \\ \frac{\partial v}{\partial x} & dv \end{vmatrix}}{J} = -\frac{1}{J}\frac{\partial v}{\partial x}du + \frac{1}{J}\frac{\partial u}{\partial x}dv, \end{aligned} \tag{3}$$

where

$$J = \frac{\partial u}{\partial x}\frac{\partial v}{\partial y} - \frac{\partial u}{\partial y}\frac{\partial v}{\partial x} \neq 0.$$

By considering $x = x(u, v)$ and $y = y(u, v)$, one can also write

$$\begin{aligned} dx &= \frac{\partial x}{\partial u}du + \frac{\partial x}{\partial v}dv, \\ dy &= \frac{\partial y}{\partial u}du + \frac{\partial y}{\partial v}dv. \end{aligned} \tag{4}$$

*This treatment also follows ref. 7.

Equating like terms in (3) and (4) and assuming $J \neq 0$:

$$J \frac{\partial x}{\partial u} = \frac{\partial v}{\partial y}, \quad J \frac{\partial x}{\partial v} = - \frac{\partial u}{\partial y},$$
$$J \frac{\partial y}{\partial u} = - \frac{\partial v}{\partial x}, \quad J \frac{\partial y}{\partial v} = \frac{\partial u}{\partial x}. \tag{5}$$

Putting (5) in (1) and rearranging terms:

$$(a^2 - v^2) \frac{\partial x}{\partial u} + uv \frac{\partial y}{\partial u} + uv \frac{\partial x}{\partial v} + (a^2 - u^2) \frac{\partial y}{\partial v} = 0,$$
$$0 \frac{\partial x}{\partial u} - \frac{\partial y}{\partial u} + \frac{\partial x}{\partial v} + 0 \frac{\partial y}{\partial v} = 0. \tag{6}$$

Equations (6) can now be treated just as (1) was treated in appendix 2. Let

$$\underset{\sim}{Z} \equiv [x, y],$$
$$O_i \equiv \frac{\partial O}{\partial i},$$
$$A \equiv \begin{bmatrix} a^2 - v^2 & uv \\ 0 & -1 \end{bmatrix}, \tag{7}$$
$$B \equiv \begin{bmatrix} uv & a^2 - u^2 \\ 1 & 0 \end{bmatrix},$$

and (6) becomes

$$A \underset{\sim}{Z}_u + B \underset{\sim}{Z}_v = 0. \tag{8}$$

Equation (8) can be solved for $\underset{\sim}{Z}_u$ which yields

$$\underset{\sim}{Z}_u + A^{-1} B \underset{\sim}{Z}_v = 0 \tag{9}$$

where

$$A^{-1}B = \begin{bmatrix} \frac{2uv}{a^2 - v^2} & \frac{a^2 - u^2}{a^2 - v^2} \\ -1 & 0 \end{bmatrix} \quad \text{if } |A| = v^2 - a^2 \neq 0. \tag{10}$$

The characteristic condition is:

$$Q = \left| A^{-1}B - \tau I \right| = \begin{vmatrix} \frac{2uv}{a^2 - v^2} - \tau & \frac{a^2 - u^2}{a^2 - v^2} \\ -1 & -\tau \end{vmatrix} = \tau^2 - \frac{2uv}{a^2 - v^2} \tau + \frac{a^2 - u^2}{a^2 - v^2} = 0 \tag{11}$$

which has roots

$$\tau_{1,2} = \frac{uv \pm a\sqrt{u^2 + v^2 - a^2}}{a^2 - v^2} . \tag{12}$$

This system is therefore hyperbolic if

$$u^2 + v^2 - a^2 > 0. \tag{13}$$

The null vectors $\underset{\sim}{\ell}^{\alpha}$ are then found to be:

$$\ell_1^{1,2} = - \frac{uv \pm a\sqrt{u^2 + v^2 - a^2}}{a^2 - u^2} \ell_2^{1,2} . \tag{14}$$

Using $\underset{\sim}{\ell}^{\alpha}$ in (9), the compatibility equations are:

$$\begin{aligned} \left(\frac{uv + a\sqrt{u^2 + v^2 - a^2}}{u^2 - a^2}\right) D_1 x &= D_1 y, \\ \left(\frac{uv - a\sqrt{u^2 + v^2 - a^2}}{u^2 - a^2}\right) D_2 x &= D_2 y. \end{aligned} \tag{15}$$

If the characteristic curves in the u, v plane are designated by Γ, then:

$$\Gamma_1 : \frac{dv}{du} = \tau_1 = - \left(\frac{uv + a\sqrt{u^2 + v^2 - a^2}}{v^2 - a^2}\right)$$

along which

$$\left(\frac{uv + a\sqrt{u^2 + v^2 - a^2}}{u^2 - a^2}\right) \frac{dx}{du_1} = \frac{dy}{du_1} , \tag{16}$$

and

$$\Gamma_2 : \frac{dv}{du} = \tau_2 = - \left(\frac{uv - a\sqrt{u^2 + v^2 - a^2}}{v^2 - a^2}\right)$$

along which

$$\left(\frac{uv - a\sqrt{u^2 + v^2 - a^2}}{u^2 - a^2}\right) \frac{dx}{du_2} = \frac{dy}{du_2} .$$

A comparison of equations (16) above and (25) in appendix 2 reveals the relation between the characteristic curves in the x, y plane and the u, v plane. Γ curves in the u, v plane are compatibility conditions in the x, y plane and C curves in the x, y plane are compatibility conditions in the u, v plane.

APPENDIX 4
CONDITIONS AT THE DETONATION FRONT

Consider a detonation front traveling in the -x direction through a rectangular slab of material whose z and x dimensions are infinite. Let D be the speed with which the front moves. To consider this as a steady state problem, the detonation front is brought to rest and assumed to be located at x = 0. The following diagrams may prove helpful in visualizing the process:

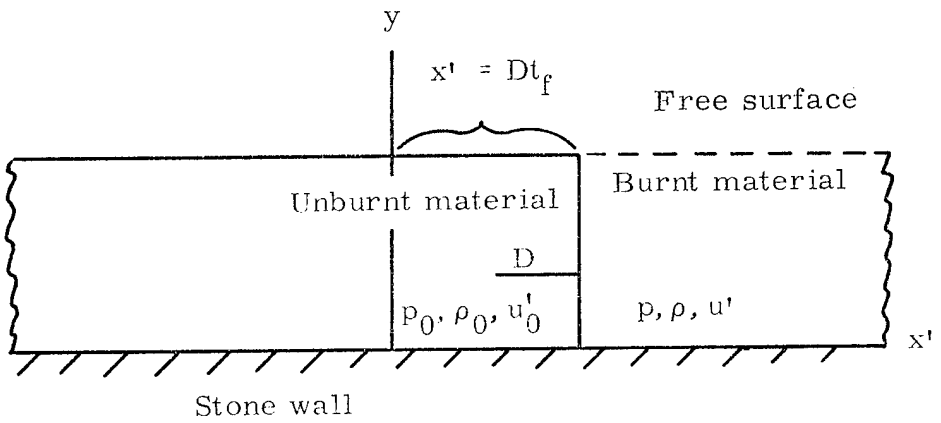

Fig. 20

The transformation -u' + D is made to bring the front to rest and (x' - Dt_f) is made to put the front at the x = 0 position. Since the slab is infinite in the x direction this last does not really play a part. The diagram now becomes:

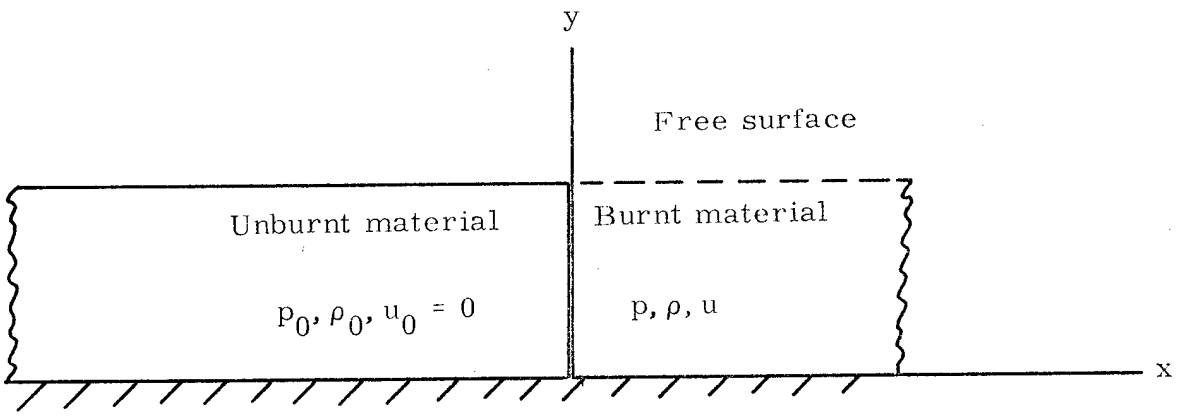

Fig. 21

At the front now the particle velocity of burnt material is $u = D - u'$ in the x direction, $v = 0$ in the y direction, where u is positive if it is in the positive x direction and v is positive if it is in the positive y direction.

The problem considered in this paper deals with the material behind the front (burnt material) and this latter coordinate system is the one used. In that case the velocity u is the velocity in the x' direction relative to the detonation front so that at $x = 0$, $u = a_{c-j}$ where a_{c-j} is the sound speed at the detonation front as determined by the Chapman-Jouguet hypothesis (see ref. 2, p. 212).

In order to determine a_{c-j} and, therefore, u at $x = 0$ consider Fig. 20 above in conjunction with the Rankine-Hugoniot equations, with the detonation speed D in place of the shock speed (see ref. 1, p. 3), that hold at the front:

$$D = \frac{(u' - u'_0)\rho}{\rho - \rho_0}, \tag{1}$$

$$p - p_0 = \rho_0 D(u' - u'_0). \tag{2}$$

For an ideal gas the sound speed at the front is given by

$$a^2_{c-j} = \frac{\gamma p}{\rho}. \tag{3}$$

The statement $u = a_{c-j}$ is equivalent to the Chapman-Jouguet hypothesis that holds at the front and may be written as

$$a_{c-j} + u' = D. \tag{4}$$

By considering the unburnt material to be at rest with $p_0 \ll p$, equations (1) and (2) become:

$$D = \frac{\rho u'}{\rho - \rho_0}, \tag{5}$$

$$p = \rho_0 D u'. \tag{6}$$

From (5) solve for

$$\frac{\rho_0}{\rho} = \frac{D - u'}{D}. \tag{7}$$

From (4) solve for

$$a_{c-j} = D - u' \ .$$

Using (3) in this last expression:

$$(D - u')^2 = \frac{\gamma p}{\rho} \ .$$

Putting (6) in this expression:

$$(D - u')^2 = \frac{\gamma \rho_0 D u'}{\rho}$$

which may be solved for

$$\frac{\rho_0}{\rho} = \frac{(D - u')^2}{\gamma D u'} \tag{8}$$

Combining (7) and (8) yields

$$\frac{D - u'}{D} = \frac{(D - u')^2}{\gamma D u'}$$

which becomes

$$\frac{D - u'}{\gamma u'} = 1 \ .$$

If now this expression is solved for,

$$u' = \frac{D}{\gamma + 1}, \tag{9}$$

and u' is substituted from (9) into (8), a_{c-j} may be written in terms of D as

$$a_{c-j} = \frac{\gamma}{\gamma + 1} D. \tag{10}$$

Hence, the boundary conditions at the detonation front are

$$u = a_{c-j} = \frac{\gamma}{\gamma + 1} D \text{ at } x = 0 \tag{11}$$

and

$$v = 0 \text{ at } x = 0.$$

If $\gamma = 3$, (11) is seen to be

$$u = a_{c-j} = \frac{3}{4} D \text{ at } x = 0,$$
$$v = 0 \text{ at } x = 0. \tag{12}$$

APPENDIX 5

GENERAL RELATIONS BETWEEN THE CHARACTERISTIC CURVES IN THE x, y PLANE AND THOSE IN THE u, v PLANE*

Introducing parameters α, β along characteristic curves C^+ and C^- respectively, the characteristic equations (25), appendix 2, and (16), appendix 3, may be written as:

$$
\begin{aligned}
C^+: \quad & y_\alpha = \left(\frac{uv + a\sqrt{u^2 + v^2 - a^2}}{u^2 - a^2} \right) x_\alpha, \\
\Gamma^+: \quad & v_\alpha = - \left(\frac{uv + a\sqrt{u^2 + v^2 - a^2}}{v^2 - a^2} \right) u_\alpha, \\
C^-: \quad & y_\beta = \left(\frac{uv - a\sqrt{u^2 + v^2 - a^2}}{u^2 - a^2} \right) x_\beta, \\
\Gamma^-: \quad & v_\beta = - \left(\frac{uv - a\sqrt{u^2 + v^2 - a^2}}{v^2 - a^2} \right) u_\beta,
\end{aligned}
\tag{1}
$$

where $A_\alpha = \frac{dA}{d\alpha}$, etc.

Using (1), one can form

$$
\begin{aligned}
u_\alpha x_\beta + v_\alpha y_\beta &= u_\alpha x_\beta \left[1 - \frac{uv + a\sqrt{u^2 + v^2 - a^2}}{v^2 - a^2} \, \frac{uv - a\sqrt{u^2 + v^2 - a^2}}{u^2 - a^2} \right] \\
&= u_\alpha x_\beta \left[1 - \frac{u^2 v^2 - a^2 (u^2 + v^2 - a^2)}{u^2 v^2 - a^2 u^2 - a^2 v^2 + a^4} \right] = 0,
\end{aligned}
$$

or

$$
\frac{u_\alpha}{v_\alpha} = - \frac{y_\beta}{x_\beta}
$$

which may be written

$$
\left. \frac{du}{dv} \right|_\alpha = - \frac{1}{\left(\frac{dx}{dy} \right)\Big|_\beta} \, . \tag{2}
$$

From (2) one concludes that if Γ^+ and C^- are plotted in the same coordinate system, then Γ^+ is perpendicular to C^-.

*The discussion here follows closely that in ref. 2, p. 259 ff.

Using (1), one can also form

$$u_\beta x_\alpha + v_\beta y_\alpha = u_\beta x_\alpha \left[1 - \frac{uv - a\sqrt{u^2 + v^2 - a^2}}{v^2 - a^2} \; \frac{uv + a\sqrt{u^2 + v^2 - a^2}}{u^2 - a^2}\right]$$

$$= 0,$$

so that one can write

$$\left(\frac{du}{dv}\right)_\beta = - \frac{1}{\left(\frac{dx}{dy}\right)\Big|_\alpha} . \tag{3}$$

From (3), one concludes that if Γ^- and C^+ are plotted in the same coordinate system, then Γ^- is perpendicular to C^+.

Consider a point x, y in the x, y plane. The flow direction θ is given by

$$\tan \theta = \frac{v}{u} . \tag{4}$$

Let the angle between the flow direction at x, y and the tangent to the C^+ curve at x, y be A, and the angle between the horizontal and the tangent to the C^+ curve be ϕ^+, then

$$\phi^+ = \theta + A \text{ (see Fig. 22)}, \tag{5}$$

whence

$$\tan \phi^+ = \tan (\theta + A) = \frac{\tan \theta + \tan A}{1 - \tan \theta \tan A} . \tag{6}$$

Let the angle between the flow direction at x, y and the tangent to the C^- curve at x, y be B, and the angle between the horizontal and the tangent to the C^- curve be ϕ^-, then

$$\phi^- = \theta - B \text{ (see Fig. 22)}, \tag{7}$$

whence

$$\tan \phi^- = \tan(\theta - B) = \frac{\tan \theta - \tan B}{1 + \tan \theta \tan B} . \tag{8}$$

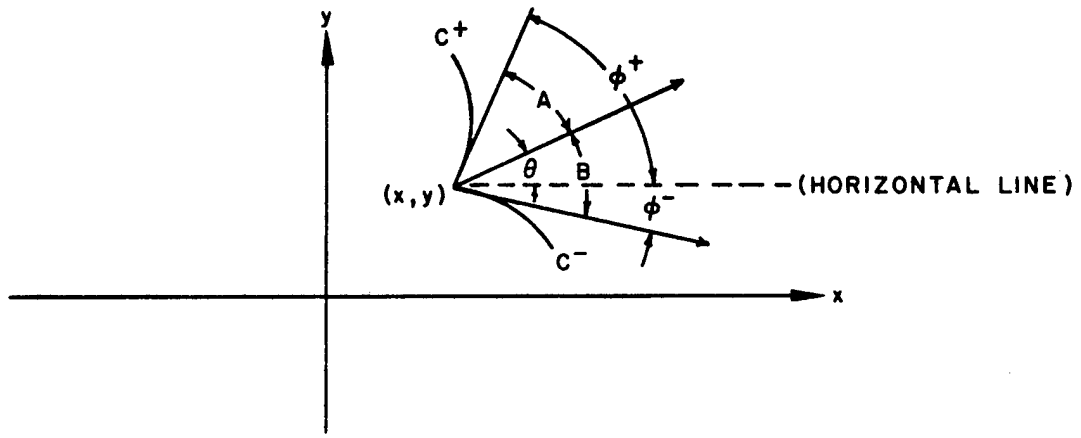

Fig. 22

From equation (1) above it is clear that

$$\tan \phi^{+} = \frac{y_{\alpha}}{x_{\alpha}} = \frac{uv + a\sqrt{u^2 + v^2 - a^2}}{u^2 - a^2}$$

and (9)

$$\tan \phi^{-} = \frac{y_{\beta}}{x_{\beta}} = \frac{uv - a\sqrt{u^2 + v^2 - a^2}}{u^2 - a^2} \quad .$$

From a comparison of (9) with equations (15) and (16) in appendix 2:

$$\tan^2 \phi^{+} + \frac{2uv}{a^2 - u^2} \tan \phi^{+} + \frac{a^2 - v^2}{a^2 - u^2} = 0,$$

and (10)

$$\tan^2 \phi^{-} + \frac{2uv}{a^2 - u^2} \tan \phi^{-} + \frac{a^2 - v^2}{a^2 - u^2} = 0.$$

Using (6) in (10.a),

$$(a^2 - u^2)\left(\frac{\tan \theta + \tan A}{1 - \tan \theta \tan A}\right)^2 + 2uv \frac{\tan \theta + \tan A}{1 - \tan \theta \tan A} + a^2 - v^2 = 0.$$

Clearing fractions and squaring:

$$a^2 \tan^2\theta + 2a^2 \tan \theta \tan A + a^2 \tan^2 A - u^2 \tan^2\theta - 2u^2 \tan \theta \tan A - u^2 \tan^2 A$$

$$+ 2uv \tan \theta + 2uv \tan A - 2uv \tan^2\theta \tan A - 2uv \tan \theta \tan^2 A + a^2$$

$$- 2a^2 \tan \theta \tan A + a^2 \tan^2\theta \tan^2 A - v^2 + 2v^2 \tan \theta \tan A - v^2 \tan^2\theta \tan^2 A = 0.$$

Using (4) in the above after eliminating the terms whose sum is zero:

$$a^2 \frac{v^2}{u^2} + a^2 \tan^2 A - v^2 - 2uv \tan A - u^2 \tan^2 A + 2v^2 + 2uv \tan A$$

$$- 2 \frac{v^3}{u} \tan A - 2v^2 \tan^2 A + a^2 + a^2 \frac{v^2}{u^2} \tan^2 A - v^2 + 2 \frac{v^3}{u} \tan A - \frac{v^4}{u^2} \tan^2 A = 0,$$

from which

$$\left(a^2 + a^2 \frac{v^2}{u^2}\right)(1 + \tan^2 A) = \tan^2 A \left(u^2 + 2v^2 + \frac{v^4}{u^2}\right).$$

Solving this last for a^2:

$$a^2 = \left(\frac{\tan^2 A}{1 + \tan^2 A}\right) \frac{u^2 + 2v^2 + v^4/u^2}{1 + v^2/u^2} = \left(\frac{\tan^2 A}{\sec^2 A}\right) \frac{u^4 + 2u^2 v^2 + v^4}{u^2 + v^2},$$

and letting $q^2 = u^2 + v^2$,

$$a^2 = q^2 \sin^2 A . \tag{11}$$

Using (4) and (8) in (10.b) by a similar calculation:

$$a^2 = q^2 \sin^2 B . \tag{12}$$

Now at the point (x, y), a and q have some fixed value so that except where $a^2 = u^2$, $u = 0$ or $1 \pm \frac{v}{u} \tan A = 0$,

$$A = B. \tag{13}$$

Hence, with the exceptions noted, the flow direction bisects the angle between C^+ and C^- and since C^+ is perpendicular to Γ^- and C^- is perpendicular to Γ^+, the flow direction bisects the angle between Γ^- and Γ^+.

Let the angle between the flow direction and the Γ^+ curve at the point (u, v) in the u, v plane corresponding to the point (x, y) in the (x, y) plane be A', and the angle between the horizontal and the tangent to the Γ^+ curve be ψ^+, then

$$\psi^+ = \theta + A'$$

or

$$\tan \psi^+ = \frac{\tan \theta + \tan A'}{1 - \tan \theta \tan A'} . \tag{14}$$

From equation (1)

$$\tan \psi^+ = \frac{v_\alpha}{u_\alpha} = -\left(\frac{uv + a\sqrt{u^2 + v^2 - a^2}}{v^2 - a^2}\right), \tag{15}$$

and comparing (15) with equations (11) and (12), appendix 3,

$$\tan^2\psi^+ - \frac{2uv}{a^2 - v^2} \tan \psi^+ + \frac{a^2 - u^2}{a^2 - v^2} = 0. \tag{16}$$

Using (14) and (4) in (16) and solving for a^2:

$$a^2\left(1 + \frac{v^2}{u^2}\right)(1 + \tan^2 A') = u^2 + 2v^2 + \frac{v^4}{u^2}$$

or

$$a^2 = q^2 \cos^2 A' \tag{17}$$

(which is another proof that Γ curves are normal to C curves). Comparing (17) and (11),

$$A' = \frac{\pi}{2} - A, \tag{18}$$

and one concludes that the component of flow normal to a C curve is equal to the sound speed and the component of flow tangent to a Γ curve is equal to the sound speed.

From (2), (3), (9), (14), and (15) it is clear that (1) can be written as

$$\begin{aligned}
&\Gamma^+: \quad v_\alpha = \tan \psi^+ \, u_\alpha , \\
&C^+: \quad y_\alpha = \frac{-1}{\tan \psi^-} x_\alpha , \\
&\Gamma^-: \quad v_\beta = \tan \psi^- \, u_\beta , \\
&C^-: \quad y_\beta = \frac{-1}{\tan \psi^+} x_\beta .
\end{aligned} \tag{19}$$

APPENDIX 6
ANALYTIC SOLUTION FOR CHARACTERISTICS IN THE HODOGRAPH PLANE*

To obtain the solution for Γ curves in the u, v plane, start with equations (15) and (17) from appendix 5:

$$\text{Along } \Gamma^+: \quad \frac{dv}{du} = \tan \psi^+. \tag{1}$$

$$\text{At (u, v):} \quad a^2 = q^2 \cos^2 A'. \tag{2}$$

Again referring to appendix 5:

$$\psi^+ = \theta + A' = \theta - A + \frac{\pi}{2}. \tag{3}$$

From (1):

$$du \sin \psi^+ - dv \cos \psi^+ = 0. \tag{4}$$

From (2) since $a \geq 0$, $q \geq 0$ and $|A'| \leq \frac{\pi}{2}$:

$$a = q \cos A'. \tag{5}$$

From (3):

$$A' = \psi^+ - \theta,$$

whence

$$\cos A' = \cos (\psi^+ - \theta) = \cos \psi^+ \cos \theta + \sin \psi^+ \sin \theta. \tag{6}$$

Since $\tan \theta = \frac{v}{u}$,

$$\sin \theta = \frac{v}{q}, \quad \cos \theta = \frac{u}{q}, \quad \text{where } q = \sqrt{u^2 + v^2}. \tag{7}$$

Using (6) and (7) in (5):

$$a = v \sin \psi^+ + u \cos \psi^+. \tag{8}$$

In appendix 5 it is shown that a ($\equiv$ sound speed) is the velocity along Γ curves, and to find the velocity g normal to the Γ curves note that the flow velocity $\underset{\sim}{q}$ is given by

$$\underset{\sim}{q} = u \underset{\sim}{i} + v \underset{\sim}{j}, \tag{9}$$

where $\underset{\sim}{i}$ and $\underset{\sim}{j}$ are unit vectors along u and v respectively, and that the unit vector along Γ^+ is

*This discussion follows ref. 2, p. 264 ff.

$$\underset{\sim}{n} = \underset{\sim}{i} \cos\psi^+ + \underset{\sim}{j} \sin\psi^+ . \tag{10}$$

Since a is the component of $\underset{\sim}{q}$ along Γ^+,

$$a = \underset{\sim}{q} \cdot \underset{\sim}{n} = u \cos\psi^+ + v \sin\psi^+$$

which checks with (8). To find the normal component of $\underset{\sim}{q}$, one takes the inner product of $\underset{\sim}{q}$ with $\underset{\sim}{\nu}$, the unit normal to Γ^+. To find $\underset{\sim}{\nu}$, note that

$$\underset{\sim}{\nu} = \frac{dn}{d\psi^+} = - \underset{\sim}{i} \sin\psi^+ + j \cos\psi^+, \tag{11}$$

whence

$$g = \underset{\sim}{q} \cdot \underset{\sim}{\nu} = v \cos\psi^+ - u \sin\psi^+. \tag{12}$$

Next, solve (8) and (12) for u and v in terms of a and g:

$$a = u \cos\psi^+ + v \sin\psi^+,$$

$$g = -u \sin\psi^+ + v \cos\psi^+.$$

The determinant of coefficients, D, is

$$D = \begin{vmatrix} \cos\psi^+ & \sin\psi^+ \\ -\sin\psi^+ & \cos\psi^+ \end{vmatrix} = 1$$

whence

$$u = \begin{vmatrix} a & \sin\psi^+ \\ g & \cos\psi^+ \end{vmatrix} = a \cos\psi^+ - g \sin\psi^+, \tag{13}$$

$$v = \begin{vmatrix} \cos\psi^+ & a \\ -\sin\psi^+ & g \end{vmatrix} = g \cos\psi^+ + a \sin\psi^+. \tag{14}$$

The solution, then, is obtained by considering ψ^+ as the variable along Γ^+ and determining a and g as functions of ψ^+.

Using (13) and (14):

$$\begin{aligned} \frac{du}{d\psi^+} &= - a \sin\psi^+ + a_{\psi^+} \cos\psi^+ - g \cos\psi^+ - g_{\psi^+} \sin\psi^+, \\ \frac{dv}{d\psi^+} &= - g \sin\psi^+ + g_{\psi^+} \cos\psi^+ + a \cos\psi^+ + a_{\psi^+} \sin\psi^+. \end{aligned} \tag{15}$$

Dividing (4) by $d\psi^+$:

$$\frac{du}{d\psi^+} \sin\psi^+ - \frac{dv}{d\psi^+} \cos\psi^+ = 0,$$

which upon substitution from (15) yields

$$- a \sin^2\psi^+ + a_{\psi^+} \sin\psi^+ \cos\psi^+ - g \sin\psi^+ \cos\psi^+ - g_{\psi^+} \sin^2\psi^+$$

$$+ g \sin\psi^+ \cos\psi^+ - g_{\psi^+} \cos^2\psi^+ - a \cos^2\psi^+ - a_{\psi^+} \sin\psi^+ \cos\psi^+ = 0$$

or

$$- a (\sin^2\psi^+ + \cos^2\psi^+) - g_{\psi^+}(\cos^2\psi^+ + \sin^2\psi^+) = 0,$$

whence

$$g_{\psi^+} = - a. \tag{16}$$

Using equation (21) from appendix 1 and equation (11) from appendix 4:

$$\frac{2}{\gamma - 1} a^2 + u^2 + v^2 = \frac{2}{\gamma - 1} a^2 + q^2 = \frac{2}{\gamma - 1} \left(a^2_{c-j}\right) + \left(a^2_{c-j}\right) + 0 = \frac{\gamma + 1}{\gamma - 1} a^2_{c-j}$$

or

$$\frac{2a^2}{\gamma - 1} = \frac{\gamma + 1}{\gamma - 1} a^2_{c-j} - q^2,$$

and if we let $\mu^2 = \frac{\gamma - 1}{\gamma + 1}$, then

$$\frac{2a^2}{\gamma - 1} = \frac{a^2_{c-j}}{\mu^2} - q^2 \quad \text{or} \quad \frac{a^2_{c-j}}{\mu^2} = q^2 + \frac{2a^2}{\gamma - 1}. \tag{17}$$

Since a and g are orthogonal components of q,

$$q^2 = a^2 + g^2, \tag{18}$$

so that using (18) in (17) yields

$$\frac{a^2_{c-j}}{\mu^2} - \frac{2a^2}{\gamma - 1} - a^2 = \frac{a^2_{c-j}}{\mu^2} - a^2\left(\frac{2 + \gamma - 1}{\gamma - 1}\right) = \frac{a^2_{c-j} - a^2}{\mu^2} = g^2$$

or

$$\frac{a^2_{c-j} - a^2}{\mu^2} = g^2. \tag{19}$$

Differentiating (19):

$$-\frac{2a\, a_{\psi^+}}{\mu^2} = 2g\, g_{\psi^+}. \tag{20}$$

Putting (16) in (20):

$$-a\, a_{\psi^+} = -\mu^2 ga$$

or

$$a_{\psi^+} = \mu^2 g\,. \tag{21}$$

Then the problem is reduced to solving (16) and (21). In addition, note the boundary condition from (19):

$$g = 0 \text{ when } a = a_{c-j}\,. \tag{22}$$

Operating on (16),

$$\frac{d^2g}{d(\psi^+)^2} + \frac{da}{d\psi^+} = 0,$$

and using (21),

$$\frac{d^2g}{d(\psi^+)^2} + \mu^2 g = 0,$$

whence

$$g = E \sin \mu(\psi^+ - \psi^+_*), \text{ where E and } \psi^+_* \text{ are constants.} \tag{23}$$

Using (23) in (21),

$$\frac{da}{d\psi^+} = \mu^2 E \sin \mu(\psi^+ - \psi^+_*),$$

whence

$$a = -\mu\, E \cos \mu(\psi^+ - \psi^+_*) + F, \text{ where F is a constant.} \tag{24}$$

Using the condition (22) in (23)

$0 = g = E \sin(\psi_0^+ - \psi_*^+)$, where ψ_0^+ is the value of ψ^+ at $a = a_{c-j}$.

This condition is satisfied if

$$\psi_0^+ = \psi_*^+,$$

and using this in (24), assuming $\Gamma = 0$,

$$a_{c-j} = -\mu E \quad \text{or} \quad E = -\frac{a_{c-j}}{\mu},$$

whence

$$a = a_{c-j} \cos \mu(\psi^+ - \psi_*^+) \text{ and } g = -\frac{a_{c-j}}{\mu} \sin \mu(\psi^+ - \psi_*^+). \tag{25}$$

Physically $a \geq 0$, so that

$$\left|\psi^+ - \psi_*^+\right| \leq \frac{\pi}{2\mu}.$$

It is shown in appendix 5 that θ bisects the angle between the Γ^+ and the Γ^- curves so that we can write the equations for Γ^- that correspond to (1), (2), and (3) as:

Along Γ^-: $\frac{dv}{du} = \tan \psi^-$. (26)

At (u, v): $a^2 = q^2 \cos^2 A'$, (27)

$$\psi^- = \theta - A'. \tag{28}$$

From (26):

$$du \sin \psi^- - dv \cos \psi^- = 0. \tag{29}$$

From (27),

$$a = q \cos A'. \tag{30}$$

From (28),

$$A' = \theta - \psi^-, \tag{31}$$

and from (31),

$$\cos A' = \cos(\theta - \psi^-) = \cos \theta \cos \psi^- + \sin \theta \sin \psi^-. \tag{32}$$

Now by inspection it is seen that (29), (30), and (32) are the same as (4), (5), and (6) with ψ^+ replaced by ψ^-. Hence, the equations for the Γ^- curves are

$$a = a_{c-j} \cos \mu(\psi^- - \psi_*^-) \text{ and } g = -\frac{a_{c-j}}{\mu} \sin \mu(\psi^- - \psi_*^-) \tag{33}$$

with

$$\left|\psi^- - \psi^-_*\right| \leq \frac{\pi}{\mu 2}\,.$$

From (12) and (3), along Γ^+:

$$g = v\cos\psi^+ - u\sin\psi^+ = v\cos(\theta + A') - u\sin(\theta + A')$$

$$= v\cos\theta\cos A' - v\sin\theta\sin A' - u\sin\theta\cos A' - u\cos\theta\sin A'.$$

Using (7):

$$g = \frac{uv}{q}\cos A' - \frac{v^2}{q}\sin A' - \frac{uv}{q}\cos A' - \frac{u^2}{q}\sin A' = -\frac{q^2}{q}\sin A'.$$

But $A' = \frac{\pi}{2} - A$ (see equation (18), appendix 5), whence

$$g = -q\sin\left(\frac{\pi}{2} - A\right) = -q\cos A, \text{ along } \Gamma^+. \tag{34}$$

From the dual of (12) for ψ^- and (28), along Γ^-:

$$g = v\cos\psi^- - v\sin\psi^- = v\cos(\theta - A') - u\sin(\theta - A')$$

$$= v\cos\theta\cos A' + v\sin\theta\sin A' - u\sin\theta\cos A' + u\cos\theta\sin A'.$$

Using (7):

$$g = \frac{uv}{q}\cos A' + \frac{v^2}{q}\sin A' - \frac{uv}{q}\cos A' + \frac{u^2}{q}\sin A'$$

but $A' = \pi/2 - A$, whence

$$g = q\sin A' = q\sin\left(\frac{\pi}{2} - A\right) = q\cos A, \text{ along } \Gamma^-. \tag{35}$$

From (34) and (35), since $|A| \leq \pi/2$, one concludes

$$g \leq 0 \text{ for } \Gamma^+, \text{ and } g \geq 0 \text{ for } \Gamma^- \text{ curves.} \tag{36}$$

Using (36) in (33) and (25):

$$\psi^+ \geq \psi^+_* \text{ and } \psi^- \leq \psi^-_*\,. \tag{37}$$

Let ψ be the variable along either Γ curve, then using (13) the solution for Γ curves is given by:

$$\frac{u}{a_{c-j}} = \cos\mu(\psi - \psi_*)\cos\psi + \frac{1}{\mu}\sin\mu(\psi - \psi_*)\sin\psi,$$

$$\frac{v}{a_{c-j}} = \cos\mu(\psi - \psi_*)\sin\psi - \frac{1}{\mu}\sin\mu(\psi - \psi_*)\cos\psi. \tag{38}$$

In order to see what the equations look like, proceed as follows:

$$\frac{u}{a_{c-j}} = \cos\mu(\psi - \psi_*)\cos\psi + \frac{1}{\mu}\sin\mu(\psi - \psi_*)\sin\psi$$

$$= \left(\frac{1}{2\mu} + \frac{1}{2}\right)\cos\psi\cos\mu(\psi - \psi_*) + \left(\frac{1}{2\mu} + \frac{1}{2}\right)\sin\psi\sin\mu(\psi - \psi_*)$$

$$- \left(\frac{1}{2\mu} - \frac{1}{2}\right)\cos\psi\cos\mu(\psi - \psi_*) + \left(\frac{1}{2\mu} - \frac{1}{2}\right)\sin\psi\sin\mu(\psi - \psi_*)$$

$$= \frac{1}{2}\left(\frac{1}{\mu} + 1\right)\cos\left[\psi - \mu(\psi - \psi_*)\right] - \frac{1}{2}\left(\frac{1}{\mu} - 1\right)\cos\left[\psi + \mu(\psi - \psi_*)\right],$$

or

$$\frac{u}{a_{c-j}} = \frac{1}{2}\left(\frac{1}{\mu} + 1\right)\cos\left[(\psi - \psi_*)(1 - \mu) + \psi_*\right] - \frac{1}{2}\left(\frac{1}{\mu} - 1\right)\cos\left[(\psi - \psi_*)(1 + \mu) + \psi_*\right]. \tag{39}$$

Now let

$$\bar{q} = \frac{1}{2}\left(\frac{1}{\mu} - 1\right)a_{c-j}, \tag{40}$$

then

$$\frac{1}{2}\left(\frac{1}{\mu} + 1\right)a_{c-j} = \frac{1}{2}\left(\frac{1}{\mu} - 1\right)a_{c-j} + a_{c-j} = \bar{q} + a_{c-j}. \tag{41}$$

Using (40) and (41) in (39):

$$u = (a_{c-j} + \bar{q})\cos\left[(1 - \mu)(\psi - \psi_*) + \psi_*\right] - \bar{q}\cos\left[(1 + \mu)(\psi - \psi_*) + \psi_*\right]. \tag{42}$$

From (40):

$$\mu = \frac{a_{c-j}}{2\bar{q} + a_{c-j}} \quad \text{and} \quad 1 - \mu = \frac{2\bar{q}}{2\bar{q} + a_{c-j}}, \tag{43}$$

and

$$1 + \mu = \frac{2\bar{q} + 2a_{c-j}}{2\bar{q} + a_{c-j}} = \left(\frac{2\bar{q}}{2\bar{q} + a_{c-j}}\right)\left(\frac{\bar{q} + a_{c-j}}{\bar{q}}\right) = (1 - \mu)\frac{\bar{q} + a_{c-j}}{\bar{q}}. \tag{44}$$

Using (43) and (44), (42) becomes:

$$u = (a_{c-j} + \bar{q}) \cos\left[(1 - \mu)(\psi - \psi_*) + \psi_*\right] - \bar{q} \cos\left[(1 - \mu)\frac{a_{c-j} + \bar{q}}{\bar{q}}(\psi - \psi_*) + \psi_*\right]. \tag{45}$$

Let

$$\beta = (1 - \mu)(\psi - \psi_*), \tag{46}$$

then (45) becomes

$$u = (a_{c-j} + \bar{q}) \cos(\beta + \psi_*) - \bar{q} \cos\left[\frac{a_{c-j} + \bar{q}}{\bar{q}}\beta + \psi_*\right]. \tag{47}$$

Similarly one finds that

$$v = (a_{c-j} + \bar{q}) \sin(\beta + \psi_*) - \bar{q} \sin\left[\frac{a_{c-j} + \bar{q}}{\bar{q}}\beta + \psi_*\right]. \tag{48}$$

Equations (47) and (48) are the parametric equations for an epicycloid generated by a circle of radius $\bar{q}$ rolling on a circle of radius a_{c-j} (see appendix 7).

Now let

$$\hat{q}^2 = \frac{a_{c-j}^2}{\mu^2} \text{ and hence, } \hat{q} = \frac{a_{c-j}}{\mu}, \tag{49}$$

then from (17):

$$q^2 + \frac{2a^2}{\gamma - 1} = \hat{q}^2 \tag{50}$$

and

$$\hat{q} - a_{c-j} = \frac{a_{c-j}}{\mu} - a_{c-j} = \left(\frac{1}{\mu} - 1\right) a_{c-j} = 2\bar{q}. \tag{51}$$

From (51) it is seen that the circle of radius $\bar{q}$ also rolls on the inside of the circle of radius $\hat{q}$. On the circle $u^2 + v^2 = a_{c-j}^2$, the speed (q) is the Chapman-Jouguet sound speed, hence this circle is called the "sonic circle." One then can say that equations (47) and (48) are epicycloids generated by a circle rolling between the sonic circle and the circle of radius $\hat{q} = \frac{a_{c-j}}{\mu}$.

Note also that from (50), when $q = \hat{q}$, $a = 0$ and conversely. This indicates that the circle $q^2 = \hat{q}^2$ is the locus of points (x, y) where there is no material or where the pressure is zero (see equation (19), appendix 1).

To investigate the mapping of x, y points to u, v points nondimensionalize (47) and (48) be letting

$$u = a_{c\text{-}j}\frac{\delta}{2} \quad \text{and} \quad v = a_{c\text{-}j}\frac{\lambda}{2} \tag{52}$$

and

$$R_2 = \frac{1}{\mu} + 1, \quad R_3 = \frac{1}{\mu} - 1 \tag{53}$$

so that substituting from (40), (41), and (44) into (47) and (48),

$$\begin{aligned} \delta &= R_2 \cos(\beta + \psi_*) - R_3 \cos\left(\frac{R_2}{R_3}\beta + \psi_*\right), \\ \lambda &= R_2 \sin(\beta + \psi_*) - R_3 \sin\left(\frac{R_2}{R_3}\beta + \psi_*\right). \end{aligned} \tag{54}$$

Using (43) and (46),

$$\beta = (1 - \mu)(\psi - \psi_*)$$

or

$$\psi - \psi_* = \frac{\beta}{1 - \mu}. \tag{55}$$

From (37) one concludes, since $1 - \mu = 1 - \left(\frac{\gamma - 1}{\gamma + 1}\right)^{1/2} > 0$, that Γ^+ curves are generated by $\beta \geq 0$, and Γ^- curves are generated by $\beta \leq 0$.

In other words, Γ^+ curves are generated by rolling the circle of radius $\bar{q}$ counterclockwise around the "sonic" circle, while Γ^- curves are generated by clockwise rotation. β is the angle subtended at the center of the "sonic" circle by the center of the circle of radius $\bar{q}$ as it rolls from its initial position to its current position, and ψ_* is the angle subtended at the center of the "sonic" circle between the radius vector to the center of the circle of radius $\bar{q}$ at its initial position and the positive u axis (see appendix 7).

From (33) and (25),

$$\left|\psi - \psi_*\right| \leq \frac{\pi}{2\mu},$$

and from (55),

$$\frac{1}{1 - \mu}\left|\beta\right| \leq \frac{\pi}{2\mu},$$

whence

$$|\beta| \leq \frac{\pi(1 - \mu)}{2\mu}, \tag{56}$$

and for $\gamma = 3$, $\mu = (2/4)^{1/2} = 1/\sqrt{2}$ so that $\frac{1 - \mu}{2} = \frac{\sqrt{2} - 1}{2\sqrt{2}}$ or

$|\beta| \leq \frac{\pi(\sqrt{2} - 1)}{2} \approx 37.26°$.

Suppose one considers the semi-infinite slab of H. E. (shown by the dotted line in Fig. 23a before detonation) in the x, y plane. In appendix 4 it is shown that along the detonation front (x = 0), $v = \lambda = 0$ and $u = a_{c\text{-}j} = \frac{\gamma}{\gamma + 1} D$ or $\delta = 2$. Hence, the entire line [1]-[4] in the x, y plane is mapped to the point $\delta = 2$, $\lambda = 0$ in the δ, λ plane (see Figs. 23a and b). From (54) this corresponds to $\beta = 0$, $\psi_* = 0$. Along y = 0, $v = \lambda = 0$ so that the x axis is mapped to the u axis between the "sonic" circle and the circle of radius $\hat{q}$. Along the line [4]-[5], $p = a = 0$, and as stated above all points where a = 0 are mapped to the circle $q^2 = \hat{q}^2$. Since there must be contact between the lines [4]-[5] and [4]-[1], the point [4] in the x, y plane is a singular point and is mapped to the Γ_0^+ curve that runs between the "sonic" circle and the circle of radius $\hat{q}$ from the point $\delta = 2$, $\lambda = 0$.

To see that [4]-[5] is indeed a straight line in the x, y plane, note that (37) implies that the Γ^+ and Γ^- curves are generated by rolling the generating circle counterclockwise and clockwise, respectively, so that the Γ curves at the point [4, 5] in the u, v plane are both tangent to the circle $q^2 = \hat{q}^2$ there. Since the flow direction $\underset{\sim}{q}$ bisects the tangent to each of Γ^+ and Γ^-, $\underset{\sim}{q}$ is normal to this circle at [4, 5]. Referring to equation (25), appendix 2, it is seen that a = 0 gives the slope of both C curves since $v/u = \tan\theta \equiv$ direction of the flow. However, the flow direction bisects the angle between C^+ and C^- curves and, in this case, must be collinear with them, so that the image in the x, y plane of [4, 5] is the flow direction of points on the upper boundary and has constant slope.

Considering the Γ_0^+ curve and (56) it is seen that the value of β at [4, 5] is given by

$$\beta = \frac{\pi(1 - \mu)}{2\mu},$$

and to generate all other Γ^+ curves in the region bounded by $\lambda = 0$, Γ_0^+, and $q^2 = \hat{q}^2$, one lets ψ_*^+ vary from 0 to $\left[-\frac{\pi(1 - \mu)}{2\mu}\right] = \psi_{v*}^+$ with the lower limit of β for each ψ_*^+ value being determined by $\lambda = 0$. Similarly, the Γ^- curves are

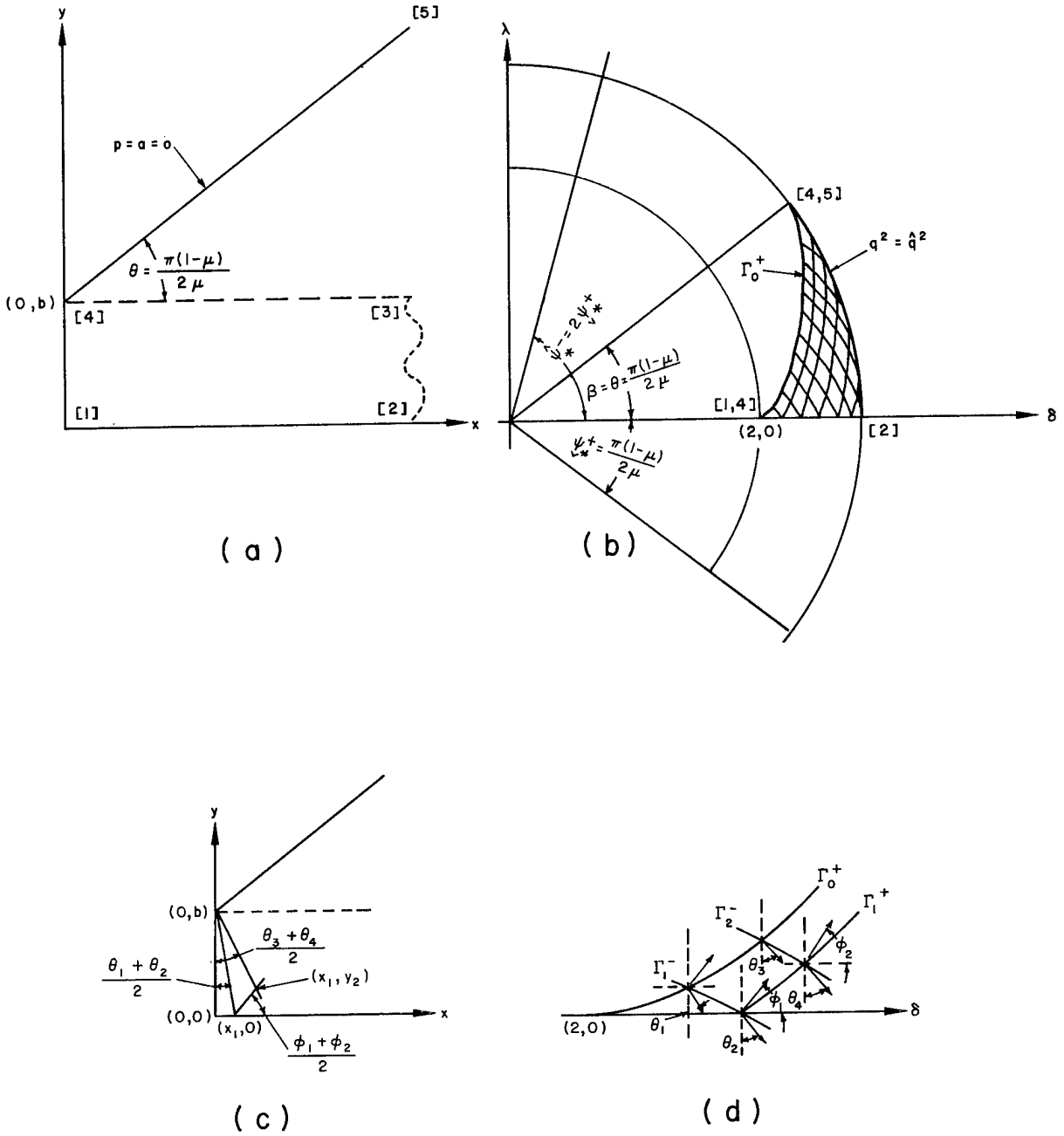

Fig. 23. Mapping.

determined by letting ψ_*^- vary between 0 and $\frac{\pi(1-\mu)}{\mu} = \hat{\psi}_*^-$ with $\beta < 0$ and the limits of β determined by Γ_0^+ and $\lambda = 0$ for $0 \leq \psi_*^- \leq \frac{\pi(1-\mu)}{2\mu}$ and by Γ_0^+ and $\beta = -\frac{\pi(1-\mu)}{2\mu}$ for $\frac{\pi(1-\mu)}{2\mu} \leq \psi_*^- \leq \hat{\psi}_*^-$. It is seen that points in the δ, λ plane are determined by assigning a pair of values ψ_*^+, ψ_*^-. Note also that along $\lambda = 0$, the intersection of a Γ^+ and Γ^- curve occurs where $\psi_*^- = -\psi_*^+$ by the way in which these curves are generated.

Using (43) and (46) above:

$$\psi = \frac{\beta}{1-\mu} + \psi_* \tag{57}$$

so that

$$\psi^+ = \frac{\beta^+}{1-\mu} + \psi_*^+ \text{ and } \psi^- = \frac{\beta^-}{1-\mu} + \psi_*^- . \tag{58}$$

Hence, by using (57) and (58) in (52) and (54), one can write equations (19) of appendix 5 as:

$$\Gamma^+: \quad \frac{2u}{a_{c-j}} = R_2 \cos\left(\beta^+ + \psi_*^+\right) - R_3 \cos\left(\frac{R_2}{R_3}\beta^+ + \psi_*^+\right),$$

$$\frac{2v}{a_{c-j}} = R_2 \sin\left(\beta^+ + \psi_*^+\right) - R_3 \sin\left(\frac{R_2}{R_3}\beta^+ + \psi_*^+\right), \tag{59}$$

$$C^+: \quad y_{\beta^+} = \frac{-1}{\tan\left(\frac{\beta^-}{1-\mu} + \psi_*^-\right)} x_{\beta^+}, \tag{60}$$

$$\Gamma^-: \quad \frac{2u}{a_{c-j}} = R_2 \cos\left(\beta^- + \psi_*^-\right) - R_3 \cos\left(\frac{R_2}{R_3}\beta^- + \psi_*^-\right),$$

$$\frac{2v}{a_{c-j}} = R_2 \sin\left(\beta^- + \psi_*^-\right) - R_3 \sin\left(\frac{R_2}{R_3}\beta^- + \psi_*^-\right), \tag{61}$$

$$C^-: \quad y_{\beta^-} = \frac{-1}{\tan\left(\frac{\beta^+}{1-\mu} + \psi_*^+\right)} x_{\beta^-} . \tag{62}$$

In appendix 2 (equation (17)) it was stated that $u^2 + v^2 - a^2 > 0$ was the condition for a hyperbolic system of equations and this condition has been assumed when (58)-(62) are given as the solution. However, at the detonation front itself $u = a_{c-j}$, $v = 0$, and $a = a_{c-j}$, whence $u^2 + v^2 - a^2 = 0$ and the

system is parabolic with the front, the line [1]-[4] in Fig. 23, in the x, y plane being both a C^+ and a C^- characteristic. This means that the solution in the region of interest, i.e., that enclosed by the lines [2]-[1], [1]-[4], [4]-[5] in the x, y plane, cannot be obtained from the known information at the front since no characteristic curves intersect the front and move into the region of interest. In the u, v plane the situation is different.

Recall that the detonation front in the x, y plane is, except for the point [4], mapped to the single point $u = a_{c-j}$, $v = 0$ in the u, v plane and the point [4] is mapped to the line Γ_0^+. Therefore along Γ_0^+ the values of x, y are known, i.e., $x = 0$, $y = b$. Along $v = 0$ the values of y are known ($y = 0$) and along $q^2 = \hat{q}^2$, $x = \infty$, and $y = \infty$ while at $u = a_{c-j}$, $v = 0$, $x = 0$, $0 \leq y \leq b$. If the point $u = a_{c-j}$, $v = 0$ is avoided then the problem can be solved by working in both planes.

In the u, v plane the problem is completely solved for u and v. Near the point $u = a_{c-j}$, $v = 0$, the Γ^- curves connecting Γ_0^+ and $v = 0$ are short (relatively) and it seems clear that at least one can be found which is accurately approximated by a straight line. The values of β and ψ_* can be selected for a point on both Γ_0^+ and $v = 0$ and x and y are known on Γ_0^+ while $y = 0$ on $v = 0$. In other words only x on $v = 0$ is not known. However, along the Γ^- curve connecting these two points, equation (62) can be used in finite difference form to find that x value. Graphically this corresponds to getting the slope of the C^- curve corresponding to this Γ^- curve and extending a line from the point [4] in the x, y plane with this slope until it intersects the line [1]-[2] (see Fig. 23c, d). With this value of x on [1]-[2] the values of x and y on the C^+ curve through this point can be found using (62) along C^- from Γ_0^+ and (60) along C^+ from Γ^- curves. In Fig. 23d the angles θ_1 and θ_2 are measured between the normals to Γ_0^+ and Γ_1^+ and the negative v axis respectively. Their average is used to drop the line from [0, b] in Fig. 23c to [x, 0] thus determining x_1. The values x_2, y_2 are determined similarly using normals to both Γ_1^-, Γ_2^-, and Γ_0^+, Γ_1^+ as indicated. That the procedure works is shown in the example problem considered.

APPENDIX 7
DERIVATION OF THE PARAMETRIC EQUATIONS FOR AN EPICYCLOID

An epicycloid is defined as the path traced out by a point on the circumference of a circle rolling on another circle. To determine the general equation for such a curve, consider the situation depicted in Fig. 24 which shows a part of the path of the point Q on the circle of radius $\bar{q}$ which was originally at point P on the circle of radius a_{c-j}. The two circles are in contact at point R and since there is no slipping allowed, the length along the inner circle from P to R (called C) is the same as the length along the other circle from Q to R.

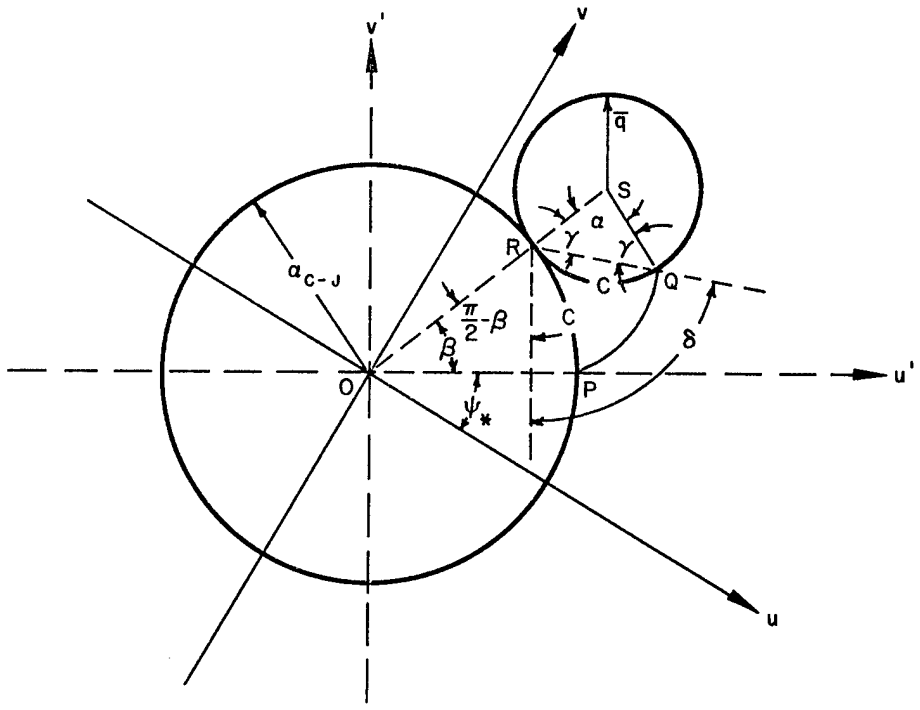

Fig. 24

From Fig. 24, note the following relations:

$$\beta = \frac{C}{a_{c-j}}, \quad \alpha = \frac{C}{\bar{q}}, \tag{1}$$

whence

$$\alpha = \frac{a_{c-j}\beta}{\bar{q}}, \tag{2}$$

$$\alpha + 2\gamma = \pi \quad \text{or} \quad \gamma = \frac{\pi}{2} - \frac{\alpha}{2}, \tag{3}$$

$$\angle \text{ORQ} = \alpha + \gamma. \tag{4}$$

Combining (3) and (4):

$$\angle \text{ORQ} = \frac{\pi}{2} + \frac{\alpha}{2}. \tag{5}$$

Using the law of sines in triangle RSQ:

$$\frac{\overline{RQ}}{\sin \alpha} = \frac{\bar{q}}{\sin \gamma}. \tag{6}$$

Using (3) in (6) and $\sin 2\theta = 2 \sin \theta \cos \theta$:

$$\overline{RQ} = \frac{\bar{q} \sin \alpha}{\sin\left(\frac{\pi}{2} - \frac{\alpha}{2}\right)} = \frac{\bar{q}\ 2 \sin \frac{\alpha}{2} \cos \frac{\alpha}{2}}{\cos \frac{\alpha}{2}} = 2\ \bar{q} \sin \frac{\alpha}{2}. \tag{7}$$

Now using (5):

$$\delta = \angle \text{ORQ} - \left(\frac{\pi}{2} - \beta\right) = \frac{\pi}{2} + \frac{\alpha}{2} - \frac{\pi}{2} + \beta = \beta + \frac{\alpha}{2}. \tag{8}$$

Putting (2) in (8):

$$\delta = \beta + \frac{a_{c-j}\beta}{2\bar{q}}. \tag{9}$$

Putting (2) in (7):

$$\overline{RQ} = 2\ \bar{q} \sin \frac{a_{c-j}\beta}{2\bar{q}}. \tag{10}$$

For the coordinates of the point Q, refer again to Fig. 24:

$$\begin{aligned} u' &= a_{c-j} \cos \beta + \overline{RQ} \sin \delta, \\ v' &= a_{c-j} \sin \beta - \overline{RQ} \cos \delta. \end{aligned} \tag{11}$$

Using (9) and (10) in the first of (11):

$$u' = a_{c-j} \cos \beta + 2\ \bar{q} \sin \frac{a_{c-j}\beta}{2\bar{q}} \sin\left(\beta + \frac{a_{c-j}\beta}{2\bar{q}}\right)$$

$$= a_{c-j} \cos \beta + 2\ \bar{q} \sin \frac{a_{c-j}\beta}{2\bar{q}} \left(\sin \beta \cos \frac{a_{c-j}\beta}{2\bar{q}} + \cos \beta \sin \frac{a_{c-j}\beta}{2\bar{q}}\right).$$

Now, $2 \sin \frac{\theta}{2} \cos \frac{\theta}{2} = \sin \theta$ and $2 \sin^2 \frac{\theta}{2} = 1 - \cos \theta$, so that this last expression may be written as

$$u' = a_{c-j} \cos \beta + \bar{q} \sin \beta \sin \frac{a_{c-j}\beta}{\bar{q}} + \bar{q} \cos \beta - \bar{q} \cos \beta \cos \frac{a_{c-j}\beta}{\bar{q}}$$

or

$$u' = (a_{c-j} + \bar{q}) \cos \beta - \bar{q} \left[\cos \beta \cos \frac{a_{c-j}\beta}{\bar{q}} - \sin \beta \sin \frac{a_{c-j}\beta}{\bar{q}} \right],$$

whence

$$u' = (a_{c-j} + \bar{q}) \cos \beta - \bar{q} \cos \frac{a_{c-j} + \bar{q}}{\bar{q}} \beta \tag{12}$$

Similarly

$$v' = (a_{c-j} + \bar{q}) \sin \beta - \bar{q} \sin \frac{a_{c-j} + \bar{q}}{\bar{q}} \beta . \tag{13}$$

To rotate the u', v' axes through the angle $-\psi_*$ as shown, use the relation

$$u + iv = e^{i\psi_*}(u' + iv'), \text{ where } i = \sqrt{-1}, \tag{14}$$

or

$$\begin{aligned} u &= u' \cos \psi_* - v' \sin \psi_*, \\ v &= u' \sin \psi_* + v' \cos \psi_*. \end{aligned} \tag{15}$$

Using (12) and (13) in (15),

$$u = (a_{c-j} + \bar{q}) \cos \beta \cos \psi_* - \bar{q} \cos \frac{a_{c-j} + \bar{q}}{\bar{q}} \cos \psi_*$$

$$- (a_{c-j} + \bar{q}) \sin \beta \sin \psi_* + \bar{q} \sin \frac{a_{c-j} + \bar{q}}{\bar{q}} \beta \sin \psi_*,$$

or

$$u = (a_{c-j} + \bar{q}) \cos (\beta + \psi_*) - \bar{q} \cos\left(\frac{a_{c-j} + \bar{q}}{\bar{q}} \beta + \psi_* \right), \tag{16}$$

and similarly

$$v = (a_{c-j} + \bar{q}) \sin (\beta + \psi_*) - \bar{q} \sin\left(\frac{a_{c-j} + \bar{q}}{\bar{q}} \beta + \psi_* \right). \tag{17}$$

It is clear from Fig. 24 that $\beta > 0$ generates curves going counterclockwise and $\beta < 0$ generates curves going clockwise, and that to sweep out all the counterclockwise curves one varies ψ_* and similarly for the clockwise curves.

APPENDIX 8
THE NEWTON-RAPHSON METHOD*

If one is given the equation $f(x) = 0$, and lets $x^i + h^i = x$ where x^i is the ith approximation of x and h^i is the error in the ith approximation, then

$$h^i = -\frac{f(x^i)}{f'(x^i)} \quad \text{where } f'(x) = \frac{df}{dx}, \tag{1}$$

and

$$x^{i+1} = x^i + h^i = x^i - \frac{f(x^i)}{f'(x^i)} \; . \tag{2}$$

Let

$$f(\beta) = \sin\left[\beta + \frac{1}{2}(\psi^+ - \psi^-)\right] - \frac{R_3}{R_2}\sin\left[\frac{R_2}{R_3}\beta + \frac{1}{2}(\psi^+ - \psi^-)\right] = 0, \tag{3}$$

then

$$f'(\beta) = \cos\left[\beta + \frac{1}{2}(\psi^+ - \psi^-)\right] - \cos\left[\frac{R_2}{R_3}\beta + \frac{1}{2}(\psi^+ - \psi^-)\right] \tag{4}$$

so that to solve (3) for β one solves by iteration:

$$\beta^{i+1} = \beta^i - \frac{\sin\left[\beta^i + \frac{1}{2}(\psi^+ - \psi^-)\right] - \frac{R_3}{R_2}\sin\left[\frac{R_2}{R_3}\beta^i + \frac{1}{2}(\psi^+ - \psi^-)\right]}{\cos\left[\beta^i + \frac{1}{2}(\psi^+ - \psi^-)\right] - \cos\left[\frac{R_2}{R_3}\beta^i + \frac{1}{2}(\psi^+ - \psi^-)\right]} \tag{5}$$

until $\dfrac{\beta^{i+1} - \beta^i}{\beta^i} \leq$ some reasonable limit.

*See ref. 8, p. 192.

APPENDIX 9
BERNOULLI' S EQUATION FOR "WILKINS" EQUATION OF STATE

The first law of thermodynamics can be written as:

$$T\, d\eta = d\epsilon + p\, d\left(\frac{1}{\rho}\right). \tag{1}$$

For isentropic flow $d\eta = 0$, whence:

$$d\epsilon = -\, p\, d\left(\frac{1}{\rho}\right). \tag{2}$$

From equation (8), appendix 1,

$$d\epsilon + u\, du + v\, dv + \frac{1}{\rho}\, dp + p\, d\left(\frac{1}{\rho}\right) = 0, \tag{3}$$

and combining (2) and (3):

$$u\, du + v\, dv = -\frac{1}{\rho}\, dp. \tag{4}$$

Now the relation (4) holds along lines where $d\eta = 0$, i. e., along path or flow lines. Hence, (4) may be written as

$$\frac{1}{2}\frac{d}{dS}(u^2 + v^2) = -\frac{1}{\rho}\frac{dp}{dS} = -\frac{a^2}{\rho}\frac{d\rho}{dS}$$

or

$$u^2 + v^2 + 2\int_{\rho(S_*)}^{\rho(S)} \frac{a^2}{\rho}\, d\rho = \text{constant}, \tag{5}$$

where S, S_* are two values of a parameter along a path line,

a^2 = sound speed defined as in appendix 1.

Equation (5) is the well-known Bernoulli' s equation.

To express (5) in terms of the Wilkins equation of state, recall the definition of relative volume,

$$V = \rho_0/\rho,$$

and the expression for a^2 from equation (2), section II, part A:

$$a^2 = \frac{1}{\rho_0}\left[\frac{AQ}{V^{Q-1}} + BRV^2\, e^{-RV} + \frac{(1+\omega)C_s}{V^{\omega}}\right].$$

Using these last two expressions, it is clear that to evaluate (5) the following expression must be integrated:

$$\int_{\rho(S_*)}^{\rho(S)} \frac{a^2 d\rho}{\rho} = \int_{V(S_*)}^{V} -\frac{1}{\rho_0}\left[\frac{AQ}{V^Q} + RBV\, e^{-RV} + \frac{(1+\omega)C_s}{V^{\omega+1}}\right] dV. \qquad (6)$$

The integration of (6) is quite straightforward and the resulting equation is:

$$\text{Const} = u^2 + v^2 + \frac{2}{\rho_0}\left[\frac{AQ}{(Q-1)V^{Q-1}} + B(V + \frac{1}{R})\, e^{-RV} + \frac{(1+\omega)C_s}{\omega V^{\omega}}\right]. \qquad (7)$$

APPENDIX 10
SOLUTION FOR CHARACTERISTICS IN THE HODOGRAPH PLANE FOR THE "WILKINS" EQUATION OF STATE

For the plane problem using the Wilkins equation of state the arguments in appendix 6 are unchanged down through equation (16). As indicated in appendix 6 the basic equations are of the same form for both sets of curves (Γ) and equation (16), appendix 6, can be written as

$$\frac{dg}{d\psi} = -a, \tag{1}$$

where ψ is the angle the tangent to a Γ curve makes with the positive u axis and g is the magnitude of the velocity component normal to a Γ curve.

If equation (7), appendix 9, is evaluated at the Chapman-Jouguet point (detonation front), then

$$q^2 + \frac{2}{\rho_0}\left[\frac{AQ}{(Q-1)V^{Q-1}} + B\left(V + \frac{1}{R}\right)e^{-RV} + \frac{(1+\omega)C_s}{\omega V^{\omega}}\right] = D \tag{2}$$

where

$$D = a_{c-j}^2 + \frac{2}{\rho_0}\left[\frac{AQ}{(Q-1)V_{c-j}^{Q-1}} + B\left(V_{c-j} + \frac{1}{R}\right)e^{-RV_{c-j}} + \frac{(1+\omega)C_s}{\omega V_{c-j}^{\omega}}\right], \tag{3}$$

and

$$q^2 = u^2 + v^2 = a^2 + g^2. \tag{4}$$

Combining (2), (3), and (4):

$$g^2 = D - a^2 - \frac{2}{\rho_0}\left[\frac{AQ}{(Q-1)V^{Q-1}} + B\left(V + \frac{1}{R}\right)e^{-RV} + \frac{(1+\omega)C_s}{\omega V^{\omega}}\right]. \tag{5}$$

Differentiating (5) with respect to ψ:

$$2g\frac{dg}{dV}\frac{dV}{d\psi} = \left(-\frac{da^2}{dV} + \frac{2a^2}{V}\right)\frac{dV}{d\psi}. \tag{6}$$

Using (1):

$$\frac{dg}{dV}\frac{dV}{d\psi} = -a. \tag{7}$$

Hence, putting (7) in (6):

$$\frac{dV}{d\psi} = \frac{2ga}{\frac{da^2}{dV} - \frac{2a^2}{V}}, \tag{8}$$

whence

$$d\psi = \frac{\frac{1}{2}\frac{da^2}{dV} - \frac{a^2}{V}}{ga}. \tag{9}$$

If (9) can be integrated, then ψ can be determined as a function of V and the relations (13) and (14) of appendix 6 can be used to determine u and v, and the equations for C^+ and C^- will determine x and y.

From the considerations in appendix 6 it is seen that for Γ^+ (and ψ^+), $g \leq 0$; and for Γ^- (and ψ^-), $g \geq 0$. If the symbol g is considered to be a positive quantity, then letting

$$F(V) = \frac{\frac{1}{2}\frac{da^2}{dV} - \frac{a^2}{V}}{ga}, \tag{10}$$

one has

$$\psi^+ = -\int_{V_*}^{V} F(V)dV + \psi^+_* \tag{11}$$

and

$$\psi^- = \int_{V_*}^{V} F(V)dV + \psi^-_*. \tag{12}$$

Hence, with g given by the square root of (5), a^2 by equation (2), section II, part A, ψ^+ by (11), and ψ^- by (12), equations (13) and (14) from appendix 6 can be used to give:

$$\Gamma^+: \quad u = a\cos\psi^+ + g\sin\psi^+, \quad v = a\sin\psi^+ - g\cos\psi^+, \tag{13}$$

$$\Gamma^-: \quad u = a\cos\psi^- - g\sin\psi^-, \quad v = a\sin\psi^- + g\cos\psi^-, \tag{14}$$

provided the integral in (11) and (12) exists and is finite.

With a considerable amount of work it can be shown numerically that

$$F(v) < \frac{M'}{\left(\frac{V}{V_{c-j}} - 1\right)^p} = F'(v)$$

where $p < 1$ and M' = constant, as $V \rightarrow V_{c-j}$. For reference:

$$M = \frac{\frac{1}{2}\left[\frac{AQ(Q+1)}{V^Q} + BR^2V^2e^{-RV} + \frac{(1+\omega)(2+\omega)C_s}{V^{\omega+1}}\right]\frac{1}{\rho_0}}{\frac{1}{\sqrt{\rho_0}}\left[\frac{AQ}{V^{Q-1}} + BRV^2e^{-RV} + \frac{(1+\omega)C_s}{V^{\omega}}\right]^{1/2}}$$

and

$$M' = Me^{RV_{c-j}/2}\sqrt{\rho_0}/(\sqrt{RB}\, V_{c-j}) .$$

Since the integral of $F'(v)$ exists for $p < 1$ for an arbitrary upper limit, the integral of $F(v)$ would also exist by the comparison test if one could be sure that the function ψ was single valued at $V = V_{c-j}$. That this is indeed true can be seen by considering Fig. 5 of UCRL-7797 which indicates that near V_{c-j} the material behaves like an ideal gas. The characteristics for the ideal gas equation of state were shown to become horizontal at $V = V_{c-j}$, and the same result should follow in this case.

It seems clear, therefore, that the integral in (11) and (12) has a finite value and can be evaluated numerically. This point is discussed further in section II, part B.

At the intersection of a Γ^+ and Γ^- curve, the relations (13) and (14) yield the following formulas for finding ψ^- in terms of ψ^+:

$$\tan\psi^- = \frac{(a^2 - g^2)\sin\psi^+ - 2ag\cos\psi^+}{(a^2 - g^2)\cos\psi^+ + 2ag\sin\psi^+} . \qquad (15)$$

Along $v = 0$, (13) and (14) yield:

$$\tan\psi^+ = \frac{g}{a} \qquad (16)$$

and

$$\psi^+ = -\psi^- . \qquad (17)$$

To find ψ^- and ψ^+ at the intersection of a Γ^- curve and $v = 0$,

$$a\sin\psi^- + g\cos\psi^- = 0$$

must be solved for ψ^-. This is done by the use of the Newton-Raphson method described in appendix 8 to find V from

$$V^i = -V^{i-1}\left[\frac{g(V^{i-1})}{a(V^{i-1})\tan\psi^-(V^{i-1})}\right] \tag{18}$$

where V^i is the ith estimate of V; ψ^- and ψ^+ are then determined from (16) and (17).

In a similar manner ψ^+ and ψ^- are determined at the intersection of Γ^+ and Γ^- by finding V from:

$$V^i = -V^{i-1}\left\{\frac{g(V^{i-1})\left[\sin\psi^+(V^{i-1}) + \sin\psi^-(V^{i-1})\right]}{a(V^{i-1})\left[\cos\psi^+(V^{i-1}) - \cos\psi^-(V^{i-1})\right]}\right\} \tag{19}$$

and ψ^+ and ψ^- are calculated from (11) and (12).

REFERENCES

1. UCRL-6797, "Shock Hydrodynamics," Wilkins, M. L., Feb. 1962.

2. Supersonic Flow in Shock Waves, Courant and Friedricks, Interscience Publishers, Inc., New York, 1948.

3. "An Investigation, by the Method of Characteristics, of the Lateral Expansion of Gases Behind a Detonating Slab of Explosive," Hill, R., and Pack, D. C., Proceedings of the Royal Society of London, Vol. 194, 1947, pp. 524-541.

4. UCRL-7797, "The Equation of State for PBX 9404 and LX-04-01," Wilkins, M. L., Squire, B., Halperin, B., 27 April 1964.

5. UCRL-7569-T, "Write-up of Subroutine ROMBRG, a General-Purpose Routine for Numerical Integration," Fritsch, Fred N., Oct. 1963.

6. Nonlinear Theory of Continuous Media, Eringen, A. C., McGraw-Hill Book Company, Inc., New York, 1962.

7. Methods of Mathematical Physics, Vol. II, Courant, R., Interscience Publishers, Inc., New York, 1962.

8. Numerical Mathematical Analysis, Scarborough, J. B., Johns Hopkins Press, 3rd Ed., 1955.

APPENDIX 11

TABLES OF OUTPUT FOR PRESSURE CURVES

Table 1. Pressure at various distances from the centerline of the H. E. as a function of distance from the front in units of the initial thickness of the slab, for the ideal gas equation of state in plane geometry.

y = 0.0[a]		y = 0.1		y = 0.2		y = 0.3		y = 0.4	
X	P	X	P	X	P	X	P	X	P
0.0013	0.3900	0.0016	0.3900	0.0022	0.3900	0.0033	0.3899	0.0066	0.3887
.0189	.3894	.0192	.3893	.0206	.3886	.0181	.3877	.0212	.3777
.0407	.3873	.0415	.3866	.0411	.3846	.0389	.3794	.0448	.3422
.0649	.3831	.0599	.3830	.0559	.3800	.0613	.3655	.0600	.3140
.0822	.3790	.0835	.3765	.0803	.3705	.0828	.3482	.0744	.2870
.1127	.3698	.1055	.3691	.1113	.3546	.1035	.3293	.0916	.2569
.1299	.3635	.1138	.3659	.1274	.3452	.1179	.3157	.1257	.2084
.1439	.3579	.1443	.3527	.1402	.3373	.1292	.3049	.1361	.1965
.1666	.3480	.1662	.3421	.1510	.3304	.1606	.2759	.1447	.1876
.1853	.3392	.1839	.3329	.1904	.3045	.1820	.2573	.1738	.1624
.2016	.3311	.1992	.3247	.2182	.2861	.1987	.2437	.2074	.1411
.2230	.3199	.2250	.3103	.2405	.2717	.2127	.2331		
.2421	.3097	.2469	.2979	.2595	.2598	– [b]		.2459	.1233
.2596	.3001	.2662	.2869	.2763	.2496	.2619	.2006	.2711	.1144
.2811	.2882	.2837	.2768	.2914	.2407	.2955	.1822	.2903	.1086
.3012	.2771	.2999	.2676	.3052	.2328			.3060	.1044
.3201	.2666	.3224	.2551	.3181	.2257	.3219	.1696		
.3427	.2542	.3431	.2437	.3415	.2133	.3441	.1602		
.3600	.2448	.3626	.2333	.3627	.2027	.3634	.1526	.3604	.0927
.3811	.2337	.3811	.2237	.3821	.1935	.3808	.1463		
.4017	.2231	.4046	.2120	.4002	.1853	.3966	.1410	.3967	.0866
.4219	.2130	.4215	.2038	.4172	.1780	.4248	.1321	.4250	.0825
.4419	.2033	.4433	.1937	.4413	.1682	.4376	.1284	.4486	.0794
.4617	.1941	.4592	.1866	.4638	.1595	.4614	.1219	.4692	.0769
.4814	.1853	.4799	.1777	.4852	.1517	.4831	.1164	.4876	.0748
.5012	.1768	.5002	.1693	.5058	.1447	.5033	.1116	.5044	.0730
.5209	.1686	.5201	.1615	.5190	.1404	.5223	.1073	.5199	.0714
.5408	.1608	.5398	.1541	.5384	.1343	.5403	.1035	.5479	.0686
.5608	.1533	.5593	.1472	.5634	.1269	.5576	.1000	.5608	.0674
.5810	.1461	.5835	.1390	.5816	.1218	.5822	.0953	.5849	.0652
.6015	.1391	.6027	.1328	.5996	.1170	.5979	.0924	.5962	.0642
.6222	.1324	.6220	.1270	.6172	.1125	.6207	.0884	.6177	.0623
.6390	.1272	.6412	.1214	.6403	.1069	.6426	.0848	.6379	.0606
.6604	.1210	.6605	.1161	.6575	.1030	.6639	.0814	.6571	.0591
.6821	.1150	.6799	.1110	.6802	.0980	.6846	.0783	.6845	.0569
.7043	.1092	.6993	.1062	.7027	.0934	.6982	.0763	.7019	.0556
.7223	.1047	.7239	.1004	.7194	.0901	.7183	.0736	.7187	.0543
.7407	.1004	.7437	.0960	.7417	.0859	.7380	.0709	.7432	.0525
.7595	.0962	.7637	.0918	.7585	.0830	.7639	.0676	.7590	.0514
.7834	.0911	.7840	.0878	.7807	.0792	.7830	.0653	.7822	.0497
.8030	.0872	.7993	.0848	.8031	.0756	.8020	.0631	.7973	.0487
.8230	.0834	.8200	.0811	.8199	.0731	.8209	.0610	.8195	.0472
.8435	.0797	.8410	.0775	.8424	.0698	.8397	.0590	.8413	.0458
.8591	.0770	.8622	.0740	.8594	.0675	.8585	.0571	.8628	.0444
.8804	.0735	.8839	.0707	.8821	.0645	.8834	.0546	.8770	.0434
.9023	.0702	.9003	.0683	.8994	.0623	.9020	.0529	.8980	.0423
.9246	.0669	.9226	.0652	.9225	.0595	.9207	.0512	.9189	.0411
.9418	.0646	.9396	.0630	.9400	.0575	.9395	.0495	.9396	.0399
.9593	.0623	.9626	.0601	.9637	.0550	.9582	.0480	.9602	.0388
0.9832	0.0593	0.9801	0.0580	0.9816	0.0531	0.9834	0.0459	0.9807	0.0377

[a] y ≡ distance from centerline in units of initial thickness.
x ≡ distance from front in units of initial thickness.
p ≡ pressure in megabars.

[b] Blank spaces were left where the calculated data did not fall near the values of the x coordinate being used in the other y = constant lines.

Table 2. Pressure at various distances from the centerline of the H. E. as a function of the distance from the front in units of the initial slab thickness, for Wilkins equation of state in plane geometry.

y = 0.0[a]		y = 0.1		y = 0.2		y = 0.3		y = 0.4	
X	P	X	P	X	P	X	P	X	P
0.0047	0.3904	0.0064	0.3903	0.0088	0.3901	–[b]			
.0211	.3893	.0192	.3894	.0204	.3886	0.0222	0.3857	0.0265	0.3656
.0404	.3863	.0388	.3860	.0375	.3842	.0393	.3763	.0436	.3310
.0601	.3813	.0593	.3807	.0618	.3745	.0637	.3558	.0592	.2951
.0788	.3762	.0779	.3744	.0796	.3649	.0779	.3411	.0817	.2462
.1002	.3684	.1013	.3645	.0981	.3530	.0977	.3188	.1021	.2090
.1216	.3590	.1208	.3545	.1212	.3362	.1162	.2973	.1250	.1760
.1417	.3489	.1400	.3438	.1396	.3222	.1417	.2684	.1450	.1537
.1617	.3378	.1606	.3311	.1597	.3061	.1574	.2515	.1630	.1376
.1817	.3257	.1810	.3178	.1792	.2904	.1788	.2303	.1797	.1254
.2021	.3128	.2011	.3042	.2037	.2708	.2026	.2091	.1989	.1138
.2187	.3019	.2213	.2902	.2229	.2559	.2214	.1939	.2198	.1035
.2399	.2877	.2416	.2760	.2418	.2417	.2396	.1807	.2390	.0958
.2618	.2729	.2622	.2617	.2605	.2282	.2596	.1677	.2569	.0897
.2799	.2607	.2778	.2509	.2790	.2154	.2829	.1542	.2769	.0839
.2985	.2481	.2990	.2366	.2976	.2033	.2981	.1462	.2991	.0784
.3177	.2354	.3207	.2224	.3225	.1880	.3205	.1356	.3208	.0738
.3377	.2225	.3373	.2119	.3413	.1772	.3424	.1263	.3408	.0701
.3584	.2095	.3600	.1980	.3603	.1670	.3569	.1207	.3566	.0675
.3801	.1964	.3775	.1878	.3795	.1572	.3785	.1129	.3824	.0637
.4027	.1833	.4015	.1744	.3989	.1479	.4000	.1059	.3993	.0614
.4205	.1735	.4201	.1646	.4188	.1390	.4216	.0995	.4159	.0594
.4389	.1638	.4392	.1551	.4390	.1306	.4433	.0936	.4402	.0566
.4580	.1542	.4590	.1457	.4596	.1225	.4579	.0898	.4561	.0549
.4780	.1447	.4794	.1366	.4808	.1148	.4800	.0846	.4799	.0525
.4990	.1354	.5005	.1277	.5025	.1074	.5024	.0796	.5037	.0503
.5209	.1262	.5225	.1191	.5173	.1027	.5176	.0765	.5195	.0489
.5439	.1172	.5376	.1136	.5401	.0959	.5408	.0720	.5434	.0469
.5599	.1114	.5611	.1055	.5637	.0894	.5565	.0691	.5594	.0456
.5765	.1056	.5773	.1002	.5798	.0852	.5806	.0650	.5837	.0437
.6027	.0972	.6026	.0926	.5964	.0812	.5970	.0624	.6001	.0424
.6209	.0918	.6201	.0877	.6220	.0754	.6222	.0586	.6167	.0412
.6400	.0864	.6382	.0829	.6396	.0716	.6395	.0562	.6421	.0395
.6598	.0812	.6570	.0783	.6577	.0680	.6571	.0538	.6593	.0383
.6806	.0762	.6764	.0739	.6765	.0645	.6843	.0504	.6768	.0372
.7023	.0713	.6965	.0695	.6957	.0612	.7030	.0482	.7037	.0355
.7250	.0666	.7174	.0654	.7156	.0579	.7223	.0461	.7220	.0344
.7369	.0643	.7392	.0614	.7361	.0548	.7420	.0441	.7408	.0334
.7615	.0598	.7619	.0575	.7573	.0518	.7623	.0421	.7600	.0323
.7874	.0555	.7856	.0538	.7792	.0489	.7832	.0402	.7796	.0313
.8009	.0535	.7978	.0520	.8020	.0461	.8047	.0383	.7997	.0302
.8291	.0494	.8231	.0485	.8257	.0434	.8157	.0374	.8204	.0292
.8438	.0475	.8362	.0468	.8378	.0421	.8383	.0356	.8416	.0282
.8590	.0456	.8634	.0436	.8629	.0396	.8617	.0339	.8634	.0273
.8746	.0437	.8776	.0420	.8759	.0384	.8858	.0323	.8745	.0268
.9075	.0401	.9069	.0390	.9026	.0361	.8982	.0315	.8973	.0258
.9248	.0384	.9222	.0376	.9164	.0349	.9237	.0299	.9208	.0249
.9427	.0368	.9379	.0362	.9449	.0328	.9368	.0291	.9450	.0240
.9612	.0352	.9541	.0348	.9597	.0317	.9638	.0277	.9574	.0235
0.9805	0.0336	0.9878	0.0322	0.9748	0.0307	0.9778	0.0270	0.9829	0.0227

[a] y ≡ distance from centerline in units of initial thickness.

x ≡ distance from front in units of initial thickness.

p ≡ pressure in megabars.

[b] Blank spaces were left where the calculated data did not fall near the values of the x coordinate being used in the other y = constant lines.

Table 3. Pressure at various distances from the centerline of the H. E. as a function of the distance from the front in units of the initial thickness of the cylinder, for Wilkins equation of state in cylindrical geometry.[a]

y = 0.0[b]		y = 0.1		y = 0.2		y = 0.3		y = 0.4	
X	P	X	P	X	P	X	P	X	P
0.0502	0.3840	–[c]							
.0519	.3832	0.0517	0.3823	0.0524	0.3784	0.0522	0.3659	0.0515	0.3119
.0539	.3822	.0540	.3813						
.0560	.3813	.0563	.3802	.0554	.3766	.0565	.3612		
.0584	.3804	.0587	.3791	.0584	.3747				
.0609	.3795	.0611	.3781	.0615	.3728	.0610	.3562		
.0637	.3782	.0635	.3771	.0647	.3707				
.0668	.3770	.0664	.3758					.0672	.2724
***		.0688	.3747						
.0701	.3756	.0715	.3734	.0711	.3663	.0700	.3458		
.0738	.3740			.0743	.3640	.0745	.3404	.0748	.2549
.0779	.3722	.0776	.3704	.0777	.3616				
.0822	.3706	.0810	.3685						
		.0847	.3665	.0844	.3564	.0837	.3290		
.0868	.3689			.0877	.3539	.0884	.3226		
.0923	.3659	.0932	.3616	.0919	.3504			.0903	.2209
.0986	.3622	.0981	.3585	.0989	.3447	.0978	.3105		
.1060	.3578	.1034	.3551	.1030	.3411	.1026	.3039	0.1048	0.1942
.1144	.3526	.1091	.3514	.1121	.3331	.1122	.2908		
				.1173	.3282	.1170	.2846		
.1241	.3461	.1224	.3419	.1289	.3173	.1269	.2713		
.1356	.3382	.1309	.3354	.1356	.3107	.1368	.2583		
		.1406	.3279			.1424	.2511		
.1493	.3281	.1518	.3187	.1505	.2960	.1532	.2381		
.1658	.3155			.1588	.2876	.1596	.2303		
		.1798	.2947	.1801	.2660	.1737	.2137		
.1861	.2986			.1932	.2530	.1898	.1963		
		.1978	.2785			.2084	.1778		
.2181	.2767	.2192	.2595	.2256	.2216	0.2184	0.1685		
.2454	.2474	.2461	.2353	.2454	.2038				
.2915	.2082			.2988	.1609				
		.3236	.1717	0.3334	0.1367				
0.3594	0.1560	.3845	.1315						
		0.4745	0.0869						

[a]This table, unlike Tables 1 and 2, includes all the output calculated by the program.

[b]y ≡ distance from centerline in units of initial thickness.

x ≡ distance from front in units of initial thickness.

p ≡ pressure in megabars.

[c]Blank spaces were left so that the x values across the table would be more or less comparable.

DISTRIBUTION

	No. of Copies
LRL Internal Distribution,	
Information Division	30
Gerald T. Richards	10
Mark L. Wilkins	25
Harlan H. Zodtner	5
External Distribution,	
A. Cemal Eringen, Purdue Univ., Lafayette, Indiana	
Charles Saalfrank, Lafayette College, Easton, Penna.	
C. M. Merrick, Lafayette College, Easton, Penna.	
TID-4500 (43rd Ed.), UC-32, Mathematics and Computers	

This report was prepared as an account of Government sponsored work. Neither the United States, nor the Commission, nor any person acting on behalf of the Commission:

A. Makes any warranty or representation, expressed or implied, with respect to the accuracy, completeness, or usefulness of the information contained in this report, or that the use of any information, apparatus, method, or process disclosed in this report may not infringe privately owned rights; or

B. Assumes any liabilities with respect to the use of, or for damages resulting from the use of any information, apparatus, method, or process disclosed in this report.

As used in the above, "person acting on behalf of the Commission" includes any employee or contractor of the Commission, or employee of such contractor, to the extent that such employee or contractor of the Commission, or employee of such contractor prepares, disseminates, or provides access to, any information pursuant to his employment or contract with the Commission, or his employment with such contractor.